Imperial College London
Department of Physics

Constraining the Higgs curvature coupling from vacuum decay during inflation

Andreas Mantziris

Thesis submitted for the fulfilment of the requirements for the degree of Doctor of Philosophy (PhD) in Theoretical Physics, July 2022.

Abstract

According to the current experimental data, the Higgs vacuum appears to be metastable due to the development of a second, lower ground state in its potential. Consequently, this leads to a non-zero rate of vacuum decay through nucleation of bubbles of true vacuum with catastrophic consequences for our false vacuum Universe. Since such an event would render our Universe incompatible with measurements, there cannot have been any such bubble nucleation events anywhere in our whole past lightcone. Thus, we are motivated to study possible stabilising mechanisms in the early universe, focusing on the period of cosmological inflation. We consider a minimal scenario of the Standard Model of particle physics together with single-field, high-scale inflation, while accounting for the time-dependence of the Hubble rate, both in the geometry of our past light-cone and in the Higgs effective potential. The latter is approximated with three-loop renormalization group improvement supplemented with one-loop curvature corrections in de Sitter. We study three one-parameter inflationary models in field theory, quadratic, quartic, and Starobinsky-like power law inflation, and the modified gravity scenario $R + R^2$, that leads to the observationally favoured model of Starobinsky inflation. We show that the survival of the vacuum state through inflation places lower bounds on the non-minimal Higgs curvature coupling ξ, the last unknown parameter of the Standard Model. The bounds are significantly stronger in Starobinsky inflation than in field theory models with no Higgs-inflaton coupling, $\xi \gtrsim 0.1 > 0.06$, but are independent of the duration of inflation. However, they are sensitive to the details of the dynamics at the end of inflation, and therefore they can be improved with a more detailed study of that period.

Statement of originality

The content of this thesis is my own work, except where otherwise referenced, with the majority being from two collaborative papers [1, 2], with additions from two single-authored conference proceedings [3, 4]. The research ideas and outcomes were developed collaboratively between myself, my supervisor Arttu Rajantie, and my collaborator Tommi Markkanen, and they were based on their previous work [5, 6]. The novel calculations and results from [1, 2] are presented and discussed in Chapters 4 and 5, respectively, with Chapters 2 and 3 covering background material which is mentioned in parts throughout these references.

My contribution to [1] was to perform the inflationary calculations within and beyond slow-roll in quadratic, quartic, and Starobinsky-like power-law inflation regarding the calculation of bubble nucleation. In addition, I developed the numerical code (based on the publicly available Mathematica package by F. Bezrukov available at http://www.inr.ac.ru/∼fedor/SM/) for the calculation and the renormalization group improvement of the effective Higgs potential with curvature corrections, and produced all the corresponding plots and tables.

In [2], I calculated analytically the embedding of the SM in the $R + R^2$ gravity scenario via the conformal transformation and field redefinitions, performed the necessary checks regarding the SM effective masses and RG improvement, computed the newly generated destabilising terms in the effective potential, extended and improved the Mathematica code from [1] to account for these developments, and produced the figures.

Acknowledgements

I would like to express my gratitude and appreciation for my supervisor's, Arttu Rajantie, continuous guidance and mentoring during my PhD studies, which were not limited just to our research project but extending to more general aspects of academic development. I would also like to thank Tommi Markkanen for an equally helpful and encouraging support, supervision, and collaboration, which again went beyond our research objectives. I am grateful for the useful discussions and help with the numerical computations from José Eliel Camargo-Molina. Moreover, I am thankful for the pastoral support from Dan Waldram and Jonathan Halliwell, and the invaluable friendship and camaraderie of the Theory Group PhD/Postdoc cohort: Matthew, Sumer, Arshia, Clement, Justin, Zhenghao, Rahim, Julius, Nat, Lucas, David, Stav, Dave, Ariana, Santi, Victor, Matt, and Ed whom we deeply miss. I would like to thank my family for all their undisputed support throughout my studies and my lockdown family for keeping us safe and sane. Finally, I thank Vana for everything.

This work was supported by an STFC DTP research studentship.

Contents

Abstract **1**

Statement of originality **2**

Acknowledgements **4**

1 Introduction **14**

1.1 Motivation and Objectives 14

1.2 Summary of results 18

2 The electroweak vacuum instability **20**

2.1 Vacuum instability in flat spacetime 20

2.2 Vacuum instability in curved spacetime 26

2.3 One-loop curvature corrections 29

3 Cosmological inflation **35**

3.1 Theoretical framework 35

3.2 Departure from the slow-roll regime 41

3.2.1 Leading order corrections 41

3.2.2 Beyond slow-roll 43

3.3 Inflationary models 45

3.3.1 Monomial potentials 45

3.3.2 Starobinsky inflation 47

4 Vacuum decay constraints from inflation 51

4.1 Bubble nucleation during inflation 51

4.2 Vacuum decay in field theory inflation 54

4.2.1 Bounds on ξ 56

4.2.2 Bubble nucleation time 58

4.2.3 Significance of the total duration of inflation 59

5 The metastability of the effective potential in Starobinsky inflation 63

5.1 The effective potential in $R + R^2$ gravity 63

5.1.1 Non-minimally coupled scalar spectator field 63

5.1.2 The effective masses in the Einstein frame 65

5.1.3 The time-dependence of the background 70

5.2 Vacuum decay in R^2 inflation 73

6 Conclusion 81

6.1 Summary 81

6.2 Field theory inflation 82

6.3 Starobinsky inflation 84

6.4 Future directions 85

Bibliography **86**

A Explicit calculations in quadratic inflation **100**

A.1 Analysis in terms of physical time 100

A.2 Analysis in terms of the scale factor 103

A.3 Analysis in terms of the number of e-foldings 104

A.4 Toy model vacuum decay in slow-roll 107

Conventions

- Sign convention $(-,-,-)$ for the metric $(+,-,-,-)$ and curvature tensors [7].
- Natural units $\hbar = c = 1$ are used.
- $M_P = (8\pi G)^{-1/2} \approx 2.435 \times 10^{18}$ GeV is the reduced Planck mass.
- G is Newton's gravitational constant.
- The Higgs-curvature coupling is positive and its conformal value is $\xi = 1/6$.
- The Lagrangian for a scalar field φ is written as $\mathcal{L} = \frac{1}{2}\partial_\mu\varphi\partial^\mu\varphi - V(\varphi)$.
- The scale factor and the Hubble rate today are $a_0 = 1$ and $H_0 \approx 1.5 \times 10^{-42}$ GeV.

Acronyms

1. SM = Standard Model of particle physics
2. BSM = beyond the SM
3. QCD = Quantum Chromodynamics
4. CMB = Cosmic Microwave Background
5. HBB = Hot Big Bang
6. QFT = Quantum Field Theory
7. EW = Electroweak
8. RG = Renormalization Group
9. RGI = RG Improvement/Improved
10. GR = General Relativity
11. HM = Hawking-Moss instanton
12. CdL = Coleman-de Lucia instanton
13. dS = de Sitter
14. AdS = Anti de Sitter
15. vev = vacuum exppectation value
16. bar = top of the barrier
17. fv = false vacuum
18. EoM = Equation of Motion
19. EH = Einstein-Hilbert
20. FRW = Friedmann-Robertson-Walker

List of Tables

2.1 Experimental values of the SM particle masses and couplings [8] at μ_{EW} used for the RGI of the Higgs potential. The couplings in bold are calculated by the SM code[7] subject to the input of m_h, m_t and a_S. Originally published in [1] (CC BY 4.0). 33

5.1 Loop corrections to the effective potential with tree-level couplings to the Higgs, from the $\tilde{W}^{\pm}$ and $\tilde{Z}^0$ bosons, the quarks $\tilde{\text{q}}$, the leptons $\tilde{l}$, the Higgs $\tilde{h}$, the Goldstone bosons $\tilde{\chi}_W$ and $\tilde{\chi}_Z$, and the ghosts $\tilde{c}_W$ and $\tilde{c}_Z$, and corrections that do not to couple to the Higgs at tree-level, from the photon $\tilde{\gamma}$, the gluons $\tilde{g}$, the neutrinos $\tilde{\nu}$, and the ghosts $\tilde{c}_\gamma$ and $\tilde{c}_g$. Table originally published in [6] (CC BY 4.0), then adapted and included in [2]. 68

List of Figures

2.1 Running of the Higgs self-interaction coupling with the renormalization scale for the central values of the Higgs mass, top mass, and strong coupling with 3σ uncertainty, according to the current experimental data [8]. Figure taken from [2]. 23

2.2 Vacuum decay of a scalar field φ for a double-well potential from a metastable vacuum to its true vacuum. Originally published in [5] (CC BY 4.0). 25

2.3 The running of non-minimal coupling $\xi(\mu)$ with various boundary conditions ξ_{EW} for top quark mass $m_t = (172.76 \pm 0.6)$ GeV. The solid lines correspond to the central value of m_t for each case, while the dashed and the dotted ones correspond to $m_t \pm 2\sigma$, respectively. Originally published in [1] (CC BY 4.0). . . 34

4.1 Evolution of the Hawking-Moss bounce action with spacetime curvature in the dS approximation (3.23), for sample value of the non-minimal coupling. The shaded areas denote 1σ and 2σ deviation from the central value of m_t, where a heavier top quark decreases the value of B_{HM} and vice versa. The solid red, blue and green arrows denote the last 60 e-foldings of inflation in quadratic, Starobinsky and quartic inflation respectively, whereas the dashed ones extend beyond that. Originally published in [1] (CC BY 4.0). 56

4.2 Constraints on the value of the curvature coupling ξ at $\mu_{\rm EW}$, by imposing $\langle\mathcal{N}\rangle_{\rm inf}(60) \approx 1$ at the bound, with a varying top quark mass and different inflationary models. The vertical dashed black line signifies the threshold below which, the Higgs self-coupling remains positive as it runs, and thus there is no formation of a second minimum in the Higgs potential. The vertical dashed orange line lies at the central value $m_t = (172.76 \pm 0.30)$ GeV, where the shaded areas denote the corresponding $\pm\sigma$ and $\pm 2\sigma$ variances [8]. The horizontal dotted black line shows the lowest $\xi_{\rm EW}$ value below which, $\xi(\mu_*)$ turns negative as it runs. Originally published in [1] (CC BY 4.0). 57

4.3 The integrands of (4.4) for the expectation value of the number of bubbles $\langle\mathcal{N}\rangle_{\rm inf}$, for three inflationary models, with $\xi_{\rm EW}$ chosen such that $\langle\mathcal{N}\rangle_{\rm inf}(60) = 1$ in each case. This means that $\xi_{\rm EW}^{\rm Star} = 0.05938$, $\xi_{\rm EW}^{\rm Quad} = 0.05998$, and $\xi_{\rm EW}^{\rm Quar} = 0.05875$ for Starobinsky, quadratic, and quartic inflation, respectively. The solid lines correspond to the central value of m_t, whereas the dashed and dotted lines to a deviation of ± 0.5 GeV, respectively. The scales of the Hubble rate, at which the bubbles are predominantly produced, are $H_{\rm Star} = 9.96 \times 10^{12}$ GeV, $H_{\rm Quad} = 1.83 \times 10^{13}$ GeV, and $H_{\rm Quar} = 1.16 \times 10^{13}$ GeV. Originally published in [1] (CC BY 4.0). 59

4.4 Factors of the integrand $\gamma(N)$ defined in Eq.(4.7) as functions of e-foldings of inflation in quartic inflation with $\xi_{\rm EW} = 0.05875$ and $m_t = 172.76$ GeV. The dynamic factor corresponds to $\Gamma(N)$, while the geometric factor to $\frac{d\mathcal{V}}{dN}$, and we have normalised all factors to one at $N = 0$. Originally published in [1] (CC BY 4.0). 60

5.1 Coefficient $m_{\rm eff}^2$ of the quadratic term in Eq.(5.52) for $\xi_{\rm EW} = 0.06$ (left) and $\xi_{\rm EW} = 0.1$ (right), calculated at Higgs field value $\rho = 10^{12}$ GeV. Figure included in [2]. 75

5.2 Bounce action (2.15) for sample values of the non-minimal coupling $\xi_{\rm EW}$ during R^2 inflation (solid) and in comparison with the field theory case (dotted). Figure included in [2]. 76

5.3 Integrands of $\langle\mathcal{N}\rangle_{\rm inf}$ with varying definition for the end of inflation. The vertical lines are at $\frac{\dot{H}}{H^2} = -1, -\frac{1}{4}, -\frac{1}{32}$ respectively, and the dotted lines correspond to the field theory inflation model discussed in Section 4.2. The plateau at $d\langle\mathcal{N}\rangle_{\rm inf}/dN \sim 10^{80}$, which the curves reach at small N, corresponds to vanishing Hawking-Moss action (2.15). In that case the expression (2.16) is not valid quantitatively, so the numerical value should be taken to be indicative of unsuppressed bubble nucleation. Figure included in [2]. 77

5.4 Dependence of the lower bound on the non-minimal Higgs curvature coupling $\xi_{\rm EW}$ on the choice of $N_{\rm end}$ in Eq. (4.4), parameterised by $\dot{H}/H^2$, for the top quark mass $m_t = 172.76$ GeV. The shaded regions below the curve denote the excluded values of the parameter space, the colour scheme ranges from the most conservative lower bounds in the darkest tone on the right to the less reliable in the lightest tone on the left and it matches with the corresponding bounds in figure 5.5. The horizontal black line lies at the conformal value $\xi = 1/6$. Figure included in [2]. 78

5.5 Lower bounds on the non-minimal Higgs curvature coupling $\xi_{\rm EW}$ as a function of the top quark mass m_t. The vertical dashed orange line with its accompanying shaded regions depict $m_t \pm \sigma\,, 2\sigma$ [8]. The darker and lighter shades of purple show the excluded areas for two different choices of $N_{\rm end}$, corresponding to $\dot{H}/H^2 = -1/4$ and $\dot{H}/H^2 = -1$, respectively. The leftmost black parts of the curves show the lowest $\xi_{\rm EW}$ values below which $\xi(\mu)$ turns negative during its running, and thus "pushes" the EW vacuum to higher field values. Previous constraints with a Starobinsky-like power-law model are shown in the dotted blue curve (see Section 4.2.1). The vertical dashed black line stands at the threshold value of m_t, below which the EW vacuum is stable. Finally, the horizontal, black line illustrates the conformal point $\xi = 1/6$. Figure included in [2]. 79

Chapter 1

Introduction

1.1 Motivation and Objectives

In 2012, the last missing particle of the Standard Model (SM) of particle physics, the Higgs boson, was observed in the Large Hadron Collider (LHC) at CERN [9, 10]. This event established firmly the validity of the SM as a self-consistent theory of nature's fundamental particles and their interactions. The SM has famously provided predictions about observables, which agree with experimental results to many decimal places and therefore render it as our most successful physical theory so far [11]. Even though there are still many open questions, unexplained phenomena and intricacies that we cannot tackle with the SM alone, it is possible that the SM could indeed describe physics beyond the few TeV's we probe with the LHC up to the Planck scale, where a theory of quantum gravity would be needed [12, 13, 14]. This implies that we could use the SM for studying the early universe, when energies were high, and thus make a promising connection between particle physics and cosmology. [12]

The Higgs boson, rather than acting just as a confirmation of the SM, has a number of interesting characteristics that may have allowed it to affect the evolution of the universe. In the context of the SM alone, the eponymous boson is the excitation of the Higgs field that permeates all of spacetime and via its coupling to matter fields, such as the leptons and quarks, it generates their corresponding masses. This is the result of spontaneous symmetry breaking

of the $SU(2) \times U(1)$ symmetry of the electroweak force into electromagnetism's U(1) symmetry, due to the field's non-zero vacuum expectation value (vev) of $v \approx 246.22$ GeV [11, 15]. The experimentally measured mass of the Higgs boson lies in a range [8] within which the Higgs self-interaction does not diverge below the Planck scale [16, 17, 18]. This has attracted significant interest in the past [19, 20, 21, 22, 23, 24, 25, 26] and it implies that the SM might be sufficient to describe our universe up to Planck scale energies, where quantum gravity effects become significant. Thus, the SM can be used as a consistent minimal model for describing the early Universe and address open questions by considering its cosmological applications [5, 12]. These revolve around cosmological phase transitions, baryon asymmetry, dark matter, the dynamics of inflation that seed the present day large scale structure and the possible death of the universe due to the electroweak vacuum instability. In this study, we focus on the last topic but for more details on these applications we refer the reader to [12].

The current parameters of the SM, in particular the masses of the Higgs boson and the top quark, suggest that the Higgs field lies currently in a metastable electroweak vacuum state [16, 17]. The corresponding decay rate is extremely small and thus a collapse into the true minimum is very unlikely in the present day universe [27, 28, 29, 30, 31, 32]. However, when considering our cosmological evolution and thus given a long enough time interval, the Higgs field will eventually decay to its true vacuum state. This can happen either via thermal fluctuations, quantum tunnelling or a combination of both. This is a local process at a particular point in spacetime that in turn excites the surrounding field in all directions to vacuum decay in a rapidly evolving chain reaction [33]. This induces the nucleation of bubbles of true vacuum that expand rapidly with velocity close to the speed of light c and consume everything in their path [34, 35]. Inside these bubbles, the physics that govern the true vacuum spacetime are very different to our false vacuum Universe and depend on the shape of the Higgs potential, high energy (UV) effects and quantum gravity [36]. However, for all practical purposes in the framework of the SM, the bubble interior is considered to collapse into a singularity [36, 37, 38, 39]. From our measurements of the relevant SM parameters and the observation that the Universe around us is still in the metastable state, we can conclude that no such bubble nucleation event took place inside our past lightcone, despite the many different mechanisms that could have

triggered it throughout our cosmological history. In other words, the probability for suppressing bubble production and thus surviving so far has to be significant [5, 38]. In the early Universe, the probability of such an event could have been close to unity, which allows us to constrain fundamental theories and their parameters leading to a wide variety of physical implications reviewed in Ref. [5], where we refer the reader for more details and references.

The cosmological implications of Higgs vacuum metastability have been studied in a variety of scenarios in recent years and reviewed in [5]. There is already a substantial body of literature investigating implications from vacuum stability during inflation [6, 13, 28, 36, 38, 40, 41, 42, 43, 44, 45, 39, 46, 47, 48, 49, 50, 51, 52, 53, 54, 55, 56, 57, 58, 59] and reheating [60, 61, 62, 63, 64, 65, 66, 67, 68, 69] and possible cosmological signatures from non-fatal scenarios as well as effects from black holes [70, 71, 37, 72, 73, 74, 75, 76, 77, 78, 79, 80]. For recent works addressing aspects of vacuum decay in de Sitter (dS) space see the Refs. [81, 82, 83, 84, 85].

In particular, vacuum stability allows us to constrain the non-minimal coupling ξ, which couples the Higgs field to spacetime curvature [38, 48, 60]. This parameter is required by the renormalizability of the theory in curved spacetime [86, 87, 88], but it is practically impossible to be measured experimentally in the current almost flat Universe, which makes it the last unknown renormalizable parameter of the SM [6, 89]. On the contrary, at the high energy scales of the early universe, the fabric of spacetime was curved significantly more so, that its effects on the Higgs field dynamics would be more evident. [5, 12]. Therefore, the constraints from cosmological vacuum instability are many orders of magnitude stronger than those from other measurements [5]. Within this context, vacuum stability during inflation [1, 2, 6, 38, 48] and after inflation [60, 67, 90] requires ξ to lie within a narrow range around the conformal value $\xi = 1/6$. For recent work on other cosmological implications of non-minimal couplings see the Refs. [91, 92, 93].

The aim of this work was to explore this possibility by calculating the probability of the Higgs field to vacuum decay during the period of cosmological inflation. It is essential for this computation to consider the entire particle spectrum of the SM and especially the effects of spacetime curvature. The bubble nucleation probability depends sensitively on the Higgs-curvature cou-

pling and the spacetime volume of the expanding universe. Most of the existing literature has, nonetheless, approximated the spacetime during inflation with a de Sitter spacetime. That means that the Hubble rate is treated as a constant free parameter. In this work, we consider the question in the context of actual inflationary models in which the Hubble rate is time-dependent and, once a model is chosen, the parameters are determined by cosmic microwave background (CMB) observations. The choice of the inflationary model affects the bubble nucleation probability in two ways: Because of the time-dependence of the Hubble rate, spacetime curvature is different, which affects the nucleation rate per unit spacetime volume. We compute this using the renormalization group improved effective Higgs potential with three-loop running [94, 95], pole matching as described in Ref. [96], and where crucially the effective potential is calculated on a curved background to one-loop order as given in Ref. [6]. The model choice also determines the geometry of the past lightcone, which is different from dS. We incorporate both of these effects and find the constraints on the Higgs-curvature coupling ξ arising from vacuum stability in three models of field theory inflation and in the modified gravity setting $R + R^2$ which leads to the observationally favourable model of Starobinsky inflation.

The format of this thesis is as follows. In Chapter 2, we provide an overview of the electroweak vacuum instability in the context of the Standard Model of particle physics. We focus on the Higgs effective potential, going from the simplest tree-level case in flat spacetime to the current state-of-the-art with 3-loops and one-loop curvature corrections. Afterwards, we review the necessary aspects of inflationary cosmology in Chapter 3, with a particular emphasis on departing from the slow-roll approximation, and present the inflationary models of interest. In Chapter 4, we introduce the framework for studying bubble nucleation during the inflationary epoch and describe our approach for the numerical computations. Additionally, we present our findings for the constraints on the non-minimal coupling ξ for the different inflationary models in field theory and a range of top quark masses. We also discuss the time of the nucleation event and its connection to the duration of inflation. In Chapter 5, we extend the analysis of Chapter 4 to study the Higgs vacuum metastability in Starobinsky inflation, in order to bound ξ from below more accurately. First, we present the analytic calculations for the transformation from the Jordan to the Einstein frame and illustrate the corresponding effects on a spectator scalar

field. We continue by discussing the particular case of the Standard Model in R^2 inflation, the renormalization group improvement of the effective Higgs potential and the effect of the time-dependent background. Furthermore, we establish the formalism of bubble nucleation in R^2 inflation and showcase our results regarding the lower ξ-bounds along with their dependence on the definition for the end of inflation. Finally in Chapter 6, we summarise the arguments for motivating this study and delineate its wider context, while highlighting its differences from the past literature. We also provide an overview of our results, where we underline their cosmological implications regarding the early universe and identify the next steps and objectives for future work.

1.2 Summary of results

In Chapter 4, which is based on Ref. [1], we studied the electroweak (EW) vacuum instability of the Standard Model (SM) Higgs field in the context of cosmological inflation in field theory to obtain lower bounds on the Higgs-curvature coupling. To that end, we developed a code based on F. Bezrukov's mathematica package (see Statement of originality), that deals with the renormalization group (RG) running of the SM parameters. We utilised a three-loop renormalization group improved effective Higgs potential calculated on a curved background and also took into account the time dependence of the Hubble rate both in the Higgs potential and in the geometry of our past lightcone. For the latter, we solved numerically the evolution equations, regarding the inflaton field and the conformal time in terms of e-foldings of inflation, subject to the choice of inflationary model.

We considered three one-parameter models of inflation, quadratic, quartic and Starobinsky-like power law inflation beyond the slow-roll regime. The effects of the inflationary models, entered the calculation indirectly through the calculation of the spacetime volume element $d\mathcal{V}$ that appears in the integral of the expectation value of true vacuum bubbles $\langle \mathcal{N} \rangle$. In addition, we tuned these inflationary models according to the famous CMB measurements, which resulted in degenerate results and behaviour between these otherwise very different models of inflation,

and managed to constrain the coupling $\xi \gtrsim 0.051 - 0.066$ depending on the top quark mass. We also demonstrated that vacuum decay is most likely to happen a few e-foldings before the end of inflation and it is independent of its total duration, unless it lasts for more than approximately 10^{60} e-folds. Then, in the very early universe, vacuum decay is enhanced, which acts as a possible hint against eternal inflation.

One of the inflationary potentials we investigated in Section 4.2 corresponded to Starobinsky inflation [97, 98], in which the inflaton field arises from a scalar metric degree of freedom when the action has a quadratic R^2 curvature term. It can be thought of as the minimal inflationary model because it does not require the introduction of any new fields, and it is also compatible with observations of inflationary observables [99]. However, in the presence of other scalar fields, specifically the Higgs field, it will give rise to derivative couplings between the fields, which we have not included in the formalism presented in Section 4.2. These terms have been investigated in the setting of mixed Higgs-Starobinsky inflation [100, 101], and also to study vacuum stability during reheating in Starobinsky inflation [90].

Chapter 5, which is based on Ref. [2], focuses on the minimal construction of the Standard Model in Starobinsky inflation as description of the early universe. In particular, we present the analytic calculations that show how the conformal transformation from $R + R^2$ gravity (Jordan frame) to Einstenian gravity with additions to the matter sector (Einstein frame), affects the SM action, the effective masses, and the renormalization group improvement process. These implications result from the non-trivial field redefinitions that are necessary to canonically diagonalise the Lagrangian, where additional destabilising terms manifest in the effective potential. Therefore, we derived stronger bounds on the non-minimal coupling $\xi \gtrsim 0.1$, which are however very sensitive to the last moments of inflation, compared to the field theory case. For this reason, we investigated bubble production with various endpoints for inflation and inferred that it is essential to incorporate the epoch of reheating in these studies, if we wish to improve our constraints further.

Chapter 2

The electroweak vacuum instability

2.1 Vacuum instability in flat spacetime

The SM is a renormalizable Quantum Field Theory (QFT), where the interactions between particles are related to the energy scale at which they take place. This is evident in the context of the path integral formulation of QFT and it is treated formally in the context of renormalization. Via this procedure we account for the UV (high energy) divergences of the theory we devised at lower energies (IR), and we see that our renormalized parameters are functions of the renormalization scale μ, which corresponds to the energy scale of the physics one is probing. If a renormalized coupling diverges (i.e., has a Landau pole) at energies lower than the Planck scale, then this means that our theory is not valid at those energies and thus we need to think of ways to fix it, such as beyond the Standard Model (BSM) physics. [5, 11, 14, 33, 102]

The Standard Model particle content can be written as [5]

$$\mathcal{L}_{\rm SM} = \mathcal{L}_{\rm YM} + \mathcal{L}_{\rm F} + \mathcal{L}_{\Phi} + \mathcal{L}_{GF} + \mathcal{L}_{GH}\,, \tag{2.1}$$

where the first three terms in eq. (2.1) come from the gauge fields (Yang-Mills), the fermions and the Higgs doublet Φ, respectively. The 'GF' and 'GH' correspond to the gauge fixing and

ghost Lagrangians, respectively. Here we show only the steps for the Higgs contribution, but the complete derivation can be found in Ref. [6] (see also a shortened derivation in Ref. [5]). The Higgs piece reads

$$\mathcal{L}_\Phi = (D_\mu \Phi)^\dagger (D^\mu \Phi) - m^2 \Phi^\dagger \Phi - \lambda (\Phi^\dagger \Phi)^2 \,, \tag{2.2}$$

where $m^2 < 0$ is the Higgs mass parameter and the SM covariant derivative is given by

$$D_\mu = \nabla_\mu - ig\tau^a A^a_\mu - ig' Y A_\mu; \qquad \tau^a = \sigma^a/2 \,, \tag{2.3}$$

where ∇_μ contains the covariant connection for Einsteinian gravity, g and g' are the $SU(2)$ and $U(1)$ gauge couplings, A^a_μ and A_μ the gauge fields, τ and Y the corresponding generators, and σ^a are the Pauli matrices. When expressing the Higgs field Φ as[1]

$$\Phi = \frac{1}{\sqrt{2}} \begin{pmatrix} -i(\chi_1 - i\chi_2) \\ h + (\chi_0 + i\chi_3) \end{pmatrix} , \tag{2.4}$$

where $h \in \mathbb{R}$ is a constant classical mean field and χ_0 and χ_i, $i \in \{1,2,3\}$, are quantum fluctuations with zero expectation value, the scalar part of the Lagrangian becomes

$$\mathcal{L}_{\rm SM} = -\frac{m^2}{2} h^2 - \frac{\lambda}{4} h^4 - \frac{1}{2} \chi_0 \left[\Box + m_h^2\right] \chi_0 - \frac{1}{2} \chi_i \left[\Box + m_\chi^2\right] \chi_i + \cdots \,, \tag{2.5}$$

and denote the flat space effective masses as

$$m_h^2 = m^2 + 3\lambda h^2 \,, \quad m_\chi^2 = m^2 + \lambda h^2 \,. \tag{2.6}$$

In a similar fashion, one may derive the quadratic terms for all degrees of freedom in the SM, with the rest of the flat space effective masses given by

$$m_W^2 = \frac{g^2}{4} h^2 \,, \quad m_Z^2 = \frac{g^2 + g'^2}{4} h^2 \,, \quad m_{\rm F}^2 = \frac{y_{\rm F}^2}{2} h^2 \,. \tag{2.7}$$

[1] Here we use the same notation as in Ref. [1], which differs slightly to that in Ref. [5] ($\varphi \leftrightarrow h$)

In the case of the Higgs field, its interaction with bosons increases its self-coupling $\lambda(\mu)$, whereas fermionic interactions decrease it. The size of these contributions scales with the mass of the corresponding particle. In the SM, the top quark and the Higgs boson are by far the heaviest of the fermions and bosons, respectively, and therefore, they dominate the contributions to the quartic coupling compared to the rest of the SM particle spectrum. Hence, if either one is significantly more massive than the other, then λ diverges to $\pm\infty$ accordingly. This implies that the only way for the SM to remain valid until the Planck scale would be for the two masses to be comparable with one another and the two competing contributions to cancel out. As it turns out, their experimentally measured masses at the electroweak (EW) scale [8] of

$$m_h = 125.10 \pm 0.14 \text{ GeV} \; ; \quad m_t = 172.76 \pm 0.30 \text{ GeV} \tag{2.8}$$

suggest exactly that. This realisation acts as a strong constraint on BSM theories that would disrupt the balance between the two masses by affecting λ's dependency on μ. Note that the quoted value for the mass of the top quark corresponds to the direct measurement, which has smaller uncertainty from cross-section measurements $m_t = 162.5^{+2.1}_{-1.5}$ GeV and pole from cross-section measurements $m_t = 172.4 \pm 0.7$ GeV [8]. [5]

The experimental values of m_h and m_t have another important implication. According to the calculation reviewed in Ref. [5], the Higgs self-coupling λ turns negative as it runs with the renormalization scale μ above approximately 10^{10} GeV. This is shown in figure 2.1 for the central values of the SM parameters [103], with 3σ uncertainty in the leading terms of the beta function β_λ calculated to 3 loops [6]. Therefore, there is an additional vacuum state of lower energy due to $\lambda < 0$ in the potential of the Higgs

$$V_{\mathrm{H}}(\mu, h) = \frac{m^2(\mu)}{2} h^2 + \frac{\lambda(\mu)}{4} h^4 \,. \tag{2.9}$$

Therefore, the current vacuum state of the quantum Higgs field is metastable, because there is a small but non-zero probability to quantum tunnel through the barrier.

Vacuum metastability in the Standard Model is a quantum effect, which appears at one loop

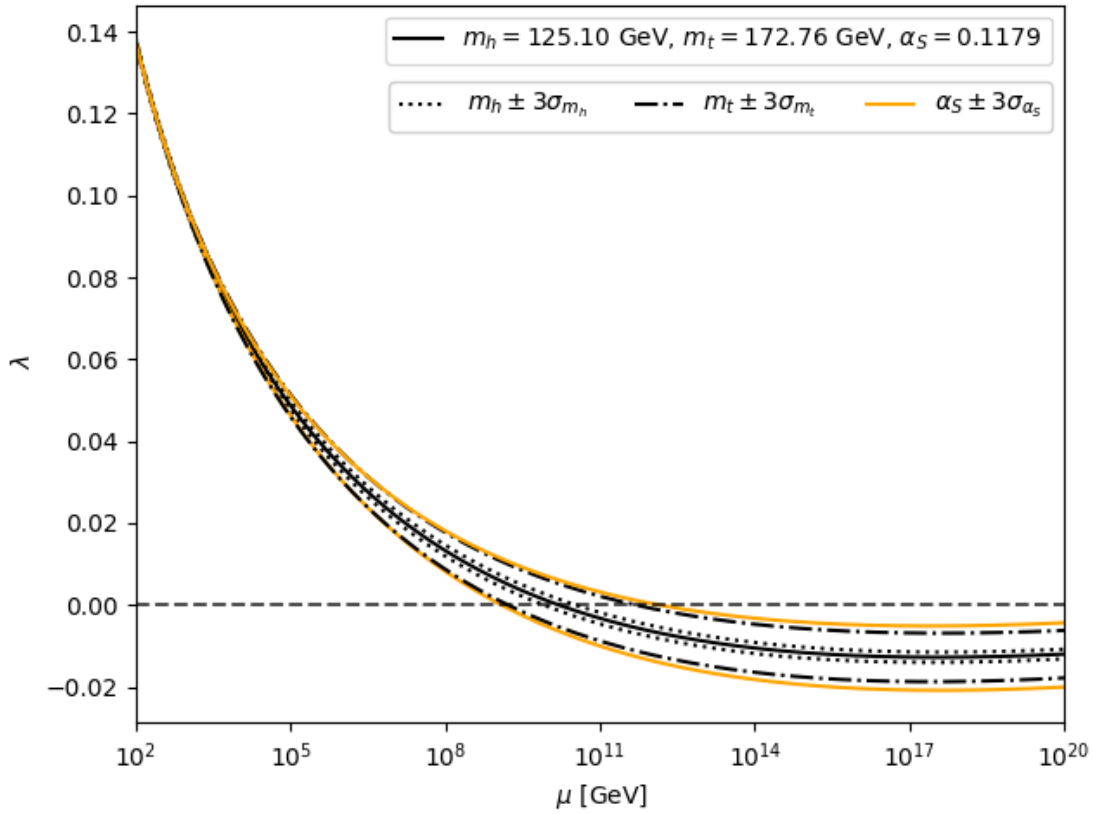

Figure 2.1: Running of the Higgs self-interaction coupling with the renormalization scale for the central values of the Higgs mass, top mass, and strong coupling with 3σ uncertainty, according to the current experimental data [8]. Figure taken from [2].

order in perturbation theory. Therefore, in order to describe it, it is essential to compute the effective Higgs potential. Although the renormalization scale μ has been an integral part of the discussion so far, our theory should not depend on it, because it is not physical but just a measure of the range of validity of the theory. The process of eliminating the μ-dependence by choosing the renormalization scale μ in an optimal and field-dependent way is called renormalization group improvement (RGI). This is a method of improving the perturbative approximation of the effective potential, which is the tree-level potential with the addition of loop corrections. In flat space and for large values of h, often a reasonable approximation for the renormalization group improved effective potential is [16]

$$V_{\mathrm{H}}(h) \approx \frac{\lambda(h)}{4} h^4 \,, \tag{2.10}$$

with the choice $\mu = h$ as the renormalization group (RG) scale for the running four-point

coupling, where we have omitted the quadratic term because it is negligible [23]. At 1-loop order, its β-function reads [6]

$$16\pi^2\beta_\lambda = 16\pi^2\mu\frac{\partial\lambda}{\partial\mu} = 24\lambda^2 - 3\lambda(g'^2 + 3g^2) + \frac{3}{4}\left(\frac{1}{2}g'^4 + g'^2g^2 + \frac{3}{2}g^4\right) + 4Y_2\lambda - 2Y_4\,, \quad (2.11)$$

where we have grouped together the terms coming from the Yukawa couplings of the up u, down d, charm c, strange s, top t, and bottom b quarks and the electron e, muon μ, and τ leptons as

$$Y_2 \equiv 3(y_u^2 + y_c^2 + y_t^2) + 3(y_d^2 + y_s^2 + y_b^2) + (y_e^2 + y_\mu^2 + y_\tau^2)\,, \quad (2.12)$$

$$Y_4 \equiv 3(y_u^4 + y_c^4 + y_t^4) + 3(y_d^4 + y_s^4 + y_b^4) + (y_e^4 + y_\mu^4 + y_\tau^4)\,, \quad (2.13)$$

but it should be solved to as high a precision as is practically feasible in order to accurately capture the running. Even though all of the SM fermions are included for completeness and because they would not increase the complexity of the numerical computations, the top quark is by far the dominant contribution to Y_4, resulting in more than 99.99996 % of its value compared to the rest of the fermions combined. The current state-of-the-art calculation [18] making use of two-loop matching conditions, three-loop RG evolution and pure QCD corrections to four-loop accuracy leads to an instability around the scale $\mu_\Lambda = 1.60 \times 10^{10}$ GeV for the central values of the m_t and m_h. However, direct loop corrections are neglected in Eq. (2.10), which may therefore be a poor approximation in some cases [5]. This can be remedied either by including the quantum corrections to 1-loop

$$\Delta V_{1-\text{loop}}(h,\mu) = \frac{1}{64\pi^2}\sum_{i=1}^{31}\left\{n_i\mathcal{M}_i^4\left[\log\left(\frac{|\mathcal{M}_i^2|}{\mu^2}\right) - d_i\right]\right\} \quad (2.14)$$

in Eq. (2.10), or by choosing explicitly the RG scale, instead of $\mu = h$, such that the quantum correction vanishes. The corresponding entries for $\mathcal{M}_i$ along with the coefficients n_i, d_i can be found in Section 5 of Ref. [6] and in Table[2] 5.1, in the flat space regime where $R = 0$.

[2]The table entries have tildes because they correspond to redefined SM fields, according to the discussion of Chapter 5. However, they look identical to the standard case and therefore their form corresponds to the usual "untilded" entries.

In general, a quantum field in a non-degenerate, double-well potential is prone to vacuum decay via quantum tunnelling, thermal excitations, or a mixture of both, as shown in Fig.2.2. We quantify the probability of decay via the decay rate Γ, which is a function of spacetime and also evidently of m_h and m_t. For an infinitely old universe, even the most infinitesimal decay rate would render it incompatible with ours. Today, our measurements indicate that we are in the metastable EW vacuum with a rate that requires more time than the age of the universe for the decay to occur [13]. This result has two important implications. Firstly, it acts as a reality check for SM extensions, which should abide by this long-lasting false vacuum. Secondly, it places constraints in our early universe theories, where a higher decay rate was favoured, as the metastable vacuum has managed to survive through its various epochs. Absolute vacuum stability is still viable within the experimental accuracy and systematic errors in our measurements, since λ can remain non-negative during its running for a sufficiently light top quark. However, the data for the central values place it well inside the metastability region within 3σ uncertainties, as shown in 2.1. [5, 33]

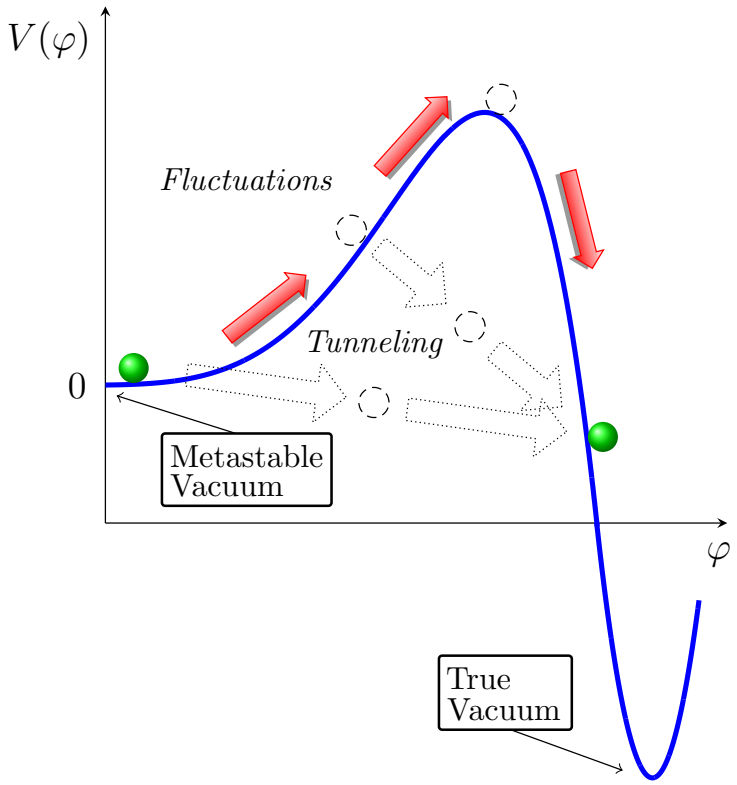

Figure 2.2: Vacuum decay of a scalar field φ for a double-well potential from a metastable vacuum to its true vacuum. Originally published in [5] (CC BY 4.0).

Vacuum decay is a local process in spacetime, where the field decays to its true vacuum and subsequently excites the surrounding field to follow. This process induces the formation of a spherically symmetric bubble of true vacuum, which expands with velocity that rapidly approaches the speed of light, see Ref. [5] and references therein, and [59, 80] for a recent discussion. The true vacuum may or may not be bounded from below, but in the context of this study this is not relevant, since we are interested in the number of bubbles that would form from the decay and not on their interiors. This is because we are focusing on the possible signatures evident in our false vacuum Universe and not on the specifics of the exotic physics inside the true vacuum bubbles, which would obviously depend on the exact form of the potential. We cannot make any definite claims about the nature of the bubble interior, but it is certain that the true vacuum universe would look very different compared to ours. At the very least, the Higgs vev would be greater resulting into heavier SM particles. However, given the high energy scales of these phenomena, for all practical purposes in the context of SM physics, we assume that spacetime collapses into a singularity inside the bubble. Such a rapidly growing singularity would be catastrophic for our false vacuum Universe, as it would devour the spacetime around it so quickly that we would not see it coming. [5, 11, 15, 16, 17, 33]

2.2 Vacuum instability in curved spacetime

There have been numerous studies of the EW metastability in flat spacetime in the past, especially before the discovery of the Higgs boson, aiming mainly at obtaining bounds on the Higgs mass and other SM parameters that were not known accurately at the time [19, 20, 21, 22, 23, 24, 25, 26, 104, 105, 106, 107]. Since then, our measurements have improved and we are placed more confidently within the metastability region of the parameter space with smaller uncertainty [5]. In addition, the present-day calculation in Minkowski space dictates a half-life for our false vacuum universe that exceeds the age of the Universe and thus there is no constraining power or further insights from studies in this regime [28, 32]. However, the persistence of the false vacuum throughout our cosmological evolution, despite the various mechanisms that could have triggered vacuum decay, motivates us to consider the implications

from the metastability of the EW vacuum in the early universe [5, 12].

In particular, we are interested in the epoch of cosmological inflation, where the universe underwent a period of accelerated expansion, before the radiation-dominated era of the Hot Big Bang model, as reviewed in chapter 3. During inflation, spacetime was highly curved, and therefore the Minkowski calculation of the vacuum decay rate is not applicable. A detailed calculation of the decay rate in a general curved spacetime would be very difficult, and therefore we approximate it locally with de Sitter, where the Ricci scalar R is constant[3]. The tunnelling process from false to true vacuum can be solved classically yielding solutions called instantons [34, 109]. The vacuum decay rate is then determined by the action of the Coleman-de Luccia instanton [35]. At sufficiently high Hubble rates $H \gtrsim 10^8$ GeV [5], it approaches the much simpler Hawking-Moss instanton [51, 108], whose action difference is given in the linear approximation limit by

$$B_{\rm HM}(R) \approx \frac{384\pi^2 \Delta V_{\rm H}}{R^2}\,, \tag{2.15}$$

where $\Delta V_{\rm H} = V_{\rm H}(h_{\rm bar}) - V_{\rm H}(h_{\rm fv})$ is the height of the potential barrier, "bar" signifies the top of the potential barrier and "fv" the false vacuum [5, 108, 110]. This is the approximation we will use throughout this study. It results in a reasonably good first approximation for the form of the decay rate as

$$\Gamma_{\rm HM}(R) \;\approx\; \left(\frac{R}{12}\right)^2 e^{-B_{\rm HM}(R)}\,, \tag{2.16}$$

where the prefactor is justified by dimensional arguments according to [5]. For light fields, $m \ll H$, this agrees with the stochastic formalism [38].

Non-zero spacetime curvature affects the effective potential of the Higgs field already at tree level, where it enters through the Higgs-curvature coupling ξ,

$$\mathcal{L}_\Phi = (D_\mu \Phi)^\dagger (D^\mu \Phi) - m^2 \Phi^\dagger \Phi - \xi R \Phi^\dagger \Phi - \lambda (\Phi^\dagger \Phi)^2\,, \tag{2.17}$$

[3]With a dynamical metric, as done in Ref. [108], the result is slightly different because of gravitational backreaction, but because the relevant energy scales are well below the Planck scale, the difference is minimal.

and appears also in the scalar part of the Lagrangian 2.5,

$$\mathcal{L}_{\rm SM} = -\frac{m^2}{2}h^2 - \frac{\lambda}{4}h^4 - \frac{1}{2}\chi_0\left[\Box + m_h^2 + \xi R\right]\chi_0 - \frac{1}{2}\chi_i\left[\Box + m_\chi^2 + \xi R\right]\chi_i + \cdots . \tag{2.18}$$

In this approximation, the Lagrangian for the Higgs field in curved spacetime is given by

$$\mathcal{L} = \frac{M_P^2}{2}R + \frac{1}{2}g^{\mu\nu}(\partial_\mu h)(\partial_\nu h) - V_{\rm H}(h,R)\,, \tag{2.19}$$

where the first term is the standard Einstein-Hilbert term that corresponds to General Relativity, with $M_P = (8\pi G)^{-1/2} \approx 2.435 \times 10^{18}$ GeV being the reduced Planck mass (and G the gravitational constant), the second is the kinetic term, and the third is the curvature-dependent Higgs potential. In the high-field approximation, the effective potential at tree level is

$$V_{\rm H}(h,R) = \frac{\xi}{2}Rh^2 + V_{\rm H}(h)\,, \tag{2.20}$$

where the first term couples the Higgs field to the Ricci scalar R and acts as a mass term [111], and $V_{\rm H}(h)$ corresponds to a general flat spacetime potential from QFT, e.g. $\lambda h^4/4$. The strength of the Higgs-curvature interaction is measured by the non-minimal coupling ξ, which is also a running SM parameter. Whenever we refer to numerical values of ξ, we mean the $\overline{\rm MS}$[4] renormalized parameter at scale $\mu = m_t$, which we denote by $\xi_{\rm EW}$ for clarity. Considering the negative quartic self-interaction from (2.10) in curved spacetime, we recover the metastable potential albeit with a stabilising term due to the positive sign of the Higgs curvature coupling, $0 \leq \xi_{\rm EW} \leq \frac{1}{6}$, where the conformal value $\xi = 1/6$ denotes the limit of applicability of the Hawking-Moss bounce solution [108]. As we will see, the relevant values for our analysis are low, $\xi \ll 1/6$, and therefore the Higgs field remains light and we should be able to trust Eq. (2.16).

To understand the effect from the non-minimal term, let us consider constant ξ and $\lambda < 0$, which is a reasonable approximation for the Higgs potential at field values $h \gg 10^{10}$ GeV. We

[4]In the *Modified Minimal Subtraction* renormalization scheme $\overline{\rm MS}$, we absorb the divergences from the perturbative result beyond leading order, the omnipresent universal constant, and the infinities from the Feynman diagrams into the counterterms [112].

may then write

$$V_{\rm H}(h,R) = \frac{\xi}{2}Rh^2 - \frac{|\lambda|}{4}h^4\,, \tag{2.21}$$

where the value of the potential at the top of the barrier is

$$V_{\rm H}(h_{\rm bar},R) = \frac{\xi^2 R^2}{4|\lambda|}\,, \tag{2.22}$$

resulting in the action difference via Eq. (2.15),

$$B_{\rm HM} \approx \frac{96\pi^2\xi^2}{|\lambda|}\,. \tag{2.23}$$

In this approximation, the action is independent of spacetime curvature and it is an increasing function of ξ. This suggests that a sufficiently high value of ξ will prevent vacuum decay during inflation and that, conversely, vacuum stability provides a lower bound on its value.

2.3 One-loop curvature corrections

Beyond tree level, spacetime curvature also enters the effective potential through loop corrections. The effective potential for the full SM on a curved background to 1-loop order was calculated in Ref. [6],

$$V_{\rm H}(h,\mu,R) = \frac{m^2}{2}h^2 + \frac{\xi}{2}Rh^2 + \frac{\lambda}{4}h^4 + V_\Lambda - \kappa R + \alpha_1 R^2 + \alpha_2 R_{\mu\nu}R^{\mu\nu} + \alpha_3 R_{\mu\nu\delta\eta}R^{\mu\nu\delta\eta} + \Delta V_{\rm loops}\,, \tag{2.24}$$

where we have suppressed all the implicit renormalisation scale dependence. In dS space,

$$R^2 = 144H^4\,, \quad R_{\mu\nu}R^{\mu\nu} = 36H^4\,, \quad R_{\mu\nu\delta\eta}R^{\mu\nu\delta\eta} = 24H^4\,, \tag{2.25}$$

and thus we can group together the pure curvature terms, resulting into

$$V_{\rm H}(h,\mu,R)=\frac{m^2}{2}h^2+\frac{\xi}{2}Rh^2+\frac{\lambda}{4}h^4+V_\Lambda-\kappa R+\frac{\alpha}{144}R^2+\Delta V_{\rm loops}\,, \tag{2.26}$$

where $\alpha\equiv 144\alpha_1+36\alpha_2+24\alpha_3$ [113]. We identify the additional terms in (2.26) as the cosmological constant correction (4th), the correction to the EH term (5th), the radiatively generated curvature correction (6th), and the loop correction (7th) summing over the SM degrees of freedom

$$\Delta V_{\rm loops}(h,\mu,R)=\frac{1}{64\pi^2}\sum_{i=1}^{31}\left\{n_i\mathcal{M}_i^4\left[\log\left(\frac{|\mathcal{M}_i^2|}{\mu^2}\right)-d_i\right]+\frac{n_i'}{144}R^2\log\left(\frac{|\mathcal{M}_i^2|}{\mu^2}\right)\right\}. \tag{2.27}$$

The various terms can be found in Section 5 of Ref. [6] and in Table 5.1, where we note that we are using $\zeta_i=1$ for the gauge fixings in this study.[5] In the early universe, spacetime is significantly curved so that the SM effective masses receive curvature corrections which, in addition to flat space contributions as in Eq. (2.6), we denote with $\mathcal{M}_i$. It is necessary to highlight that we will be neglecting the mass term for the Higgs, because it is negligible compared to the high scales of the Hubble rates in the inflationary models of this study. Setting $m=0$ implies that we can also disregard all dimensionful couplings of our theory, having a renormalization group flow fixed point at $m=0, V_\Lambda=0, \kappa=0$ [113]. Hence, we end up with

$$V_{\rm H}(h,\mu,R)=\frac{\xi(\mu)}{2}Rh^2+\frac{\lambda(\mu)}{4}h^4+\frac{\alpha(\mu)}{144}R^2+\Delta V_{\rm loops}(h,\mu,R)\,. \tag{2.28}$$

In this result, μ is an arbitrary dimensionful constant. The convergence of the perturbative expansion depends on the chosen value, and in general there is no single choice that gives good convergence for all values of h. It is expected that the choice $\mu=h$ will not be a sufficiently good approximation, since it misses the contribution from curvature which is expected to be the dominant one [5]. A simple scale choice that incorporates the effect of curvature with the form $\mu^2=ah^2+bR$, where a and b are constants, was suggested in [48] and has since widely been used in the literature, see e.g. Ref. [39, 54, 75, 114]. With that choice, the direct loop

[5] Regarding the value of the potential at the top of the barrier, we have checked that there is no significant difference between using gauge fixings $\zeta_i=0$ and $\zeta_i=1$ in the loop contribution.

corrections do not cancel exactly and should therefore be included in the effective potential for full accuracy. On the other hand, it avoids the issue that in some cases Eq. (2.29) does not have a continuous solution covering all field values [6]. In our approach, this issue does not arise and therefore, we use the exact scale choice from (2.29). We eliminate the dependence on the scale μ in Eq. (2.28) via RGI, where we fix $\mu = \mu_*(h, R)$ choosing μ_* in such a way as to result in null loop corrections to the potential [115], i.e. as a solution of

$$\Delta V_{\text{loops}}(h, \mu_*, R) = 0. \tag{2.29}$$

This leads to the RGI effective potential with no direct loop contribution

$$V_{\text{H}}^{\text{RGI}}(h, R) = \frac{\xi(\mu_*(h,R))}{2} R h^2 + \frac{\lambda(\mu_*(h,R))}{4} h^4 + \frac{\alpha(\mu_*(h,R))}{144} R^2 \,, \tag{2.30}$$

which implies a well-defined loop expansion[6]. Because the renormalization scale μ_* is approximately equal to the largest of h and R, it follows that when $R \lesssim 10^{20}$ GeV^2, the RGI effective potential (2.30) has a barrier at $h \sim 10^{10}$ GeV that makes the vacuum metastable. On the other hand, when $R \gtrsim 10^{20}$ GeV^2 the barrier disappears altogether, making the vacuum unstable unless it is stabilised by a sufficiently large and positive non-minimal coupling term ξ [6, 60].

The beta functions for the non-gravitational couplings of the SM are well known [96], in some cases up to three loops. Therefore, we provide here explicitly only the 1-loop couplings associ-

[6] In Eq. (2.30) h refers to the field renormalized at a scale μ_*, which is related to the field h_0 renormalized at some fixed physical scale μ_0 via the anomalous dimension γ as

$$h = h_0 \exp\Big(- \int_0^{\log\left(\frac{\mu_*}{\mu_0}\right)} \gamma(t) \mathrm{d}t \Big). \tag{2.31}$$

Arguably, here the relevant physical quantity is the field renormalized at the electroweak scale instead of h. The Hawking-Moss instanton however is independent of this subtlety, since it does not affect the barrier height, and for simplicity we may then perform our calculation in terms of h.

ated with curvature, the non-minimal coupling and α, as a reference [48],

$$16\pi^2 \frac{d\xi}{d\ln\mu} = 16\pi^2\beta_\xi = \left(\xi - \frac{1}{6}\right)\left(12\lambda + 6y_t^2 - \frac{3}{2}g'^2 - \frac{9}{2}g^2\right), \tag{2.32}$$

$$16\pi^2 \frac{d\alpha}{d\ln\mu} = 16\pi^2\beta_\alpha = 288\xi^2 - 96\xi - \frac{1751}{30}. \tag{2.33}$$

Assuming given electroweak-scale values $\xi_{\rm EW} = \xi(\mu_{\rm EW})$ and $\alpha_{\rm EW} = \alpha(\mu_{\rm EW})$, these equations determine their scale-dependence, which enters Eq. (2.30). The differential equations above are sensitive to the initial condition of ξ but not of α, since the right-hand sides on Eq. (2.32) and Eq. (2.33) are independent of α. Although we will not be limiting our analysis to strict dS space, it is still a good approximation to make use of the dS form of (2.26): the higher order curvature invariants R^2, $R_{\mu\nu}R^{\mu\nu}$ and $R_{\mu\nu\alpha\beta}R^{\mu\nu\alpha\beta}$ couple to the Higgs only via loop corrections [6] and reduce to a single term at the dS limit, indicating that our approximation captures the leading contribution, which we have checked is already a small contribution.

Solving Eq. (2.29) and calculating the barrier height of (2.30) require us to incorporate the entire SM particle spectrum. Firstly, we need to obtain the running of λ, y_t, g', g according to the corresponding beta functions and the accompanying pole-matching [95]. Using the publicly available Mathematica code[7], which is based on Refs.[94, 95, 96], we calculate the three-loop Minkowski space β-functions of the running couplings in (2.30). The code takes as input parameters the fine structure constant α_S, and the masses of the Higgs boson m_h and the top quark m_t renormalized at the electroweak scale, and then calculates the running of the SM parameters. After this, we obtain $\xi(\mu)$ and $\alpha(\mu)$ by solving the remaining beta functions (2.32) and (2.33). Finally, we can calculate the maximum of Eq.(2.30), after having obtained μ_* via Eq.(2.29), including the masses of all the SM particles. The overview of all the input values along with the evaluated SM couplings is shown in Table 2.1.

In Fig.2.3, we illustrate the effect of the running of $\xi(\mu)$, according to Eq. (2.32), for a range of boundary conditions at $\mu_{\rm EW}$. We can see that below $\xi_{\rm EW} \approx 0.03$, ξ switches sign as it runs, resulting in a negative term in the potential (2.30). This can potentially destabilise the Higgs vacuum, depending on how the other couplings in Eq. (2.30) run. It is also evident that even a

[7] By Fedor Bezrukov, available at http://www.inr.ac.ru/∼fedor/SM/.

	Masses [GeV]		
Higgs	$m_h = 125.10$		$v = 246.22$
Quarks	$m_t = 172.76$	$m_s = 93 \times 10^{-3}$	$m_u = 2.16 \times 10^{-3}$
	$m_b = 4.18$	$m_c = 1.27$	$m_d = 4.67 \times 10^{-3}$
Leptons	$m_\tau = 1.77686$	$m_\mu = 105.6583745 \times 10^{-3}$	$m_e = 510.9989461 \times 10^{-6}$
	Dimensionless couplings		
gauge couplings	$\alpha_S = 0.1179$	$\boldsymbol{g = 0.648382}$	$\boldsymbol{g' = 0.358729}$
couplings		$\boldsymbol{\lambda = 0.126249}$	$\boldsymbol{y_t = 0.934843}$

Table 2.1: Experimental values of the SM particle masses and couplings [8] at $\mu_{\rm EW}$ used for the RGI of the Higgs potential. The couplings in bold are calculated by the SM code[7] subject to the input of m_h, m_t and a_S. Originally published in [1] (CC BY 4.0).

2σ deviation in m_t does not affect the running of ξ significantly, at the energy scales of interest. In particular, it seems to produce a more observable effect beyond scales of order 10^{18} GeV and for smaller values of $\xi_{\rm EW}$. We have not considered any deviation in m_h and kept it fixed at its central value throughout our calculations, because of its smaller experimental uncertainty compared to the top quark's.

Finally, it is worth clarifying the loop order of this calculation. Even though our discussion in this chapter has been with reference to 1-loop effects, and we have included 1-loop curvature corrections to the Higgs potential 2.26, the β-functions of the non-gravitational SM couplings have been calculated to 3-loops. Evidently, this is an inconsistency in our approach, where different couplings and terms have been computed to different loop orders. However, performing the entirety of the calculation to 3-loops would be extremely complicated and beyond the scope of this work. In addition, incorporating the β-functions to 3-loops results only in a numerical error in the choice of μ_*, since it is the solution of $\Delta V_{1-\rm loop} = 0$ and not $\Delta V_{3-\rm loop} = 0$. Thus, the potential errors from this inconsistency will be well below the accuracy of the numerical results, when taking into account other factors such as our cosmological history.

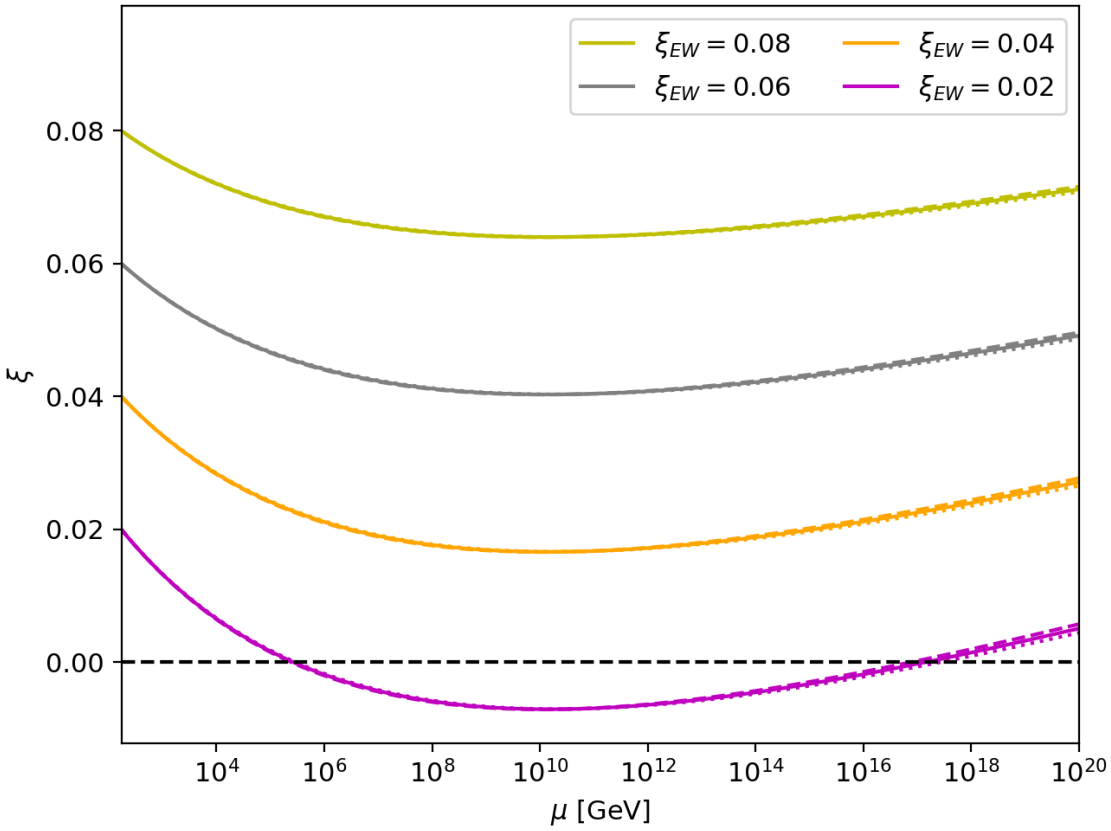

Figure 2.3: The running of non-minimal coupling $\xi(\mu)$ with various boundary conditions ξ_{EW} for top quark mass $m_t = (172.76 \pm 0.6)$ GeV. The solid lines correspond to the central value of m_t for each case, while the dashed and the dotted ones correspond to $m_t \pm 2\sigma$, respectively. Originally published in [1] (CC BY 4.0).

Chapter 3

Cosmological inflation

3.1 Theoretical framework

The theory of cosmological inflation postulates that there was a period of accelerated expansion of the universe before the Hot Big Bang (HBB) and the epochs of cosmological evolution that followed. Initially, inflation was proposed as a possible solution to the standard cosmological problems of the time, namely the horizon, flatness and relic abundance problems, but without interfering with the successes of the HBB model [97, 116]. Inflation's major success however, lies in its ability to explain the origin of large scale structure observed today in galaxy surveys, via the amplification of the initial quantum fluctuations, while recovering the HBB era through the process of reheating. Even though there are still issues that need to be addressed for the theory to be fully consistent, there exists a plethora of significant evidence in support of inflation coming from the measurements of the cosmic microwave background (CMB) anisotropies, whereas the future cosmological surveys promise to provide more insight. Refer to [117, 118, 119, 120, 121] for a more in depth discussion of inflation.

The theoretical framework to study inflation is field theory in the Lagrangian formalism, where the minimisation of the action gives the field's equation of motion (EoM), which describes its dynamics. In the simplest case, inflation is driven by a single scalar field, known as the inflaton

ϕ, subject to a potential $V_{\rm I}(\phi)$,

$$S = \int d^4x\sqrt{-g}\left(\frac{1}{2}\partial_\mu\phi\partial^\mu\phi - V_{\rm I}(\phi)\right), \tag{3.1}$$

where $g = det(g_{\mu\nu})$ [117] and $g_{\mu\nu}$ is the spacetime metric. A homogeneous and isotropic universe, that is expanding, is described by the Friedmann-Robertson-Walker (FRW) metric

$$ds^2 = a(\eta)^2\left(d\eta^2 - d\vec{x}^2\right), \tag{3.2}$$

where η is the conformal time, defined as

$$d\eta = \frac{dt}{a(t)} = \frac{da}{a^2H(a)}, \tag{3.3}$$

and $a(t)$ is the scale factor that quantifies the expansion of the universe [117, 121]. The stress-energy tensor for a perfect cosmological fluid can be written in terms of its energy density ρ and pressure p, which are related through the fluid's equation of state $p = w\rho$, as

$$T_{\mu\nu} = (\rho + p)\, u_\mu u_\nu - p g_{\mu\nu}, \tag{3.4}$$

where u^μ is the local 4-velocity of the fluid normalised at $u^2 = 1$. In general, the stress-energy tensor of a Lagrangian $\mathcal{L}$ is given by varying $g_{\mu\nu}$ in its action [117]

$$T_{\mu\nu} = 2\frac{\partial\mathcal{L}}{\partial g^{\mu\nu}} - g_{\mu\nu}\mathcal{L}\,. \tag{3.5}$$

In the case of the action (3.1) in FRW, $w = -1$ and the stress-energy tensor reads

$$T_{\mu\nu} = \partial_\mu\phi\partial_\nu\phi - g_{\mu\nu}\left(\frac{1}{2}\left(\partial\phi\right)^2 - V_{\rm I}(\phi)\right). \tag{3.6}$$

Thus, we can express the energy density and pressure of the universe in terms of the inflaton field and its potential, as

$$\rho = \frac{1}{2}\dot{\phi}^2 + V_{\rm I}(\phi)\,, \quad p = \frac{1}{2}\dot{\phi}^2 - V_{\rm I}(\phi)\,, \tag{3.7}$$

where the dot denotes differentiation with respect to time t.

Solving the Einstein field equations in FRW results famously in the Friedmann equation [117], which gives the rate of the expansion in terms of the energy density ρ,

$$H^2 = \left(\frac{\dot{a}}{a}\right)^2 = \frac{\rho}{3M_P^2}\,, \tag{3.8}$$

where H is the Hubble rate, and the acceleration equation

$$\frac{\ddot{a}}{a} = -\frac{\rho + 3p}{6M_P^2}\,, \tag{3.9}$$

respectively. The curvature scalar R in FRW is expressed in terms of Eqs. (3.8) and (3.9) as

$$R = 6\left(\frac{\dot{a}^2}{a^2} + \frac{\ddot{a}}{a}\right)\,. \tag{3.10}$$

The corresponding EoM gives the evolution of the inflaton,

$$\ddot{\phi} + 3H\dot{\phi} + V_{\rm I}'(\phi) = 0\,, \tag{3.11}$$

where the prime denotes differentiation with respect to the field. Apart from the second term, which is known as the "Hubble drag", because of the friction experienced by the field from the universe's expansion, the above EoM corresponds to the standard Klein-Gordon equation for a spatially homogeneous field in flat spacetime. [117]

In order to obtain the accelerated expansion of the universe during inflation, the energy density has to be approximately constant. Therefore, the inflaton field has to be "slowly rolling" towards the minimum of its potential, i.e. its potential $V(\phi)$ has to be a very slowly varying function of ϕ, so that it is approximately flat [117, 119]. The necessary conditions for the

inflaton potential to exhibit this behaviour are called the slow-roll conditions and are famously given by

$$\epsilon = \frac{M_{\rm P}^2}{2}\left(\frac{V_{\rm I}'(\phi)}{V_{\rm I}(\phi)}\right)^2 \ll 1\,, \quad |\eta| = \left|M_P^2\frac{V_{\rm I}''(\phi)}{V_{\rm I}(\phi)}\right| \ll 1\,, \tag{3.12}$$

which should be satisfied for a sufficiently long time so that the inflationary solution to approach the attractor [117]. They lead to the desired attractor solutions when they also imply $\dot{\phi}^2 \ll V$ and $\ddot{\phi} \ll H\phi$, and then we can write (3.8) and (3.11) in the slow-roll regime as

$$H^2 \approx \frac{V_{\rm I}(\phi)}{3M_P^2}\,, \tag{3.13}$$

$$3H\dot{\phi} \approx -V_{\rm I}'(\phi)\,. \tag{3.14}$$

Within the slow-roll approximation, for a given model of inflation with potential $V(\phi)$, the power spectrum of curvature perturbations has the expression [117]

$$\mathcal{P}_\zeta(k) = \frac{V_{\rm I}(\phi)}{24\pi^2 M_{\rm P}^4\epsilon}\,. \tag{3.15}$$

Current CMB observations set the amplitude of the power spectrum to be $\mathcal{P}_\zeta(k_*) \approx 2.1\times10^{-9}$ at the pivot scale $k_* = 0.05{\rm Mpc}^{-1}$ [99], where the scale factor is chosen to be $a_0 = 1$ today. When precisely the comoving scale corresponding to the pivot scale exits the horizon, during inflation, depends on the cosmic history and in particular, on the reheating epoch. However, when determining the input parameters for inflationary models, we will assume that this takes place 60 e-folds before the end of inflation, which in turn we take to occur when the potential slow-roll parameter is explicitly violated, $\epsilon = 1$. All inflationary models studied in this work involve just one parameter and therefore, they are completely determined once the correct amplitude has been fixed [117].

We quantify the amount of inflation that has occurred via the number of e-foldings N,

$$N(t) = \ln\left(\frac{a_{\rm inf}}{a(t)}\right)\,, \tag{3.16}$$

where $a_{\rm inf}$ is the scale factor at the end of inflation[1]. The ratio of the comoving Hubble lengths today and at the end of inflation is given by

$$e^{\tilde{N}} = \frac{a_{\rm inf} H_{\rm inf}}{a_0 H_0} \,, \tag{3.17}$$

where $\tilde{N} \approx 60 + \ln\left(\frac{V_{\rm I}^{1/4}(\phi_{\rm inf})}{10^{16}\ {\rm GeV}}\right)$ according to the approximation used in [5]. This allow us to express the boundary conditions on the scale factor in terms of the inflationary model, as

$$a_{\rm inf} = \left(\frac{a_0 H_0 e^{60}}{10^{16}\ {\rm GeV}}\right) \frac{V_{\rm I}^{1/4}(\phi_{\rm inf})}{H_{\rm inf}} \,, \tag{3.18}$$

$$a_{\rm start} = a_{\rm inf} \exp(-N_{\rm start}) \,, \tag{3.19}$$

where the Hubble constant today is $H_0 \approx 1.5 \times 10^{-42}$ GeV, according to cosmological measurements [117, 122, 123]. As we mentioned previously, we adopt the convention that inflation ends at $N_{\rm inf} = 0$, when the slow roll condition is explicitly violated[2] at $\epsilon \to 1$. In order to comply with observations, inflation has to last for at least ~ 60 e-folds [117], but we cannot place any upper constraint to its duration from experimental measurements. We can only claim that there is a maximum value of $N(t_{\rm start})$, where the energy density has reached the Planck scale $\rho \approx M_p^4$, beyond which we would need a theory of quantum gravity [117].

The post-inflationary energy/matter density of the universe is given by

$$\rho(a) = \rho_{\rm tot}^0 \left(\Omega_\Lambda + \Omega_{\rm mat}\left(\frac{a_0}{a}\right)^3 + \Omega_{\rm rad}\left(\frac{a_0}{a}\right)^4\right) \,, \tag{3.20}$$

where the Ω's denote density ratios with respect to the total density $\rho_{\rm tot}^0 = \rho_{\rm crit} = \frac{3H_0^2}{8\pi G} = 3M_P^2 H_0^2$, with $\Omega_\Lambda = 0.69$ corresponding to the cosmological constant/dark energy component, $\Omega_{\rm mat} = 0.31$ to the matter component (baryonic and dark), and $\Omega_{\rm rad} = 5.4 \times 10^{-5}$ to radiation (photons γ and neutrinos ν). According to [5], integrating the post-inflationary comoving radius

[1]Note that with this definition, higher N corresponds to earlier time during inflation.

[2]This is not entirely true for Chapter 5, where we are explicitly investigating the effect from different definitions for the end of inflation.

of the past lightcone $r(\eta) = \eta_0 - \eta$, in terms of the scale factor via (3.8) and (3.20), results to

$$\eta_0 - \eta_{\rm inf} = \int_0^{a_0} \frac{da}{a^2 H(a)} = \int_0^{a_0} \frac{da}{a^2 \sqrt{\frac{\rho(a)}{3M_P^2}}} = \frac{1}{H_0} \int_0^{a_0} \frac{da}{\sqrt{\Omega_\Lambda a^4 + \Omega_{\rm mat} a_0^3 a + \Omega_{\rm rad} a_0^4}} = \frac{3.21}{a_0 H_0} \,. \tag{3.21}$$

This corresponds to the total conformal time between the end of inflation and today, and it is a useful result that we will use in Section 4.1. On the other hand, we can express the comoving radius during inflation in terms of e-foldings as

$$\eta_{\rm inf} - \eta(N) = \int_N^0 dN' \left(\frac{-e^{N'}}{a_{\rm inf} H(N')} \right) . \tag{3.22}$$

The total comoving radius of our past lightcone is the addition of (3.21) and (3.22), $r(\eta) = \eta_0 - \eta = (\eta_0 - \eta_{\rm inf}) + (\eta_{\rm inf} - \eta(N))$, for a variable start point of inflation N.

The slow-roll approximations are valid away from the minimum of the inflationary potential, where we can use (3.13) and (3.14) to infer the dependence of the field and the Hubble rate on t, a, η or any other quantity that is expressed in terms of these, see for example the explicit calculations for quadratic inflation in Appendix A. Within the slow-roll regime, the acceleration equation (3.9) reduces to H^2 to leading order and therefore, we can write the Ricci scalar as

$$R = 12H^2. \tag{3.23}$$

However, it is necessary to go beyond the slow-roll approximation, if we wish to have a better understanding of the inflationary dynamics towards the end of inflation. This is necessary for the purposes of this study in particular, as we will see in Chapters 4 and 5, because vacuum decay is expected to take place close to the end of inflation. Since we will be integrating over the duration of inflation, the spacetime volume $\mathcal{V}$, that multiplies the decay rate Γ (i.e. the probability for decay per spacetime volume), has reached its largest value during the inflationary period. Therefore, vacuum decay is expected to be more prominent when the product $\Gamma\mathcal{V}$ is large. See Chapter 4 for a more thorough explanation.

3.2 Departure from the slow-roll regime

3.2.1 Leading order corrections

The first point where we can include slow-roll corrections to leading order is the Ricci scalar (3.10), through the the $\ddot{a}/a$ term. We calculate this term explicitly by differentiating (3.8) with respect to t, while making use of the slow-roll approximations (3.13) and (3.14), and noting that the primes denote differentiation with respect to ϕ,

$$2\frac{\dot{a}}{a}\frac{\ddot{a}a-\dot{a}^2}{a^2}=\frac{\dot{V}_{\rm I}}{3M_P^2}\;\Rightarrow\;2H\left(\frac{\ddot{a}}{a}-H^2\right)=\frac{\dot{\phi}V_{\rm I}'}{3M_P^2}\;\Rightarrow$$

$$\frac{\ddot{a}}{a}=H^2+\frac{\dot{\phi}V_{\rm I}'}{6M_P^2H}=H^2-\frac{V_{\rm I}'^2}{18M_P^2H^2}=H^2-\frac{V_{\rm I}'^2}{6V_{\rm I}}\left(\frac{3M_P^2}{V_{\rm I}}\right)H^2=H^2\left[1-\frac{M_P^2}{2}\left(\frac{V_{\rm I}'}{V_{\rm I}}\right)^2\right]\;\Rightarrow$$

$$\frac{\ddot{a}}{a}=H^2\left(1-\epsilon\right)\,, \tag{3.24}$$

which results in the following correction to the curvature scalar,

$$R=6\left[H^2+H^2(1-\epsilon)\right]=12H^2\left(1-\frac{\epsilon}{2}\right). \tag{3.25}$$

For a further departure from slow-roll, we can solve the full Friedmann equation (3.8), instead of its slow-roll version (3.13), to obtain a leading order correction to H^2. We are still disregarding the higher order correction in the inflaton's EoM (3.11), and use (3.14) instead. This combination results in a quadratic equation in H^2,

$$\frac{27M_P^4}{V_{\rm I}^2}H^4-\frac{9M_P^2}{V_{\rm I}}H^2-\epsilon=0\,, \tag{3.26}$$

which accepts only positive solutions. Its solution to leading order in slow-roll is

$$H^2 \approx \frac{V_{\rm I}}{3M_P^2}\left(1+\frac{\epsilon}{3}\right) . \tag{3.27}$$

Understandably, there is a corresponding correction to R, again via the acceleration term. By inserting Eq. (3.14) in (3.8) and (3.9), we can write them respectively, as

$$H^2 = \frac{V_{\rm I}}{3M_P^2} + \frac{1}{2}\frac{\left(V_{\rm I}'\right)^2}{27M_P^2H^2} , \tag{3.28}$$

$$\frac{\ddot{a}}{a} = \frac{V_{\rm I}-\dot{\phi}^2}{3M_P^2} = \frac{V_{\rm I}}{3M_P^2} - \frac{\left(V_{\rm I}'\right)^2}{27M_P^2H^2} . \tag{3.29}$$

We can eliminate the $V_{\rm I}/3M_P^2$ term, and therefore, we obtain the following expression to second order in slow-roll,

$$\frac{\ddot{a}}{a} = H^2\left[1-\frac{\left(V_{\rm I}'\right)^2}{18M_P^2H^4}\right] \approx H^2\left[1-\epsilon+\frac{2}{3}\epsilon^2\right] . \tag{3.30}$$

Hence, combining (3.27) and (3.30) in Eq. (3.10), allow us to express the Ricci scalar to second order in slow-roll, as

$$R \approx 12H^2\left[1-\frac{\epsilon}{2}+\frac{\epsilon^2}{3}\right] . \tag{3.31}$$

These results illustrate the considerations that allow us to go beyond the slow-roll regime, with leading order corrections to the Hubble rate and Ricci scalar, which invalidate the dS relation (3.23) between them when $\epsilon \sim 1$. Thus far, our procedure has been to gradually drop the slow-roll approximations in the Friedmann equation and the inflaton's EoM, in order to deviate increasingly from slow-roll. Hence, we are naturally led to the point where we should drop all slow-roll approximations, if we want to depart completely from dS.

3.2.2 Beyond slow-roll

We can write completely general expressions, without assuming any slow-roll conditions, if we consider the general Friedmann equation (3.8) and inflaton's EoM (3.11). It is convenient to continue this discussion in terms of e-foldings of inflation, for the purposes of our analysis in Chapters 4 and 5. Therefore, by using the change of variables

$$\frac{d\phi}{dt} = -\frac{d\phi}{dN} H \,, \tag{3.32}$$

we can express the Hubble rate from the Friedmann equation in terms of N, as

$$H^2 = \frac{V_{\rm I}}{3M_P^2} \left[1 - \frac{1}{6M_P^2} \left(\frac{d\phi}{dN} \right)^2 \right]^{-1} \,. \tag{3.33}$$

Now, we have to find an expression for $d\phi/dN$, but unfortunately the calculations will be more involved, since we will not be disregarding any higher derivative terms. To utilise the EoM (3.11), we must first calculate

$$\ddot{\phi} = -H \frac{d}{dN} \left(-H \frac{d\phi}{dN} \right) = H \left(H \frac{d^2\phi}{dN^2} + \frac{d\phi}{dN} \frac{dH}{dN} \right) \,, \tag{3.34}$$

where we need to account for the last term by differentiating (3.33)

$$\begin{aligned} 2H \frac{dH}{dN} &= \left[\frac{1}{3M_P^2} \frac{dV_{\rm I}}{dN} \left(1 - \frac{1}{6M_P^2} \left(\frac{d\phi}{dN} \right)^2 \right) - \frac{V_{\rm I}}{3M_P^2} \left(\frac{-2}{6M_P^2} \frac{d\phi}{dN} \frac{d^2\phi}{dN^2} \right) \right] \left[1 - \frac{1}{6M_P^2} \left(\frac{d\phi}{dN} \right)^2 \right]^{-2} \\ &= \frac{\frac{V_{\rm I}'}{3M_P^2} \frac{d\phi}{dN}}{1 - \frac{1}{6M_P^2} \left(\frac{d\phi}{dN} \right)^2} + \frac{\frac{V_{\rm I}}{9M_P^4} \frac{d\phi}{dN} \frac{d^2\phi}{dN^2}}{\left[1 - \frac{1}{6M_P^2} \left(\frac{d\phi}{dN} \right)^2 \right]^2} = \frac{d\phi}{dN} \left[H^2 \frac{V_{\rm I}'}{V_{\rm I}} + \frac{H^4}{V_{\rm I}} \frac{d^2\phi}{dN^2} \right] \,, \end{aligned} \tag{3.35}$$

which results into

$$\frac{dH}{dN} = \frac{H}{2V_{\rm I}} \frac{d\phi}{dN} \left(V_{\rm I}' + H^2 \frac{d^2\phi}{dN^2} \right) \,. \tag{3.36}$$

Inserting (3.34) and (3.36) in the EoM (3.11) leads to

$$3H^2\frac{d\phi}{dN} = \left(V_{\mathrm{I}}' + H^2\frac{d^2\phi}{dN^2}\right)\left(1 + \frac{H^2}{2V_{\mathrm{I}}}\left(\frac{d\phi}{dN}\right)^2\right), \tag{3.37}$$

which simplifies to

$$\frac{d\phi}{dN} = M_P^2\frac{V_{\mathrm{I}}'}{V_{\mathrm{I}}} + \frac{\frac{1}{3}\frac{d^2\phi}{dN^2}}{1 - \frac{1}{6M_P^2}\left(\frac{d\phi}{dN}\right)^2}, \tag{3.38}$$

after eliminating the H^2 terms. Similarly as before, we can express the acceleration equation in terms of derivatives of the inflaton field, without making use of slow-roll approximations, as

$$\frac{\ddot{a}}{a} = H^2 - \frac{\dot{\phi}^2}{2M_P^2} = H^2\left[1 - \frac{1}{2M_P^2}\left(\frac{d\phi}{dN}\right)^2\right], \tag{3.39}$$

leading to a general expression for the Ricci scalar

$$R = 12H^2\left[1 - \frac{1}{4M_P^2}\left(\frac{d\phi}{dN}\right)^2\right]. \tag{3.40}$$

One necessary remark regarding (3.38) consists of how $\phi(N)$ is calculated according to (3.38). Since this is a second order differential equation, we need to provide two boundary conditions, one for the field ϕ and one for its derivative $\frac{d\phi}{dN}$. We choose the boundary point to be far away from the end of inflation, e.g. at $N = 10^6$ e-foldings, where the slow-roll approximations are valid and spacetime approximates dS. It is not necessary to consider such early times for the slow-roll approximations to hold, but we are interested in Section 4.2.3 to look further back in time. In this case, we can use the slow-roll solution from (3.14) for $\phi(N)$, with the boundary condition $\phi_{\mathrm{inf}} = \phi(0)|_{\epsilon=1}$, in order to obtain the values of the inflaton at sufficiently early times, which are then used as the boundary values when solving Eq. (3.38) explicitly. Thus, we can study how the inflaton behaves near the end of inflation, without making any assumptions about that period.

However, there is some freedom when defining the inflationary endpoint and it is not just the evolution of the attractor solution to $N = 0$, which originates deep inside the slow-roll regime.

Therefore, the actual behaviour of the inflaton is given by $\phi(N + N_{\rm shift})$, where we determine $N_{\rm shift}$ according to the definition for the end of inflation. There are two conditions that seem natural as definitions for the inflationary finale, either that acceleration (3.39) halts $\ddot{a}|_{N_{\rm shift}} = 0$, which corresponds to $\epsilon = 1$, or that the curvature (3.40) vanishes $R(N_{\rm shift}) = 0$. The inflaton field oscillates at these late times, before decaying into the SM particles during reheating [117]. Therefore, we should be cautious and choose the first numerical solution for each $N_{\rm shift}$, before the oscillatory behaviour takes over. This discussion continues in Section 4.2.

3.3 Inflationary models

3.3.1 Monomial potentials

So far in this chapter, we have been discussing inflation and performing various calculations, in a general manner without specifying a particular inflationary model. This has been a beneficial approach to obtain model-independent results, but as we will see in Chapter 4, we have to choose an inflationary potential $V_{\rm I}(\phi)$, in order to compute the spacetime volume of the integral which gives the expectation value of true vacuum bubbles $\langle \mathcal{N} \rangle$ (see Eq. (4.4) later). First, for the sake of simplicity, we will be considering two single-field, monomial models, which allow to perform almost the entirety of the necessary calculations analytically.

In *quadratic inflation*, the inflaton potential has only a quadratic term

$$V_{\rm quad}(\phi) = \frac{1}{2} m_\phi^2 \phi^2 \,, \tag{3.41}$$

where $m_\phi = 1.4 \times 10^{13}$ GeV acts as the inflaton mass, which is fixed from CMB measurements and Eq. (3.15). Away from the end of inflation, we can solve Eqs. (3.38), (3.33), and (3.22) analytically (see Appendix A for a detailed calculation) to leading order in slow-roll to obtain the expressions for the inflaton, the Hubble rate, and the comoving radius of the past lightcone, respectively, as

$$\phi(N) = \left(M_P\sqrt{2}\right)\sqrt{1+2N} \approx 2M_P\sqrt{N}\,, \tag{3.42}$$

$$H(N) = (m_\phi/\sqrt{3})\sqrt{1+2N} \approx m_\phi\sqrt{\frac{2N}{3}}\,, \tag{3.43}$$

$$\begin{aligned}\eta_0 - \eta(N) &= \frac{3.21}{a_0 H_0} + \frac{1}{a_{\rm inf} m_\phi}\sqrt{\frac{3\pi}{2e}}\left[\mathrm{erfi}\left(\sqrt{N+\frac{1}{2}}\right) - \mathrm{erfi}\left(\sqrt{\frac{1}{2}}\right)\right] \\ &\approx \sqrt{\frac{3}{2}}\frac{1}{m_\phi a_{\rm inf}}\frac{e^N}{\sqrt{N}}\,,\end{aligned} \tag{3.44}$$

where erfi is the imaginary error function and the approximate forms are valid at $N \gg 1$. The first term in Eq. (3.44) is the post inflationary contribution 3.21, which is subdominant when $N \gtrsim 60$. The requirement that the Hubble rate does not reach trans-Planckian values, $H(N_{\rm start}) \ll M_P$, places an upper bound to the duration of inflation at

$$N_{\rm start} \ll \frac{3}{2}\left(\frac{M_P}{m_\phi}\right)^2 \approx 10^{10}\,. \tag{3.45}$$

Another common monomial model is *quartic inflation* with the characteristic potential

$$V_{\rm quar}(\phi) = \frac{1}{4}\lambda_\phi\phi^4\,, \tag{3.46}$$

where $\lambda_\phi = 1.4\times10^{-13}$ comes from Eq. (3.15) and is not to be confused with the running self-coupling $\lambda(\mu)$ of the Higgs. In a similar manner as before, we obtain the slow-roll solution for the inflaton, Hubble rate and conformal time, as

$$\phi(N) = \left(2M_P\sqrt{2}\right)\sqrt{1+N} \approx 2M_P\sqrt{2N}\,, \tag{3.47}$$

$$H(N) = 4M_P\sqrt{\frac{\lambda_\phi}{3}}(1+N) \approx \left(4M_P\sqrt{\frac{\lambda_\phi}{3}}\right)N\,, \tag{3.48}$$

$$\eta_0 - \eta(N) = \frac{3.21}{a_0 H_0} + \frac{\sqrt{3/\lambda_\phi}}{4M_P a_{\rm inf} e}\left[\mathrm{Ei}(N+1) - \mathrm{Ei}(1)\right] \approx \left(\frac{\sqrt{3/\lambda_\phi}}{4M_P a_{\rm inf}}\right)\frac{e^N}{N}\,, \tag{3.49}$$

where Ei is the exponential integral function. The approximate forms are valid for large N and the constraint arising from trans-Planckian Hubble rates is

$$N_{\text{start}} \ll \frac{1}{4}\sqrt{\frac{3}{\lambda_\phi}} \approx 10^6 \,. \tag{3.50}$$

The quadratic and quartic models do not provide a very good fit to data, regarding the spectral index of scalar perturbations and the scalar-to-tensor ratio [99]. Nevertheless, we are including them in our study because of their simplicity and to act as a comparison to a more realistic model. An example of such a model would be Starobinsky inflation [97, 124], which complies with observational data very well and can draw connections between different inflationary models [117, 125].

3.3.2 Starobinsky inflation

Given the inevitable generation of gravitational terms beyond the simple EH term $\propto R$

$$S = \int d^4x\sqrt{-g}\frac{M_P^2}{2}R \,, \tag{3.51}$$

due to, for example, the gravitational induced renormalization group running of the conformal anomaly (see Ref. [6, 126]), Starobinsky modified gravity by including such terms already at the tree-level action [124]. This formalism provided simple extensions to General Relativity, a subset of which is grouped together as $f(R)$ theories. Their action is given by a different function of the Ricci scalar,

$$S = \int d^4x\sqrt{-g_J}\frac{M_P^2}{2}f(R_J) \,, \tag{3.52}$$

where J denotes the original metric $g_{J\mu\nu}$ in which the theory is defined, and is known as the Jordan frame. As we will see, it is possible to carry out a change of variables to a different metric $g_{\mu\nu}$ in which the action has the Einstein-Hilbert form (3.51), and which is known as the Einstein frame. The simplest and most studied $f(R)$ model emerges by adding a quadratic term to the curvature scalar of the EH action [127],

$$f(R_J) = R_J + \frac{R_J^2}{6M^2M_P^2}\,, \tag{3.53}$$

where M is a small dimensionless parameter. This is equivalent to the inflationary model proposed by Starobinsky in 1980 [97, 98], which is known as *Starobinsky* or R^2 *inflation*.

In order to describe the physics of this theory, it is convenient to carry out the transformation to Einstein frame. To do that, we first remove the quadratic term R_J^2 by introducing an auxiliary scalaron field s, and thus the action reads

$$S = \int d^4x\sqrt{-g_J}\left[\frac{M_P^2}{2}\left(1+\frac{s}{3M^2M_P^2}\right)R_J - \frac{s^2}{12M^2}\right]. \tag{3.54}$$

Its classical equation of motion is $s = R_J$ on-shell and thus, it reproduces the action from (3.52) and (3.53). Now, the action can be turned into the EH form (3.51) through a conformal transformation

$$g_{\mu\nu} = \Omega^2 g_{J\mu\nu}\,, \tag{3.55}$$

$$\Omega^2 = 1 + \frac{s}{3M^2M_P^2}\,. \tag{3.56}$$

Because the conformal transformation is not a coordinate transformation, it affects the Ricci scalar. As a result, the Ricci scalars R_J and R corresponding to the Jordan and Einstein frames, respectively, are related by the equation

$$R_J = \Omega^2\left[R - 3\Box\ln\Omega^2 + \frac{3}{2}g^{\mu\nu}\partial_\mu\ln\Omega^2\partial_\nu\ln\Omega^2\right], \tag{3.57}$$

which gives rise to new terms in the action.

To write this in a more convenient form, we carry out a new change of variables and introduce a scalar field ϕ, which we refer to as the inflaton, through

$$\Omega^2 = 1 + \frac{s}{3M^2M_P^2} = e^{\sqrt{\frac{2}{3}}\frac{\phi}{M_P}} . \tag{3.58}$$

In terms of ϕ, the relation between the two Ricci scalars (3.57) becomes

$$R_J = \Omega^2 \left[R - \frac{\sqrt{6}}{M_P}\Box\phi + \frac{1}{M_P^2} g^{\mu\nu}\partial_\mu\phi\partial_\nu\phi \right] . \tag{3.59}$$

The essence of the conformal transformation is that it corresponds to a field redefinition, which maps an nonstandard gravitational theory (the Jordan frame) to GR with additions in the matter sector (the Einstein frame). In this case, we have $R + R^2$ gravity $\rightarrow$ GR + inflaton field [117]. Therefore, in the Einstein frame, the action (3.57) is written in terms of ϕ as

$$S = \int d^4x\sqrt{-g}\left[\frac{M_P^2}{2}R + \frac{1}{2}\partial_\mu\phi\partial^\mu\phi - V_{\rm S}(\phi) \right] , \tag{3.60}$$

where we have omitted the $\Box\phi$ term because it is a total derivative, and we have obtained the potential of *Starobinsky inflation*

$$V_{\rm S}(\phi) = \frac{3M^2M_P^4}{4}\left(1 - e^{-\sqrt{\frac{2}{3}}\frac{\phi}{M_P}} \right)^2 . \tag{3.61}$$

In conclusion, we saw that the modified gravity theory defined by Eq. (3.53) can be equivalently viewed as Einsteinian gravity with an additional scalar field ϕ with potential $V_{\rm S}(\phi)$. When $\phi \gtrsim M_P$, the potential satisfies the slow-roll conditions and the scalar field is slowly rolling in its potential, giving rise to inflation. Because it does not require an introduction of any additional fields by hand, only a small and well-justified modification of the gravitational action, it can be viewed as the minimal model of inflation. It is also in great agreement with observational constraints [99], thus making it one of the most promising models to describe the inflationary epoch. The value of the single free parameter M can be determined from the observed amplitude of the CMB temperature anisotropies to be $M = 1.1 \times 10^{-5}$ [99, 117].

For plateau models, such as the Starobinsky-type potential in Eq. (3.61), the energy density quickly approaches a constant for large $N_{\rm start}$, and thus remains strictly sub-Planckian. Therefore, it does not give rise to an upper limit on the total number of e-foldings. The slow-roll solution of Eqs. (3.38), (3.33) and (3.22) is

$$\phi(N) = M_P\sqrt{\frac{3}{2}}\left[\ln F - F - \frac{4}{3}N - W_{-1}\left[-e^{\ln F - F - \frac{4N}{3}}\right]\right] \approx M_P\sqrt{\frac{3}{2}}\ln N\,, \tag{3.62}$$

$$H(N) = \frac{MM_P}{2}\left[1 - \frac{1}{F}e^{\left(F\sqrt{\frac{2}{3}}+\frac{4N}{3}+W_{-1}\left[-e^{\ln F - F - \frac{4N}{3}}\right]\right)}\right] \approx \frac{MM_P}{2}\,, \tag{3.63}$$

$$\eta_0 - \eta(N) \approx \frac{3.21}{a_0 H_0} + \frac{2\left(e^N - 1\right)}{a_{\rm inf} MM_P} \approx \frac{2e^N}{a_{\rm inf} MM_P}\,, \tag{3.64}$$

where we have defined $F = 1 + 2/\sqrt{3}$ and W_{-1} is the -1 branch of the Lambert function [128].

Chapter 4

Vacuum decay constraints from inflation

4.1 Bubble nucleation during inflation

The observation that our Universe is still in the metastable phase implies that no bubble nucleation event took place in our cosmological history. Denoting the probability that there were $\mathcal{N}$ bubble nucleation events in our past lightcone by $\mathcal{P}(\mathcal{N})$, we require $\mathcal{P}(0) \approx 1$, because otherwise our existence would be highly unlikely. Since we are interested in cases where bubble nucleation is extremely unlikely, we can assume that this probability distribution follows Poisson statistics and thus, we can relate it to the expectation number of true-vacuum bubbles $\langle \mathcal{N} \rangle$ through

$$\mathcal{P}(0) = e^{-\langle \mathcal{N} \rangle} \,. \tag{4.1}$$

The condition for vacuum stability can therefore be expressed as $\langle \mathcal{N} \rangle \lesssim 1$. This is convenient because if we know the cosmological evolution of our Universe and can compute the nucleation

rate per spacetime volume $\Gamma(x)$ as a function of spacetime position x, then

$$\langle \mathcal{N} \rangle = \int_{\text{past}} d^4x \sqrt{-g} \Gamma(x) \,, \tag{4.2}$$

where the subscript "past" indicates that the integral is taken over the past lightcone, and the decay rate Γ depends on the shape of the Higgs potential during our cosmological history [5].

In this study, we focus on the contribution from the period of inflation, which we denote by $\langle \mathcal{N} \rangle_{\text{inf}}$. Because the integrand in Eq. (4.2) is positive, the contribution from the rest of the cosmological history is positive, and therefore $\langle \mathcal{N} \rangle \geq \langle \mathcal{N} \rangle_{\text{inf}}$. This means that if any inflationary scenario gives $\langle \mathcal{N} \rangle_{\text{inf}} > 1$, it is ruled out. The expected number of bubbles nucleated between the start of inflation η_{start} and the end of inflation η_{inf} is therefore given by [5]

$$\langle \mathcal{N} \rangle_{\text{inf}} = \frac{4\pi}{3} \int_{\eta_{\text{start}}}^{\eta_{\text{inf}}} d\eta a(\eta)^4 (\eta_0 - \eta)^3 \Gamma(a(\eta)) \,. \tag{4.3}$$

Instead of conformal time η, it is convenient to express this as an integral over the number of e-foldings of inflation N,

$$\langle \mathcal{N} \rangle_{\text{inf}} = \int_{N_{\text{end}}}^{N_{\text{start}}} dN \frac{4\pi}{3H(N)} \left(\frac{a_{\text{inf}} \left[\eta_0 - \eta \left(N \right) \right]}{e^N} \right)^3 \Gamma(N) \,, \tag{4.4}$$

where a_{inf} is given by (3.18), and we use Eq. (2.16) to approximate the decay rate in the time-dependent inflationary spacetime, by replacing the inflaton-dependent quantities, such as the Ricci scalar (3.40), by their time-dependent values

$$\Gamma(N) \approx \Gamma_{\text{HM}} \left(R(N) \right) . \tag{4.5}$$

For future reference, it is instructive to note that the integrand in Eq. (4.4), which we will denote by $\gamma(N)$, is a product of a geometric factor

$$\frac{d\mathcal{V}}{dN} = \frac{4\pi}{3H(N)} \left(\frac{a_{\text{inf}} \left[\eta_0 - \eta \left(N \right) \right]}{e^N} \right)^3 , \tag{4.6}$$

and a dynamical factor $\Gamma(N)$, i.e.

$$\gamma(N) \equiv \frac{d\langle \mathcal{N} \rangle}{dN} = \frac{d\mathcal{V}}{dN}\Gamma(N). \tag{4.7}$$

The dynamical factor depends on the spacetime geometry only through the Ricci scalar and it is given by Eq. (2.16), whereas the geometric factor depends on the inflationary model.

For a general single-field inflationary model, the spacetime geometry is determined by the Friedmann and field equations. By solving these, one can obtain $\phi(N), H(N)$ and $\eta(N)$ and hence calculate the integral (4.4) for a given a bubble nucleation rate $\Gamma(N)$. In practice, for the numerical evaluation of (4.4), it is convenient to express it as a system of coupled differential equations, using N as the time variable,

$$\frac{d\langle \mathcal{N} \rangle}{dN} = \gamma(N) = \frac{4\pi}{3}\left[a_{\rm inf}\left(\frac{3.21e^{-N}}{a_0 H_0} - \tilde{\eta}(N)\right)\right]^3 \frac{\Gamma(N)}{H(N)}\,, \tag{4.8}$$

$$\frac{d\tilde{\eta}}{dN} = -\tilde{\eta}(N) - \frac{1}{a_{\rm inf} H(N)}\,, \tag{4.9}$$

$$\frac{d^2\phi}{dN^2} = \frac{V_{\rm I}(\phi)}{M_P^2 H^2}\left(\frac{d\phi}{dN} - M_P^2 \frac{V_{\rm I}'(\phi)}{V_{\rm I}(\phi)}\right)\,, \tag{4.10}$$

where $\tilde{\eta} = e^{-N}\eta$. The Hubble rate $H(N)$ is given by Eq.(3.33), and we use the Ricci scalar (3.40) for the nucleation rate $\Gamma(N)$ according to Eq. (2.16). The time dependence in $H(N)$ and $R(N)$ enters through the solution of (3.38). Note that all the expressions and quoted equations above do not assume the slow-roll approximations, and therefore remain valid as we are approaching the inflationary finale.

The choice of the limits of integration in Eq. (4.4), $N_{\rm start}$ and $N_{\rm end}$, is a compromise between stronger and more reliable bounds. Specifically, they have to be chosen in such a way that the approximation (4.5) for the decay rate $\Gamma(N)$ is valid throughout. This is only the case when spacetime can be well approximated by de Sitter. Deviation from dS can be characterised by the adiabaticity parameter $\dot{H}/H^2$, which would be equal to zero in dS. One can therefore expect

Eq. (4.5) to be valid when

$$\left|\frac{\dot{H}}{H^2}\right| \ll 1\,. \tag{4.11}$$

As $N \to \infty$, $\dot{H}/H^2 \to 0$ monotonically from below. Therefore, the further back in time we go, the better the de Sitter approximation (4.5) becomes. This means that Eq. (4.11) does not constrain the upper limit $N_{\rm start}$, and we could even consistently choose $N_{\rm start} = \infty$. On the other hand, empirically we have only evidence for roughly 60 e-foldings of inflation, somewhat dependent on the post-inflationary evolution [117]. Conversely, the further forward we go in time, the more $\dot{H}/H^2$ deviates from zero. Defining $N_{\rm end} = 0$ where $R = 0$ in (3.40) implies that $\dot{H}/H^2 = -2$. In the case when $\ddot{a}/a = 0$ in (3.39), which is often defined to be the end of inflation, it corresponds to $N_{\rm end} \approx 0.19$ and $\dot{H}/H^2 = -1$. Therefore, in order to ensure that the condition (4.11) is satisfied, $N_{\rm end}$ needs to be sufficiently large, $N_{\rm end} \gtrsim O(1)$. We will parameterise the choice of $N_{\rm end}$ by the corresponding value of the adiabaticity parameter $\dot{H}/H^2$, which lies in the range

$$-2 \leq \frac{\dot{H}}{H^2} < 0\,. \tag{4.12}$$

4.2 Vacuum decay in field theory inflation

In this section, we present the cosmological implications from the metastability of the electroweak vacuum during inflation. These computations were performed in field theory, where there were no portals between the inflaton and the Higgs, but the two fields were completely decoupled. This resulted in two parallel calculations, one regarding the barrier height of the RGI effective Higgs potential $V_{\rm H}^{\rm RGI}$, and one for the relevant cosmological quantities, namely the Hubble rate H and the comoving radius $\eta_0 - \eta$, for each inflationary model. For the latter, we solve the system of (4.8)-(4.10) numerically using Mathematica, starting from determining the boundary conditions for Eq. (4.10) using its slow-roll solution at sufficiently early times. To be precise, we fix the boundary values of $\phi(N)$ and $\phi'(N)$ at $N = 10^6$ e-foldings before the

end of inflation, and then integrate the equations down towards lower N, until the field reaches the point $\phi_{\rm inf}$ where inflation ends. In this way, we derive lower bounds on the non-minimal coupling ξ in section 4.2.1, while investigating also the time of predominant bubble nucleation in 4.2.2 and its dependence on the total duration of inflation in 4.2.3.

In this section, we consider the monomial inflationary models of Section 3.3.1 and a Starobinsky-like power-law model with the potential given by (3.61). This potential does not include cross-couplings between the Higgs and the inflaton, which in the Starobinsky model in Chapter 5, they are introduced when the initial Lagrangian is parameterised in terms of an additional R^2-term [100, 101]. Therefore, in Chapter 4, we will not be considering what is strictly defined as Starobinsky inflation, but rather a toy model version of it. However, we will refer to it as *Starobinsky inflation* throughout the remainder of this chapter for the sake of brevity. It is also important to highlight that all the following computations assume that inflation lasts for 60 e-folds, and its end $N(\phi_{\rm inf}) = 0$ is set at the point where the expansion of the universe no longer accelerates,

$$\left.\frac{\ddot{a}}{a}\right|_{\phi=\phi_{\rm inf}} = H^2 \left[1 - \frac{1}{2M_P^2}\left(\frac{d\phi}{dN}\right)^2\right]\Bigg|_{\phi=\phi_{\rm inf}} = 0\,. \tag{4.13}$$

In this calculation, we use the Higgs effective potential (2.30), which is approximated with three-loop renormalization group improvement and supplemented with one-loop curvature corrections, according to Section 2.3. In Fig. 4.1, we see how the corresponding Hawking-Moss action difference $B_{\rm HM}$ (2.15) scales with the Ricci scalar/Hubble rate for different values of the non-minimal coupling, and for a mass range of 2σ for the top quark. The choice of the depicted $\xi_{\rm EW}$ values is motivated by the bounds obtained in Section 4.2, as the ones of interest, which also parallel the corresponding ones in Fig. 2.3. The three arrows denote the last 60 e-folds of each inflationary model, where their dashed tails extend to earlier times. Hence, the relevant range of the $B_{\rm HM}$ values, for this study, is the one coinciding with the arrow of each model. We observe that as m_t increases, the bounce action becomes less sensitive to the curvature. At high R, the action becomes approximately constant, in line with the analytic approximation (2.23).

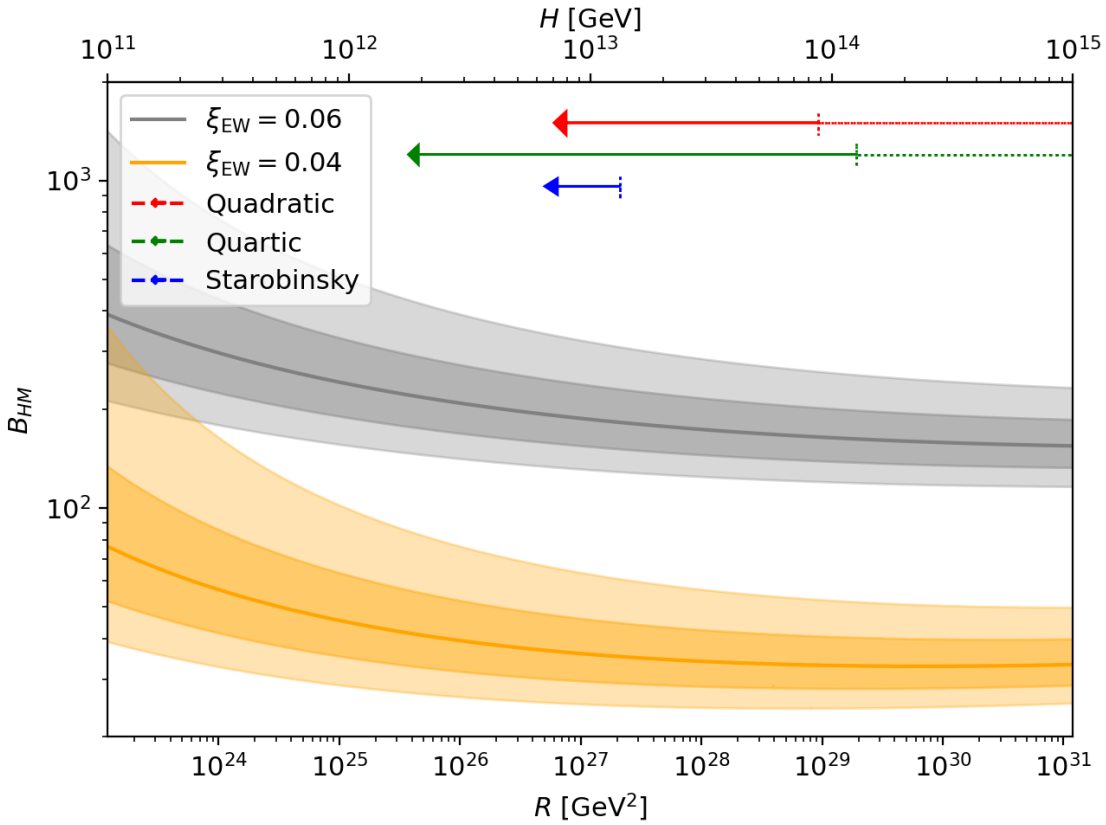

Figure 4.1: Evolution of the Hawking-Moss bounce action with spacetime curvature in the dS approximation (3.23), for sample value of the non-minimal coupling. The shaded areas denote 1σ and 2σ deviation from the central value of m_t, where a heavier top quark decreases the value of $B_{\rm HM}$ and vice versa. The solid red, blue and green arrows denote the last 60 e-foldings of inflation in quadratic, Starobinsky and quartic inflation respectively, whereas the dashed ones extend beyond that. Originally published in [1] (CC BY 4.0).

4.2.1 Bounds on ξ

Assuming a particular inflationary model, and given the values of the top quark mass and other SM parameters, one can obtain a lower bound on the Higgs-curvature coupling ξ, by solving Eqs. (4.8)–(4.10) and requiring that $\langle \mathcal{N} \rangle_{\rm inf} \leq 1$. The precise bound will depend on the duration of inflation, which we discuss in Section 4.2.3 in more detail. Because in Eq. (4.8), $\gamma(N) > 0$, the longer inflation lasts, the stricter the bound on ξ. In Fig. 4.2, we show these lower bounds calculated for different values of m_t, in the three inflationary models of Section 3.3.1, based on the minimal assumption that inflation lasts for $N = 60$ e-foldings. We can see that all three inflationary models lead to very similar bounds, which indicates that, at least to some extent, they can be considered to be model-independent.

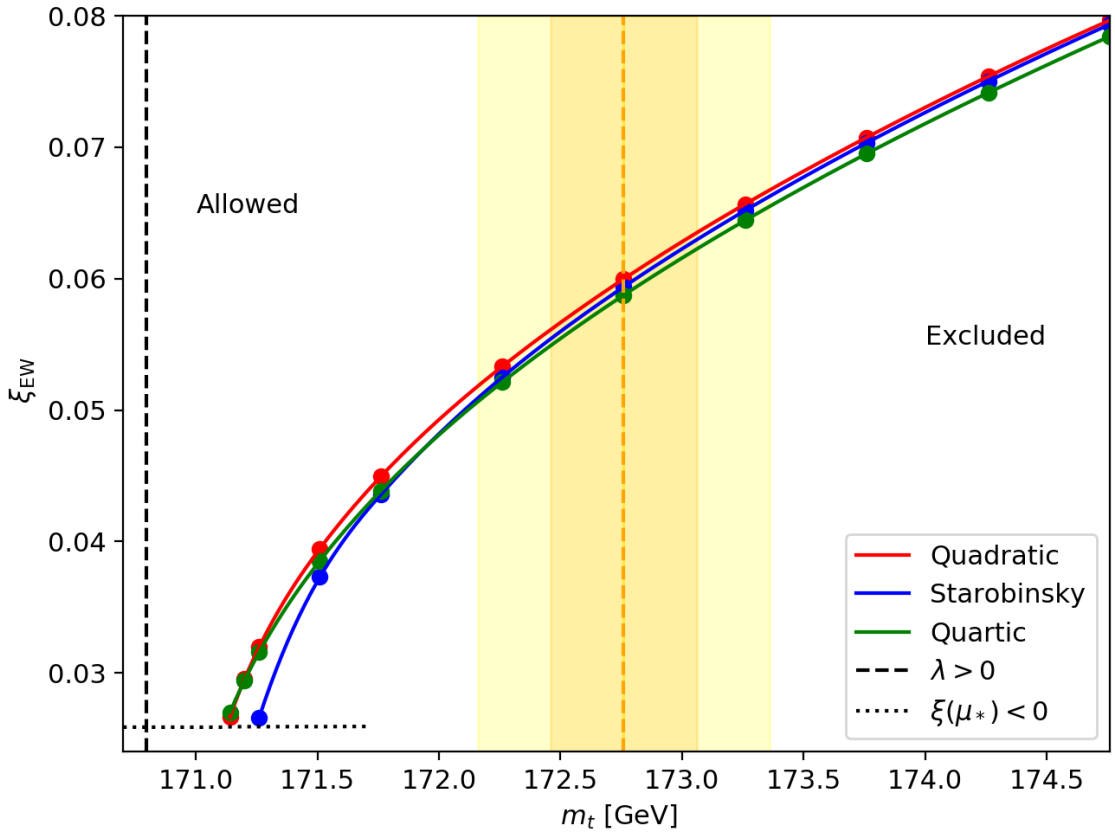

Figure 4.2: Constraints on the value of the curvature coupling ξ at $\mu_{\rm EW}$, by imposing $\langle \mathcal{N} \rangle_{\rm inf}(60) \approx 1$ at the bound, with a varying top quark mass and different inflationary models. The vertical dashed black line signifies the threshold below which, the Higgs self-coupling remains positive as it runs, and thus there is no formation of a second minimum in the Higgs potential. The vertical dashed orange line lies at the central value $m_t = (172.76 \pm 0.30)$ GeV, where the shaded areas denote the corresponding $\pm\sigma$ and $\pm 2\sigma$ variances [8]. The horizontal dotted black line shows the lowest $\xi_{\rm EW}$ value below which, $\xi(\mu_*)$ turns negative as it runs. Originally published in [1] (CC BY 4.0).

On the other hand, the bound depends quite significantly on the mass of the top quark. If it is sufficiently low, as indicated by the vertical black dashed line, the bound disappears completely because the electroweak vacuum becomes the true minimum. However, already at $m_t \approx 171.2$ GeV, the instability requires negative ξ at the relevant scale μ_*, as indicated by the horizontal dotted line. With a negative $\xi(\mu_*)$, the Higgs field gets displaced from its electroweak value during inflation. This changes its dynamics so much that we cannot use the same estimate (4.8) for the expected number of bubbles, and more work is required to determine the actual constraints. Therefore we terminate the curves at that line.

Finally, for completeness, we state explicitly the ξ-bounds for $m_t \pm 2\sigma$ in each model,

$$\text{Quadratic}: \ \xi_{\rm EW} \geq 0.060^{+0.007}_{-0.008}\,, \tag{4.14}$$

$$\text{Quartic}: \ \xi_{\rm EW} \geq 0.059^{+0.007}_{-0.008}\,, \tag{4.15}$$

$$\text{Starobinsky}: \ \xi_{\rm EW} \geq 0.059^{+0.007}_{-0.009}\,, \tag{4.16}$$

where the numerical errors in the $\xi_{\rm EW}$'s, for a fixed m_t, are approximately $< 1\%$ of their values.

4.2.2 Bubble nucleation time

In addition to the overall constraint on ξ, it is instructive to calculate the time during inflation at which bubbles are most likely to nucleate. This is important for two reasons. First, if bubbles were predominantly nucleated very close to the end of inflation, for example during the last e-folding, it would suggest that the constraints in Fig. 4.2 may not be reliable. This is because Eq. (2.16) is calculated in dS spacetime, and near the end of inflation spacetime geometry deviates increasingly from dS. Secondly, if bubble formation was most likely to happen early on during inflation, before the last 60 e-foldings, then the bounds in Fig. 4.2 would depend significantly on the early stages of inflation, which we have not accounted for.

In Fig. 4.3, we show the probability of bubble nucleation per e-folding $\gamma(N)$ for the three inflationary models. In each case, m_t has been assumed to have its experimental value, and $\xi_{\rm EW}$ is fixed to the value that gives $\langle \mathcal{N} \rangle_{\rm inf} = 1$. We can see that in all three cases, the function has a clear localised peak. This means that there is a definite, fairly well-defined time during inflation, when the vacuum decay is most likely to happen. In quadratic and quartic models, this peak is a few e-foldings before the end of inflation, which means that the constraints on ξ should be reliable, and even in Starobinsky inflation it is more than one e-folding before the end. Also note that a lighter top quark "pushes" the peak to earlier times, while a heavier one towards the end of inflation.

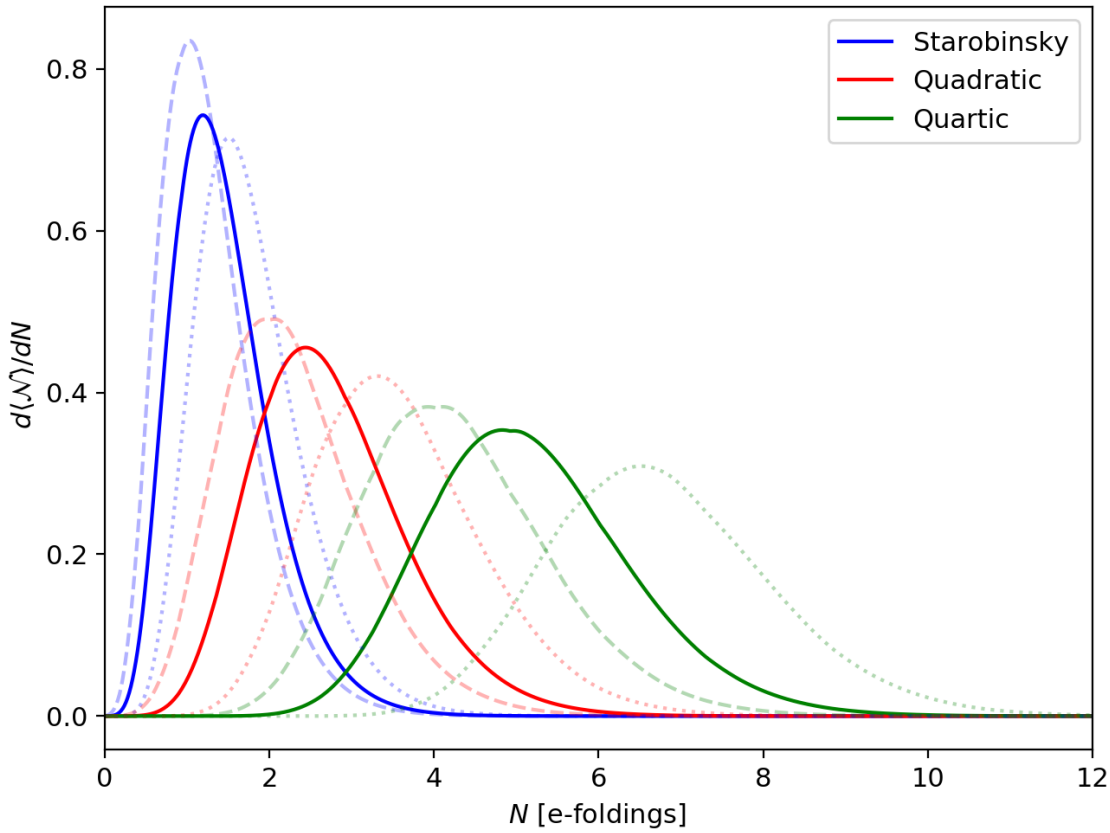

Figure 4.3: The integrands of (4.4) for the expectation value of the number of bubbles $\langle\mathcal{N}\rangle_{\rm inf}$, for three inflationary models, with $\xi_{\rm EW}$ chosen such that $\langle\mathcal{N}\rangle_{\rm inf}(60) = 1$ in each case. This means that $\xi_{\rm EW}^{\rm Star} = 0.05938$, $\xi_{\rm EW}^{\rm Quad} = 0.05998$, and $\xi_{\rm EW}^{\rm Quar} = 0.05875$ for Starobinsky, quadratic, and quartic inflation, respectively. The solid lines correspond to the central value of m_t, whereas the dashed and dotted lines to a deviation of ± 0.5 GeV, respectively. The scales of the Hubble rate, at which the bubbles are predominantly produced, are $H_{\rm Star} = 9.96 \times 10^{12}$ GeV, $H_{\rm Quad} = 1.83 \times 10^{13}$ GeV, and $H_{\rm Quar} = 1.16 \times 10^{13}$ GeV. Originally published in [1] (CC BY 4.0).

The reason for this localised peak can be seen in Fig. 4.4. As pointed out in Eq. (4.7), the overall probability $\gamma(N)$ consists of two factors, a dynamical and a geometric one. Due to the expansion of space, the geometric factor decreases exponentially as a function of N. The dynamical factor $\Gamma(N)$ increases, but not exponentially. Thus, the product $\gamma(N)$ has a maximum.

4.2.3 Significance of the total duration of inflation

As discussed in the previous section, and is also evident from Fig. 4.3, bubble nucleation is strongly dominated by the dynamics close to the end of inflation. This implies that bounds from vacuum stability are relatively insensitive to the total duration of inflation, as long as it is larger than around ten e-folds. However, in principle inflation can last for many orders of

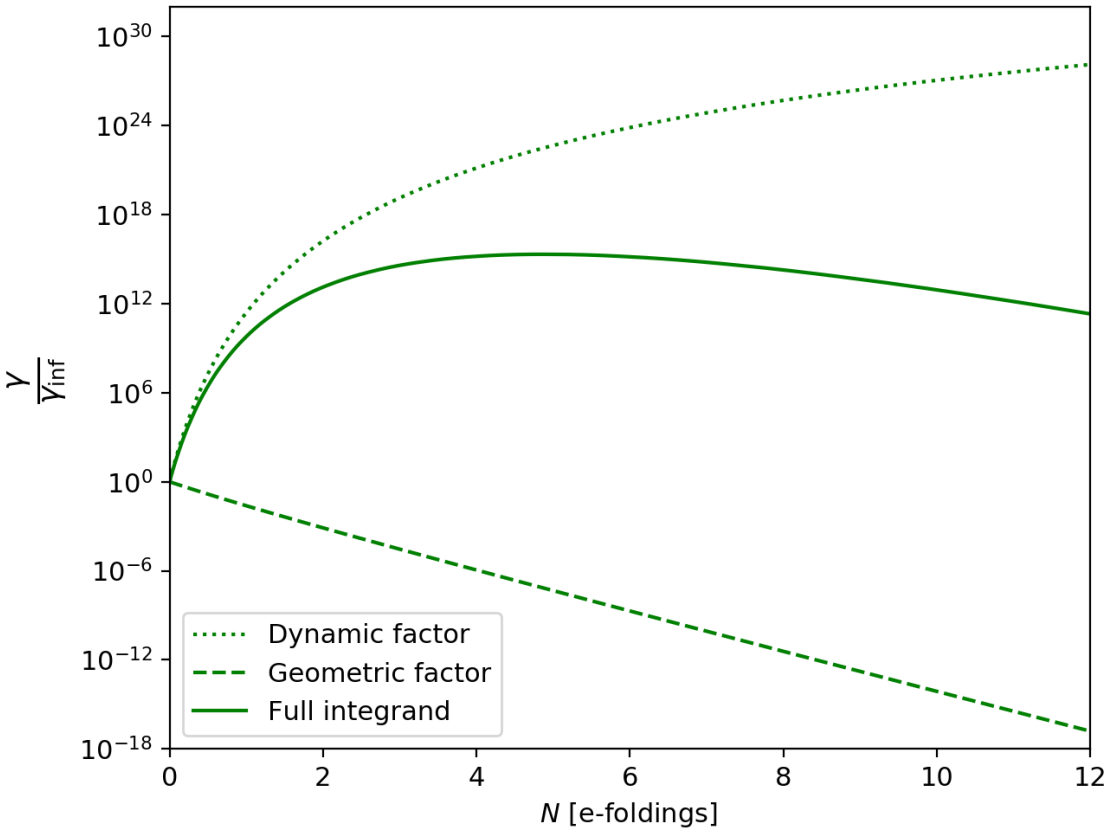

Figure 4.4: Factors of the integrand $\gamma(N)$ defined in Eq.(4.7) as functions of e-foldings of inflation in quartic inflation with $\xi_{\rm EW} = 0.05875$ and $m_t = 172.76$ GeV. The dynamic factor corresponds to $\Gamma(N)$, while the geometric factor to $\frac{d\mathcal{V}}{dN}$, and we have normalised all factors to one at $N = 0$. Originally published in [1] (CC BY 4.0).

magnitude longer than this, and therefore it is important to check whether the behaviour at very large N can change this conclusion.

To consider a long period of inflation, we split the integral (4.4) into two pieces,

$$\langle \mathcal{N} \rangle_{\rm inf}(N_{\rm start}) = \langle \mathcal{N} \rangle_{\rm inf}(60) + \int_{60}^{N_{\rm start}} dN\, \gamma(N)\,, \tag{4.17}$$

where we have already computed the first term numerically for the calculations presented earlier. If we choose the parameter values at the threshold, then by definition $\langle \mathcal{N} \rangle_{\rm inf}(60) = 1$. The second term, on the other hand, can be computed using the slow-roll approximation, which is valid at early times.

Based on Eq. (2.23) and as implied also by Fig. 4.1, we assume that the Hawking-Moss action $B_{\rm HM}$ is approximately constant at early times, so that $\Gamma(N) \approx H(N)^4 e^{-B_{\rm HM}}$, where we have

used the dS approximation (3.23) for the Ricci scalar. Under these approximations, and using the slow-roll expressions for H and η, in the quadratic (3.43)-(3.44), quartic (3.48)-(3.49), and Starobinsky (3.63)-(3.64) models, Eq. (4.17) is simplified to

$$\langle \mathcal{N} \rangle (N_{\rm start}) \approx 1 + \frac{4\pi e^{-B_{\rm HM}}}{3} N_{\rm start} \,. \tag{4.18}$$

However, this is true for all monomial potentials and all plateau models, where the Hubble rate is constant at early times. For the latter case, this is immediately evident when writing the early-time contribution to Eq. (4.17) in the slow-roll approximation,

$$\langle \mathcal{N} \rangle (N_{\rm start}) \approx 1 + \frac{4\pi e^{-B_{\rm HM}}}{3} \int_{60}^{N_{\rm start}} \left[\frac{H(N) a_{\rm inf}}{e^N} \left(\int_0^N \frac{e^{N'} dN'}{H(N') a_{\rm inf}} \right) \right]^3 dN \,, \tag{4.19}$$

where the nested integral, in terms of N', corresponds to the conformal factor

$$\eta_0 - \eta(N) = \frac{1}{a_{\rm inf}} \int_0^N \frac{e^{N'}}{H(N')} dN' \,, \tag{4.20}$$

after having dropped the post-inflationary contribution of (3.21), because it is negligible compared to (4.20) for large values of N.

In the case of monomial models of inflation with

$$V(\phi) = r\phi^q \;, \quad \forall \; r, q > 0 \quad , \tag{4.21}$$

solving the inflaton's equation of motion in slow-roll results in

$$\phi(N) = M_P \sqrt{q(2N + q/2)} \,. \tag{4.22}$$

This allows to express the Hubble rate in the slow-roll limit as well,

$$H(N) = \sqrt{\frac{r}{3}} M_P^{\frac{q-2}{2}} \left[q(2N + q/2) \right]^{q/4} = K(N + p)^p \,, \tag{4.23}$$

where we have redefined $q = 4p$ and rewritten the constant factor as $K = \sqrt{\frac{r}{3}} M_P^{2p-1} (8p)^p$.

Inserting the above expression to (4.20) and integrating by parts leads to

$$a_{\rm inf}(\eta_0-\eta(N)) \approx \int_0^N \frac{e^{N'}dN'}{K(N'+p)^p} = \frac{1}{K}\left[\frac{e^N}{(N+p)^p}-\frac{1}{p^p}\right]+\frac{p}{K}\int_0^N \frac{e^{N'}dN'}{K(N'+p)^{p+1}}\,. \quad (4.24)$$

By performing consecutive integrations by parts in the same manner, we end up with

$$\begin{aligned} a_{\rm inf}(\eta_0-\eta(N)) \approx{}& \frac{e^N}{K(N+p)^p}\left[1+\frac{p}{N+p}+\frac{p(p+1)}{(N+p)^2}+\frac{p(p+1)(p+2)}{(N+p)^3}+...\right] \\ &-\frac{1}{Kp^p}[1+1+1+1+...]\,, \end{aligned} \quad (4.25)$$

which in the large-N limit, can be approximated by the leading order of the first term,

$$a_{\rm inf}(\eta_0-\eta(N)) \approx \frac{e^N}{K(N+p)^p}\,. \quad (4.26)$$

Finally, inserting (4.23) and (4.26) in Eq. (4.19) produces the result quoted in Eq. (4.18),

$$\begin{aligned} \langle\mathcal{N}\rangle(N_{\rm start}) &\approx 1+\frac{4\pi e^{-B_{\rm HM}}}{3}\int_{60}^{N_{\rm start}}\left[\frac{K(N+p)^p}{e^N}\left(\frac{e^N}{K(N+p)^p}\right)\right]^3 dN \\ &\approx 1+\frac{4\pi e^{-B_{\rm HM}}}{3}\,(N_{\rm start}-60) \approx 1+\frac{4\pi e^{-B_{\rm HM}}}{3}N_{\rm start}\,. \end{aligned} \quad (4.27)$$

Therefore, the early-time contribution is only important if $N_{\rm start} \gtrsim e^{B_{\rm HM}} \sim 10^{58-69}$, depending on the value of $m_t \pm 0.5$ GeV and the corresponding $\xi_{\rm EW}$. For comparison, according to Eqs. (3.45) and (3.45), the Hubble rate does not reach trans-Planckian values in quadratic inflation until 10^{10} e-folds, and in quartic inflation until 10^6 e-folds. Therefore, one can conclude that in these models, early bubble production is never important. This observation can also be obtained in a naive toy model calculation shown in Appendix A.4. For plateau models, where H approaches a constant at high N, such as the Starobinsky-type potential (3.61), the asymptotic behaviour of the expected number of bubbles is again Eq. (4.18). Therefore, if inflation lasts for a very long time, such that $N_{\rm start} \gtrsim e^{B_{\rm HM}} \approx 10^{60}$, the vacuum stability bounds on ξ become stronger.

Chapter 5

The metastability of the effective potential in Starobinsky inflation

5.1 The effective potential in $R + R^2$ gravity

5.1.1 Non-minimally coupled scalar spectator field

We wish to go beyond the field theory case of Starobinsky inflation, that was presented in Chapter 4, and study the metastability of the Higgs potential in the actual $R + R^2$ gravity setting of Section 3.3.2. Since we are interested in the evolution of the Higgs field, we need to understand how the scalar field action appears in the Einstein frame. Let us, therefore, consider a spectator scalar doublet field Φ, which is non-minimally coupled to spacetime curvature, and has the potential V_Φ in the Jordan frame. Its action reads

$$S = \int d^4x\sqrt{-g_J}\left[\frac{M_P^2}{2}\left(1 - \frac{\xi\Phi^\dagger\Phi}{M_P^2}\right)R_J + \frac{1}{12M^2}R_J^2 + \frac{1}{2}g_J^{\mu\nu}(\partial_\mu\Phi^\dagger)(\partial_\nu\Phi) - V_\Phi\right], \tag{5.1}$$

where we emphasise that $\xi = 1/6$ corresponds to the conformal point. We assume that Φ is a quantum field in the classical background metric, and we ignore the backreaction of Φ on the metric. As in Eq. (3.54), we remove the quadratic curvature term by introducing the auxiliary

field s, so that the action becomes

$$S = \int d^4x\sqrt{-g_J}\left[\frac{M_P^2}{2}\left(1+\frac{s}{3M^2M_P^2}\right)R_J - \frac{1}{12M^2}s^2 + \frac{1}{2}g_J^{\mu\nu}(\partial_\mu\Phi^\dagger)(\partial_\nu\Phi) - \frac{\xi}{2}\Phi^\dagger\Phi R_J - V_\Phi\right]. \tag{5.2}$$

Then, we use the conformal transformation (3.58) to write the action in the Einstein frame as

$$S = \int d^4x\sqrt{-g}\left[\frac{M_P^2}{2}R + \frac{1}{2}\partial_\mu\phi\partial^\mu\phi\left(1-\frac{\xi e^{-\sqrt{\frac{2}{3}}\frac{\phi}{M_P}}\Phi^\dagger\Phi}{M_P^2}\right) + \sqrt{\frac{3}{2}}\frac{\xi e^{-\sqrt{\frac{2}{3}}\frac{\phi}{M_P}}\Phi^\dagger\Phi}{M_P}\Box\phi + \frac{e^{-\sqrt{\frac{2}{3}}\frac{\phi}{M_P}}}{2}\partial_\mu\Phi^\dagger\partial^\mu\Phi - U(\phi,\Phi)\right], \tag{5.3}$$

having neglected the first $\Box\phi$ term, because it was coupled to the constant quantity $\frac{M_P^2}{2}$ and thus, it would not survive the subsequent integration by parts. We have grouped the potential terms together as

$$U(\phi,\Phi) = V_S(\phi) + \frac{\xi}{2}\frac{\Phi^\dagger\Phi R}{e^{\sqrt{\frac{2}{3}}\frac{\phi}{M_P}}} + \frac{V_\Phi}{e^{2\sqrt{\frac{2}{3}}\frac{\phi}{M_P}}}, \tag{5.4}$$

having obtained the potential of Starobinsky inflation (3.61), and exponential suppression to the scalar doublet's potential terms.

To canonically normalise the scalar field Φ, we rescale it with the field redefinition

$$\Phi = e^{\frac{1}{2}\sqrt{\frac{2}{3}}\frac{\phi}{M_P}}\tilde{\Phi}, \tag{5.5}$$

which turns the action (5.3) to

$$S = \int d^4x\sqrt{-g}\left[\frac{M_P^2}{2}R + \frac{1}{2}\partial_\mu\phi\partial^\mu\phi\left(1+\left(-\xi+\frac{1}{6}\right)\frac{\tilde{\Phi}^\dagger\tilde{\Phi}}{M_P^2}\right) + \sqrt{\frac{3}{2}}\left(-\xi+\frac{1}{6}\right)\frac{\partial^\mu\phi}{M_P}\partial_\mu\left(\tilde{\Phi}^\dagger\tilde{\Phi}\right) + \frac{1}{2}\partial_\mu\tilde{\Phi}^\dagger\partial^\mu\tilde{\Phi} - \tilde{U}(\phi,\tilde{\Phi})\right], \tag{5.6}$$

with the potential now written in terms of the redefined field as

$$\tilde{U}(\phi, \tilde{\Phi}) = V_{\rm S}(\phi) + \frac{\xi}{2}\tilde{\Phi}^\dagger\tilde{\Phi}R + e^{-2\sqrt{\frac{2}{3}}\frac{\phi}{M_P}} V_\Phi\left(e^{\frac{1}{2}\sqrt{\frac{2}{3}}\frac{\phi}{M_P}}\tilde{\Phi}\right) . \tag{5.7}$$

In the case of a renormalizable tree-level potential

$$V_\Phi(\Phi) = \frac{1}{2}m^2\Phi^\dagger\Phi + \frac{1}{4}\lambda\left(\Phi^\dagger\Phi\right)^2 , \tag{5.8}$$

the potential reads

$$\tilde{U}(\phi, \tilde{\Phi}) = V_{\rm S}(\phi) + \frac{\xi}{2}\tilde{\Phi}^\dagger\tilde{\Phi}R + \frac{1}{2}e^{-\sqrt{\frac{2}{3}}\frac{\phi}{M_P}} m^2\tilde{\Phi}^\dagger\tilde{\Phi} + \frac{1}{4}\lambda\left(\tilde{\Phi}^\dagger\tilde{\Phi}\right)^2 . \tag{5.9}$$

This shows that in the Einstein frame, and when expressed in terms of $\tilde{\Phi}$, the potential has the same form as in the original Jordan frame, but with a scaled mass term.

We also observe that the transformation from Jordan to Einstein frame has given rise to two non-renormalizable coupling terms between ϕ and Φ. We will discuss these terms, and their effect on the scalar field dynamics, in Section 5.1.3. However, we can already note that if the non-minimal coupling is conformal, $\xi = 1/6$, or if ϕ is constant so that $\partial_\mu\phi = 0$, these terms vanish, and therefore the scalar field action has its standard form. The latter requirement is a good approximation during inflation, and we make use of it in the next section, when computing the quantum corrections to the effective Higgs potential.

5.1.2 The effective masses in the Einstein frame

The discussion and results presented in Section 2.3 are applicable in an almost identical manner in the $R + R^2$ gravity scenario. We assume a constant spacetime curvature R and a constant inflaton field ϕ, meaning that $\partial_\mu\phi = 0$, and also that we can eliminate the inflaton field ϕ from the equations using the relation

$$e^{-\sqrt{\frac{2}{3}}\frac{\phi}{M_P}} = 1 - \frac{2H}{MM_P} = 1 - \frac{2\sqrt{R/12}}{MM_P}\,, \tag{5.10}$$

which follows from the Friedmann equation (3.8) in dS. Considering first the Higgs field, we can see from Eq. (5.9) that within our approximations, the relevant part of the action has the same form as in Einsteinian gravity, apart from a modified mass term. In terms of the rescaled mean field

$$\tilde{h} = \Omega^{-1}h = e^{-\frac{1}{2}\sqrt{\frac{2}{3}}\frac{\phi}{M_P}}h\,, \tag{5.11}$$

the effective masses of the Higgs and Goldstone modes are

$$\tilde{m}_h^2 = m^2 e^{-\sqrt{\frac{2}{3}}\frac{\phi}{M_P}} + 3\lambda\tilde{h}^2\,, \tag{5.12}$$

$$\tilde{m}_\chi^2 = m^2 e^{-\sqrt{\frac{2}{3}}\frac{\phi}{M_P}} + \lambda\tilde{h}^2\,. \tag{5.13}$$

In a similar way, all SM fields can be rescaled in such a way, that the form of the quadratic terms in the action is identical to GR, but with potentially modified mass terms, denoted with a tilde ($\sim$).

Therefore, for any fermion ψ we define a rescaled field $\tilde{\psi}$ and mass $\tilde{m}_\psi^2$, by demanding that

$$S_\psi = \int d^4x\sqrt{-g_J}\left(i\bar{\psi}\hat{\mathcal{D}}\psi - m_\psi\bar{\psi}\psi\right) = \int d^4x\sqrt{-g}\left(i\bar{\tilde{\psi}}\hat{\tilde{\mathcal{D}}}\tilde{\psi} - \tilde{m}_\psi\bar{\tilde{\psi}}\tilde{\psi}\right)\,, \tag{5.14}$$

where the covariant derivative $\hat{\tilde{\mathcal{D}}}$ transforms under the conformal transformation as [129]

$$\hat{\mathcal{D}} = \Omega\hat{\tilde{\mathcal{D}}} = e^{\frac{1}{\sqrt{6}}\frac{\phi}{M_P}}\hat{\tilde{\mathcal{D}}}\,. \tag{5.15}$$

This implies that the fermion field is rescaled as

$$\psi = \left(\Omega^2\right)^{3/4}\tilde{\psi} = e^{\frac{3}{4}\sqrt{\frac{2}{3}}\frac{\phi}{M_P}}\tilde{\psi}\,, \tag{5.16}$$

and its mass as

$$\tilde{m}_\psi^2 = \frac{y_\psi^2}{2}\tilde{h}^2 \,. \tag{5.17}$$

For W-bosons (and identically for Z-bosons), with gauge fixings $\zeta_i = 1$, there is no field redefinition as $\left(W^J\right)_\mu^+ = W_\mu^+$, since the exponential factors coming from the conformal transformation are cancelling one another in the kinetic term of the action

$$\begin{aligned} S_W &= \int d^4x\sqrt{-g_J}\left(-g_J^{\mu\nu}g_J^{\sigma\rho}\partial_\sigma W_\mu^+\partial_\rho W_\nu^- + m_W^2 g_J^{\mu\nu}W_\mu^+W_\nu^- + W_\mu^+ R_J^{\mu\nu}W_\nu^-\right) \\ &= \int d^4x\sqrt{-g}\left(-g^{\mu\nu}g^{\sigma\rho}\partial_\sigma W_\mu^+\partial_\rho W_\nu^- + \tilde{m}_W^2 g^{\mu\nu}W_\mu^+W_\nu^- + W_\mu^+\left(R^{\mu\nu} + ...\right)W_\nu^-\right) \,, \end{aligned} \tag{5.18}$$

where the dots $(\ldots)$ indicate terms that vanish because we are assuming constant ϕ. Therefore, this has the same form as in Einstein gravity, with the masses given in terms of the transformed Higgs field by

$$\tilde{m}_W^2 = \frac{g^2}{4}\tilde{h}^2 \,, \tag{5.19}$$

$$\tilde{m}_Z^2 = \frac{g^2 + (g')^2}{4}\tilde{h}^2 \,. \tag{5.20}$$

From Eqs. (5.17), (5.19) and (5.20), we can see that the particle masses have their standard expressions, when written in terms of the transformed Higgs field, with the exception of the Higgs (5.12) and the Goldstone (5.13) bosons that receive an exponential suppression to their constant term. Because in these rescaled variables, the action has the same form as in Einstein gravity, the one-loop curvature correction to the effective potential is also identical to Eq. (2.27) when expressed in terms of $\tilde{h}$, but with modified effective masses in curved space $\tilde{\mathcal{M}}_i$, which are given in Table 5.1,

$$\Delta V_{\rm loops}(\tilde{h}, \mu_*, R) = \frac{1}{64\pi^2}\sum_{i=1}^{31}\left\{n_i\tilde{\mathcal{M}}_i^4\left[\log\left(\frac{|\tilde{\mathcal{M}}_i^2|}{\mu_*^2}\right) - d_i\right] + \frac{n_i'}{144}R^2\log\left(\frac{|\tilde{\mathcal{M}}_i^2|}{\mu_*^2}\right)\right\}. \tag{5.21}$$

Table 5.1: Loop corrections to the effective potential with tree-level couplings to the Higgs, from the $\tilde{W}^{\pm}$ and $\tilde{Z}^0$ bosons, the quarks $\tilde{\mathrm{q}}$, the leptons $\tilde{l}$, the Higgs $\tilde{h}$, the Goldstone bosons $\tilde{\chi}_W$ and $\tilde{\chi}_Z$, and the ghosts $\tilde{c}_W$ and $\tilde{c}_Z$, and corrections that do not to couple to the Higgs at tree-level, from the photon $\tilde{\gamma}$, the gluons $\tilde{g}$, the neutrinos $\tilde{\nu}$, and the ghosts $\tilde{c}_\gamma$ and $\tilde{c}_g$. Table originally published in [6] (CC BY 4.0), then adapted and included in [2].

$\tilde{\Psi}$	i	n_i	d_i	n'_i	$\tilde{\mathcal{M}}_i^2$
$\tilde{W}^{\pm}$	1	2	3/2	$-34/15$	$\tilde{m}_W^2 + R/12$
	2	6	5/6	$-34/5$	$\tilde{m}_W^2 + R/12$
	3	-2	3/2	4/15	$\tilde{m}_W^2 - R/6$
$\tilde{Z}^0$	4	1	3/2	$-17/15$	$\tilde{m}_Z^2 + R/12$
	5	3	5/6	$-17/5$	$\tilde{m}_Z^2 + R/12$
	6	-1	3/2	2/15	$\tilde{m}_Z^2 - R/6$
$\tilde{\mathrm{q}}$	$7-12$	-12	3/2	38/5	$\tilde{m}_q^2 + R/12$
$\tilde{l}$	$13-15$	-4	3/2	38/15	$\tilde{m}_l^2 + R/12$
$\tilde{h}$	16	1	3/2	$-2/15$	$\tilde{m}_h^2 + (\xi - 1/6)R$
$\tilde{\chi}_W$	17	2	3/2	$-4/15$	$\tilde{m}_\chi^2 + \zeta_W \tilde{m}_W^2 + (\xi - 1/6)R$
$\tilde{\chi}_Z$	18	1	3/2	$-2/15$	$\tilde{m}_\chi^2 + \zeta_Z \tilde{m}_Z^2 + (\xi - 1/6)R$
$\tilde{c}_W$	19	-2	3/2	4/15	$\zeta_W \tilde{m}_W^2 - R/6$
$\tilde{c}_Z$	20	-1	3/2	2/15	$\zeta_Z \tilde{m}_Z^2 - R/6$
$\tilde{\gamma}$	21	1	3/2	$-17/15$	$R/12$
	22	3	5/6	$-17/5$	$R/12$
	23	-1	3/2	2/15	$-R/6$
$\tilde{g}$	24	8	3/2	$-136/15$	$R/12$
	25	24	5/6	$-136/5$	$R/12$
	26	-8	3/2	16/15	$-R/6$
$\tilde{\nu}$	$27-29$	-2	3/2	19/15	$R/12$
$\tilde{c}_\gamma$	30	-1	3/2	2/15	$-R/6$
$\tilde{c}_g$	31	-8	3/2	16/15	$-R/6$

In analogy with Eqs. (2.29) and (2.30), the RGI improved effective potential is given by

$$V_{\rm H}^{\rm RGI}(\tilde{h}, R) = \frac{\xi(\mu_*(\tilde{h}, R))}{2} R\tilde{h}^2 + \frac{\lambda(\mu_*(\tilde{h}, R))}{4}\tilde{h}^4 + \frac{\alpha(\mu_*(\tilde{h}, R))}{144} R^2 \,, \tag{5.22}$$

where the renormalization scale $\mu_*(\tilde{h}, R)$ is determined by demanding

$$\Delta V_{\rm loops}(\tilde{h}, \mu_*, R) = 0. \tag{5.23}$$

In this study, we are assuming classical gravity, with the inflaton field ϕ also treated as a classical background field. Therefore, neither ϕ nor the graviton loops contribute to the β-functions. As a consequence of this, the β-functions used to obtain the running couplings in Eq. (5.22) are the standard ones, and not the ones shown in Ref. [130]. This is a good approximation because the relevant energy scales, the highest of which is the Hubble rate during inflation $H_{\rm inf} \approx 10^{13}$ GeV, are well below the Planck scale. Because of this, and since the masses $\tilde{\mathcal{M}}_i$ appearing in the loops are almost identical to $\mathcal{M}_i$, the quantum corrections to the Higgs effective potential are very similar to those in Einstein gravity, apart from the rescaling of the field h.

Even though we will be taking into account the time-dependence of the background in the next section, the calculation of the RG scale via (5.21) is performed on dS with constant ϕ. After the RG improvement of the effective potential, we take into account the time-dependence of the Ricci and the inflaton in the terms that involve them (see Section 5.1.3). Naturally, this approximation starts to break down as we are approaching the end of inflation, where spacetime deviates increasingly from dS. At that stage, the time-dependence of all these objects cannot be ignored, but a proper calculation would be more involved and beyond the scope of this work. Therefore, the adoption of the dS approximation will introduce some level of uncertainty in our numerical results, as explained in Section 5.2, but inevitably towards the inflationary finale, there are other factors that would complicate the calculations. An obvious example would be the non-trivial transition to the reheating period, or the appearance of mass hierarchies when $R \to 0$, which would not allow to utilise (5.23) due to the different divergences in the logarithms of (5.21) that render the approximate behaviours $\tilde{\mathcal{M}}_i \propto R$ and $\mu_* \propto R$ as invalid.

5.1.3 The time-dependence of the background

While, as we found in the previous section, the quantum corrections are very similar to Einstein gravity, the extra classical terms in Eq. (5.6) play a very important role, because of the time-dependence of the classical background. In order to incorporate this dependence in the effective RG improved Higgs potential, we have to rewrite the action (5.6) in a canonical form, without neglecting the terms consisting of the inflaton field and its derivatives. We start by rewriting the Lagrangian (5.6) more compactly as

$$\mathcal{L} = \frac{M_P^2}{2}R + \frac{A(\tilde{h},\mu_*)}{2}\partial_\mu\phi\partial^\mu\phi + B(\tilde{h},\mu_*)\partial_\mu\tilde{h}\partial^\mu\phi + \frac{1}{2}\partial_\mu\tilde{h}\partial^\mu\tilde{h} - \tilde{U}(\phi,\tilde{h},\mu_*)\,, \tag{5.24}$$

where we have included the chosen RG scale explicitly and made the following definitions for compactness,

$$A(\tilde{h},\mu_*) = 1 - \Xi(\mu_*)\left(\frac{\tilde{h}}{M_P}\right)^2\,, \tag{5.25}$$

$$B(\tilde{h},\mu_*) = -\sqrt{6}\Xi(\mu_*)\frac{\tilde{h}}{M_P}\,, \tag{5.26}$$

$$\Xi(\mu_*) = \xi(\mu_*) - \frac{1}{6} \leq 0\,. \tag{5.27}$$

In the remainder of this section, we will be suppressing the μ_*-dependence for clarity.

In order to eliminate the mixing term, we can perform a field redefinition of the inflaton

$$\phi = \tilde{\phi} + f(\tilde{h})\,. \tag{5.28}$$

Hence, the Lagrangian now reads, after having suppressed the $\tilde{h}$-dependence,

$$\mathcal{L} = \frac{M_P^2}{2}R + \frac{A}{2}\partial_\mu\tilde{\phi}\partial^\mu\tilde{\phi} + \left[f'A + B\right]\partial_\mu\tilde{h}\partial^\mu\tilde{\phi} + \frac{1}{2}\partial_\mu\tilde{h}\partial^\mu\tilde{h}\left[1 + 2Bf' + f'^2A\right] - \tilde{U}(\tilde{\phi},h)\,. \tag{5.29}$$

Since the function $f(\tilde{h})$ is an arbitrary one, we can define it as such, so that the coefficient of the mixing term vanishes exactly,

$$f(\tilde{h}) = -M_P\sqrt{\frac{3}{2}}\ln\left[1 - \Xi\left(\frac{\tilde{h}}{M_P}\right)^2\right] . \tag{5.30}$$

Therefore, imposing the field redefinition (5.28) with (5.30) simplifies (5.24) into

$$\mathcal{L} = \frac{M_P^2}{2}R + \frac{A(\tilde{h})}{2}\partial_\mu\tilde{\phi}\partial^\mu\tilde{\phi} + \frac{C(\tilde{h})}{2}\partial_\mu\tilde{h}\partial^\mu\tilde{h} - \tilde{U}(\tilde{\phi},\tilde{h}) , \tag{5.31}$$

where we have defined the following function for brevity

$$C(\tilde{h}) = 1 - \frac{6\Xi^2\left(\frac{\tilde{h}}{M_P}\right)^2}{1 - \Xi\left(\frac{\tilde{h}}{M_P}\right)^2} . \tag{5.32}$$

There is a possible field redefinition of $\tilde{h}$ that can bring the kinetic term in canonical form, e.g.

$$\rho = g(\tilde{h})\tilde{h} , \tag{5.33}$$

since $C(\tilde{h})$ is not a function of $\tilde{\phi}$, which reduces to (5.31), when

$$\left(g(\tilde{h}) + \tilde{h}g'(\tilde{h})\right)^2 = C(\tilde{h}) . \tag{5.34}$$

Solving the above equation results into

$$g(\tilde{h}) = \frac{E\left(\text{ArcSin}\left(\sqrt{z}\right)|6\xi\right)}{\sqrt{z}} , \tag{5.35}$$

where $E(\phi|m)$ is the incomplete elliptic integral of the second kind, and we have defined the function $z(\tilde{h}) = \Xi\left(\frac{\tilde{h}}{M_P}\right)^2$ for convenience. We can expand (5.35) in a power series around zero, given that $\tilde{h} \ll M_P$ since the Higgs field is a spectator field, as

$$g(\tilde{h}) \approx \frac{\sqrt{z} - \Xi z^{3/2} + \mathcal{O}(z^{5/2})}{\sqrt{z}} = 1 - \Xi^2\left(\frac{\tilde{h}}{M_P}\right)^2 - \mathcal{O}\left((\tilde{h}/M_P)^5\right) . \tag{5.36}$$

Then, we can express the field redefinition (5.33) explicitly in terms of $\tilde{h}$ via (5.36) as

$$\rho \approx \tilde{h} - \Xi^2 \frac{\tilde{h}^3}{M_P^2} \,. \tag{5.37}$$

If we write (5.37) as $\rho \approx \tilde{h}\left[1 - \Xi^2 \epsilon_{\tilde{h}}^2\right]$ with $\epsilon_{\tilde{h}} = \tilde{h}/M_P \ll 1$, then we can obtain approximately the inverse function from $\tilde{h} \approx \rho\left[1 - \Xi^2\epsilon_{\tilde{h}}^2\right]^{-1} \approx \rho\left[1 + \Xi^2\epsilon_{\tilde{h}}^2\right]$, after keeping only the leading term in $\epsilon_{\tilde{h}} = \frac{\rho}{M_P} + \frac{\rho\Xi^2\epsilon_{\tilde{h}}^2}{M_P}$, as

$$\tilde{h} \approx \rho\left[1 + \Xi^2\left(\frac{\rho}{M_P}\right)^2 + \mathcal{O}(\rho^4)\right] . \tag{5.38}$$

Thus, finally we have an approximately diagonalised theory

$$\mathcal{L} \approx \frac{M_P^2}{2}R + \frac{1}{2}\partial_\mu\tilde{\phi}\partial^\mu\tilde{\phi} + \frac{1}{2}\partial_\mu\rho\partial^\mu\rho - \tilde{U}(\tilde{\phi},\rho)\,, \tag{5.39}$$

where we have grouped all the potential terms in $\tilde{U}(\tilde{\phi},\rho) = V_{\rm S}(\tilde{\phi}) + V_{\rm H}^{\rm RGI}(\tilde{\phi},\rho)$, with the first term corresponding to the Starobinsky potential (3.61) for $\tilde{\phi}$, and the second to the RG improved effective Higgs potential

$$V_{\rm H}^{\rm RGI}(\tilde{\phi},\rho) = \frac{\alpha}{144}R^2 + \left[\xi R + \Delta m^2\right]\frac{\rho^2}{2} + \left[\lambda + \Delta\lambda_1 + \Delta\lambda_2\right]\frac{\rho^4}{4} + \frac{\Xi^2}{M_P^2}\left[\lambda + \Delta\lambda_1 + \frac{\Delta\lambda_2}{8}\right]\rho^6\,, \tag{5.40}$$

with the additional terms that were generated by the field redefinitions being

$$\Delta m^2 = 3M^2M_P^2\Xi\left(1 - e^{-\sqrt{\frac{2}{3}}\frac{\tilde{\phi}}{M_P}}\right)e^{-\sqrt{\frac{2}{3}}\frac{\tilde{\phi}}{M_P}} + \frac{\Xi}{M_P^2}\partial_\mu\tilde{\phi}\partial^\mu\tilde{\phi}\,, \tag{5.41}$$

$$\Delta\lambda_1 = 3M^2\Xi^2 e^{-2\sqrt{\frac{2}{3}}\frac{\tilde{\phi}}{M_P}}\,, \tag{5.42}$$

$$\Delta\lambda_2 = \frac{4\Xi^2}{M_P^2}\left[\xi R + 3M^2M_P^2\Xi\left(1 - e^{-\sqrt{\frac{2}{3}}\frac{\tilde{\phi}}{M_P}}\right)e^{-\sqrt{\frac{2}{3}}\frac{\tilde{\phi}}{M_P}}\right] + \frac{4\Xi^3}{M_P^4}\partial_\mu\tilde{\phi}\partial^\mu\tilde{\phi}\,. \tag{5.43}$$

Because we are interested in field values well below the Planck scale, the ρ^6 term is Planck suppressed, and we do not include it in the following numerical calculations.

5.2 Vacuum decay in R^2 inflation

Let us now apply the general framework, that was introduced in Section 4.1, to the case of the Standard Model in the setting of $R + R^2$ gravity, with the particular aim of constraining the value of the non-minimal coupling ξ. In Section 4.2.1, we carried out the same analysis for the field theory case with the same inflationary potential as in the current case, and obtained the bound

$$\xi_{\rm EW} \gtrsim 0.059^{+0.007}_{-0.009}\,, \tag{5.44}$$

to which we will compare our findings in this chapter. For consistency of comparison, we are using the same inputs for the numerical computation, namely the Hubble rate today $H_0 = 1.5 \times 10^{-42}$ GeV [117] and at the end of inflation $H_{\rm inf} = 6.5 \times 10^{12}$ GeV, where the latter is estimated from the solution of Eq. (4.10) with $\phi_{\rm inf} = 0.6 M_P$ and $a_{\rm inf} = 1.25 \times 10^{-29}$ estimated at $\dot{H}/H^2 = -1$.

For the numerical evaluation of the integral (4.4), we express it as a system of coupled differential equations, similarly as described in Section 4.1, with the difference that $\tilde{\phi}$ acts as the inflaton in this context,

$$\frac{d\langle\mathcal{N}\rangle}{dN} = \gamma(N) = \frac{4\pi}{3}\left[a_{\rm inf}\left(\frac{3.21e^{-N}}{a_0 H_0} - \tilde{\eta}(N)\right)\right]^3 \frac{\Gamma(N)}{H(N)}\,, \tag{5.45}$$

$$\frac{d\tilde{\eta}}{dN} = -\tilde{\eta}(N) - \frac{1}{a_{\rm inf} H(N)}\,, \tag{5.46}$$

$$\frac{d^2\tilde{\phi}}{dN^2} = \frac{V_{\rm I}(\tilde{\phi})}{M_P^2 H^2}\left(\frac{d\tilde{\phi}}{dN} - M_P^2 \frac{V_{\rm I}'(\tilde{\phi})}{V_{\rm I}(\tilde{\phi})}\right)\,, \tag{5.47}$$

where again $\tilde{\eta} = e^{-N}\eta$. The boundary conditions for the field $\tilde{\phi}$ and its derivative were set at $\tilde{\phi} = 20 M_P$ by demanding that the right-hand-side of Eq. (4.10) vanishes, according to the slow-roll approximation. Eq. (5.47) was then evolved forwards in time, to find the point at which the Ricci scalar (3.40) vanishes, $R = 0$, which defines the origin $N = 0$[1]. The full set of Eqs. (5.45)–(5.47) was then evolved towards larger N, with the additional boundary conditions

[1]This definition differs slightly from the one used in Section 4.2, corresponding to shift by $\Delta N = 0.192212$ in the definition of N, but this is well below the accuracy of Eq. (3.18).

$$\langle \mathcal{N} \rangle_{\rm inf}(0) = 0\,, \tag{5.48}$$

$$\tilde{\eta}(0) = 0\,. \tag{5.49}$$

For the calculation of the decay rate (2.16), we replace R and $\tilde{\phi}$ by their time-dependent values,

$$\Gamma(N) \approx \Gamma_{\rm HM}\left(\tilde{\phi}(N), R(N)\right)\,, \tag{5.50}$$

and use the RGI effective potential (5.40), without the Planck-suppressed sixth-order term,

$$V_{\rm H}^{\rm RGI}(N,\rho) = \alpha(\mu_*)\frac{R^2(N)}{144} + m^2_{\rm eff}(\mu_*, N)\frac{\rho^2}{2} + \lambda_{\rm eff}(\mu_*, N)\frac{\rho^4}{4}\,, \tag{5.51}$$

where

$$m^2_{\rm eff} = \xi(\mu_*)R(N) + 3M^2M_P^2\Xi(\mu_*)\left(1 - e^{-\sqrt{\frac{2}{3}}\frac{\tilde{\phi}(N)}{M_P}}\right)e^{-\sqrt{\frac{2}{3}}\frac{\tilde{\phi}(N)}{M_P}} + \frac{\Xi(\mu_*)H^2(N)}{M_P^2}\left(\frac{d\tilde{\phi}}{dN}\right)^2\,, \tag{5.52}$$

$$\begin{aligned}\lambda_{\rm eff} = {}& \lambda(\mu_*) + 3M^2\Xi^2(\mu_*)e^{-2\sqrt{\frac{2}{3}}\frac{\tilde{\phi}(N)}{M_P}} + \frac{4\Xi^3(\mu_*)H^2(N)}{M_P^4}\left(\frac{d\tilde{\phi}}{dN}\right)^2 \\ & + \frac{4\Xi^2(\mu_*)}{M_P^2}\left[\xi(\mu_*)R(N) + 3M^2M_P^2\Xi(\mu_*)\left(1 - e^{-\sqrt{\frac{2}{3}}\frac{\tilde{\phi}(N)}{M_P}}\right)e^{-\sqrt{\frac{2}{3}}\frac{\tilde{\phi}(N)}{M_P}}\right]\,,\end{aligned} \tag{5.53}$$

with μ_* containing the implicit dependence on ρ and N through Eq. (5.23). Therefore, the potential is not a polynomial. Nevertheless, to understand the shape of the potential, it is instructive to think of $m^2_{\rm eff}$ and $\lambda_{\rm eff}$ as the coefficients of the quadratic and quartic terms, respectively, and consider their dependence on N.

In Fig. 5.1, we show the N-dependence of the coefficient $m^2_{\rm eff}$ of the quadratic term for two different values of $\xi_{\rm EW}$. We can see that the extra contribution Δm^2, which is not present in the field theory inflation model considered in Section 4.2, is negative and dominates over the non-minimal coupling term ξR towards the end of inflation, which destabilises the potential.

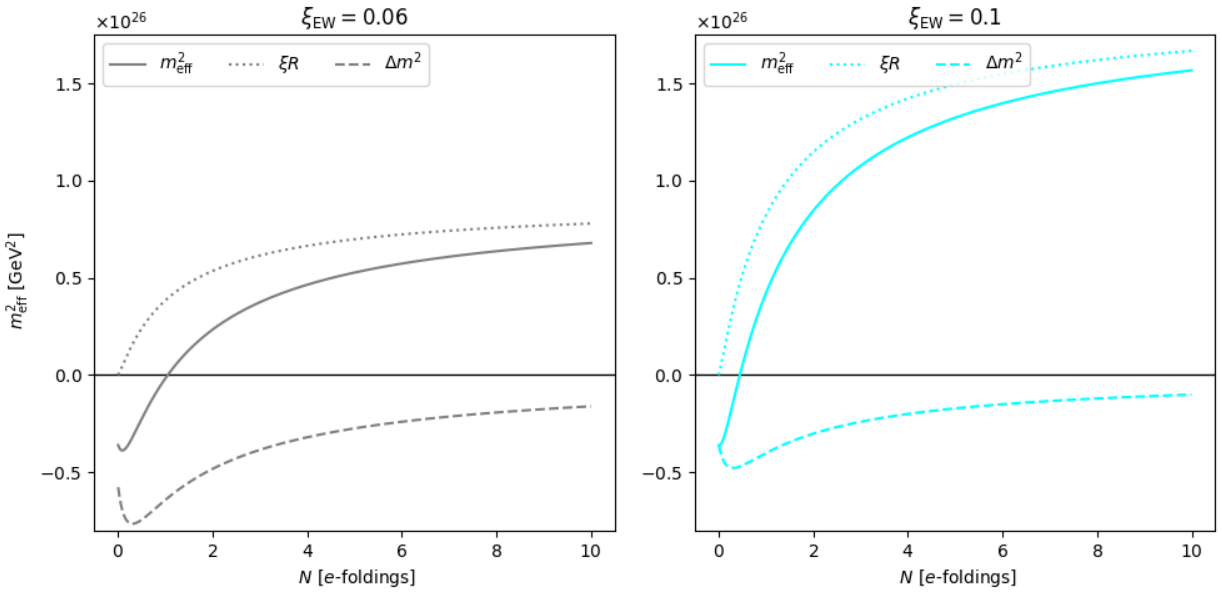

Figure 5.1: Coefficient m^2_{eff} of the quadratic term in Eq.(5.52) for $\xi_{\text{EW}} = 0.06$ (left) and $\xi_{\text{EW}} = 0.1$ (right), calculated at Higgs field value $\rho = 10^{12}$ GeV. Figure included in [2].

This can be seen more concretely in Fig. 5.2, where the value of the Hawking-Moss action (2.15) as a function of N is compared to the field theory case, which is shown with dotted lines. Because the Hawking-Moss bounce is lower than in the field theory model, the decay rate (2.16) is higher, and thus vacuum stability will require a higher value of ξ_{EW}. The vanishing action at low N indicates unsuppressed bubble nucleation, but only if the validity condition (4.11) is satisfied, which means that the lower ξ-bounds are going to depend on the choice of N_{end}.

Early on during inflation, when $N \gg 1$, the slow-roll approximations hold and spacetime looks approximately de Sitter, with the Hubble rate tending to a constant value $H \to H_{\text{dS}} = \frac{MM_P}{2}$. The extra terms in the effective potential (5.51) are negligible, and therefore we find identical behaviour as in Section 4.2.3. This can also be seen by the behaviour of the bounce action in Fig. 5.2 for high values of N, where the two different curves overlap for each ξ_{EW}. Finally, as stated in Section 2.2, the gravitational backreaction to B_{HM} is negligible, and thus we can safely omit it. This is explicitly evident when considering the corrections arising in the Hawking-Moss

bounce action, if we do not use the linear approximation [5],

$$B_{\rm HM}(N) = 24\pi^2 M_P^4 \left[\frac{1}{\tilde{U}(N,\rho_{\rm fv})} - \frac{1}{\tilde{U}(N,\rho_{\rm bar})}\right] = 24\pi^2 M_P^4 \left[\frac{\Delta V_{\rm H}(N)}{V_{\rm S}^2(N)\left(1+\frac{V_{\rm H}^{\rm RGI}(N,\rho_{\rm fv})+V_{\rm H}^{\rm RGI}(N,\rho_{\rm bar})}{V_{\rm S}(N)}+\frac{V_{\rm H}^{\rm RGI}(N,\rho_{\rm fv})V_{\rm H}^{\rm RGI}(N,\rho_{\rm bar})}{V_{\rm S}^2(N)}\right)}\right], \quad (5.54)$$

If we use the dS expression for the Ricci scalar (3.23), $R = \frac{4V_{\rm S}}{M_P^2}$, we can express the corrections in the denominator of $B_{\rm HM}$ in manner which is directly comparable to (2.15) and amounts to corrections of order less than one in a billion due to their Planck suppression,

$$B_{\rm HM}(N) = \frac{384\pi^2\Delta V(N)}{R^2(N)}\left[1+\left(\frac{4V_{\rm H}^{\rm RGI}(N,\rho_{\rm fv})}{M_P^2R(N)}+\frac{4V_{\rm H}^{\rm RGI}(N,\rho_{\rm bar})}{M_P^2R(N)}\right)+\left(\frac{4V_{\rm H}^{\rm RGI}(N,\rho_{\rm fv})}{M_P^2R(N)}\right)\left(\frac{4V_{\rm H}^{\rm RGI}(N,\rho_{\rm bar})}{M_P^2R(N)}\right)\right]^{-1}. \quad (5.55)$$

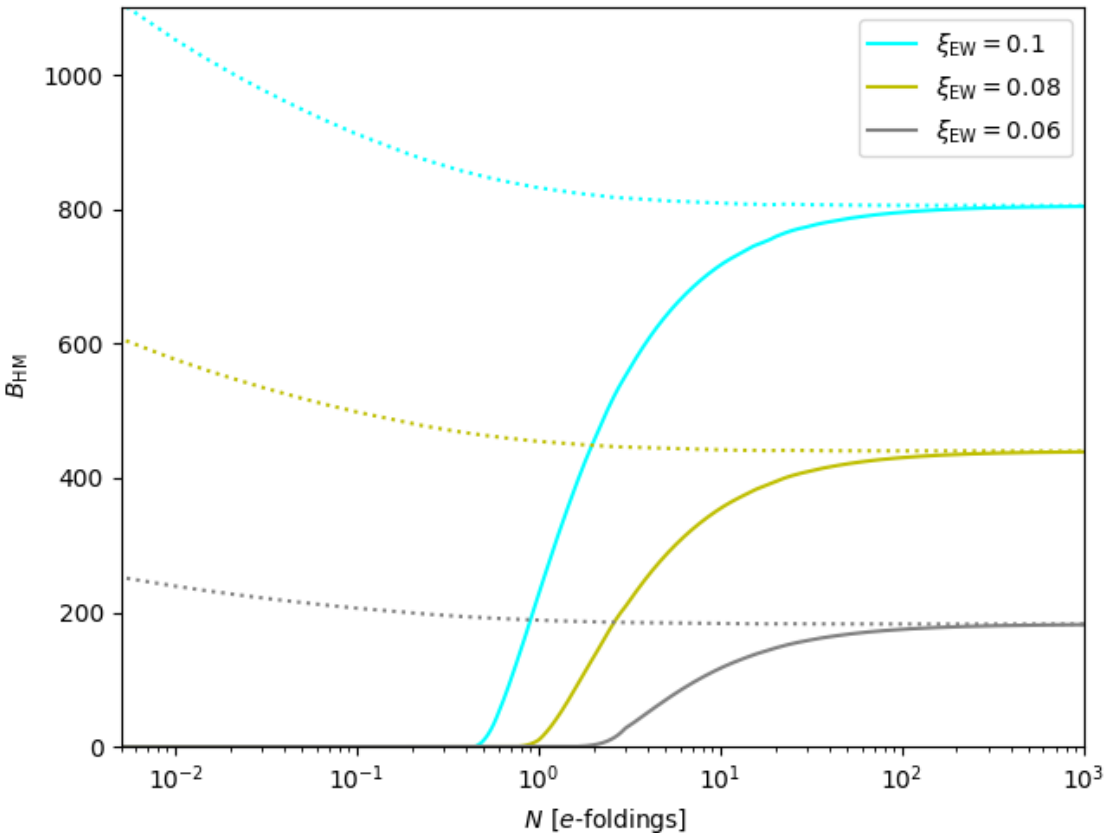

Figure 5.2: Bounce action (2.15) for sample values of the non-minimal coupling $\xi_{\rm EW}$ during R^2 inflation (solid) and in comparison with the field theory case (dotted). Figure included in [2].

The comparison between the field theory example of Section 4.2 and the proper implementation

of R^2 inflation can be also made at the full integrand level, as shown in Fig. 5.3. Once again, each pair of curves approach each other at earlier times, but they show very different evolution at the final moments of inflation. The destabilising new terms lead to significantly higher integrands, that result in an greater expectation number of true-vacuum bubbles, i.e. we have an enhancement of vacuum decay at late times. This effect is very sharply localised close to the very end of inflation, meaning that bubble nucleation takes place predominantly moments before the inflationary finale. The vertical lines, shown in varying shades of purple, denote different choices of $N_{\rm end}$, as indicated in the caption. On the other hand, because the integrand decreases rapidly as a function of N, the number of bubbles $\langle\mathcal{N}\rangle_{\rm inf}$ and hence the bounds on $\xi_{\rm EW}$ are almost independent of the choice of $N_{\rm start}$, unless $N_{\rm start} \gtrsim 10^{60}$ as discussed in Section 4.2.3. In practice, we therefore we only need to integrate up to $N = 5$ to obtain precise bounds.

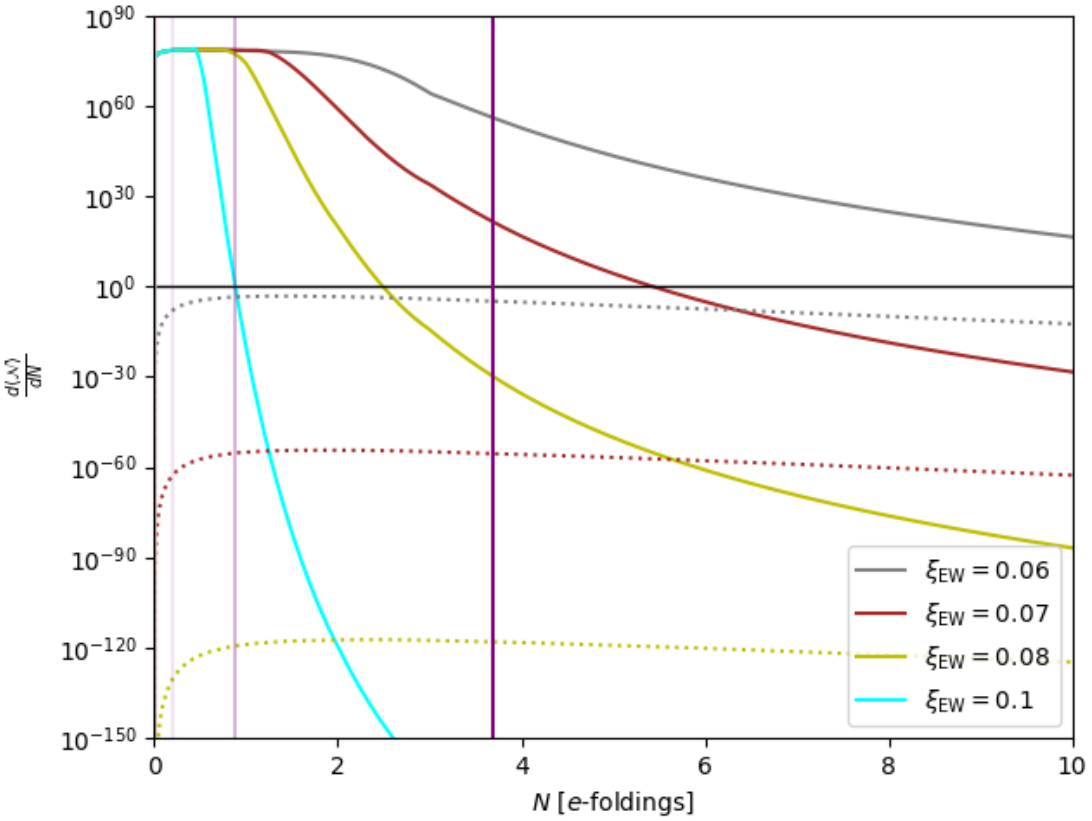

Figure 5.3: Integrands of $\langle\mathcal{N}\rangle_{\rm inf}$ with varying definition for the end of inflation. The vertical lines are at $\frac{\dot{H}}{H^2} = -1, -\frac{1}{4}, -\frac{1}{32}$ respectively, and the dotted lines correspond to the field theory inflation model discussed in Section 4.2. The plateau at $d\langle\mathcal{N}\rangle_{\rm inf}/dN \sim 10^{80}$, which the curves reach at small N, corresponds to vanishing Hawking-Moss action (2.15). In that case the expression (2.16) is not valid quantitatively, so the numerical value should be taken to be indicative of unsuppressed bubble nucleation. Figure included in [2].

Finding $\langle \mathcal{N} \rangle_{\rm inf}$ by solving the system of differential equation (5.45)-(5.47), and demanding that $\langle \mathcal{N} \rangle_{\rm inf} < 1$, results in a lower bound on the non-minimal Higgs curvature coupling $\xi_{\rm EW}$. This calculation is sensitive to the input SM parameters, and because the uncertainty in the estimation of the mass of the top quark is by far the greatest, we explore the parameter space around its central value (2.8). For a detailed account of the input parameters we use in this calculation, see Table 2.1. This computation is also dependent on the choice of $N_{\rm end}$.

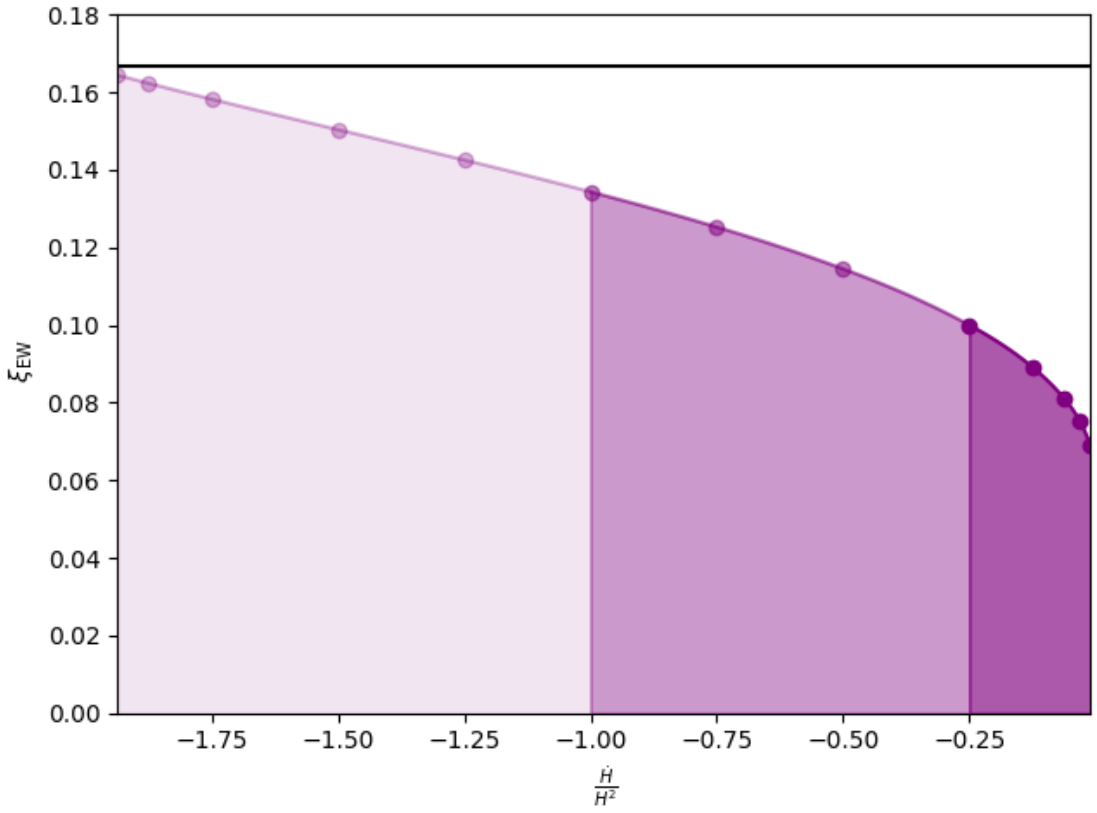

Figure 5.4: Dependence of the lower bound on the non-minimal Higgs curvature coupling $\xi_{\rm EW}$ on the choice of $N_{\rm end}$ in Eq. (4.4), parameterised by $\dot{H}/H^2$, for the top quark mass $m_t = 172.76$ GeV. The shaded regions below the curve denote the excluded values of the parameter space, the colour scheme ranges from the most conservative lower bounds in the darkest tone on the right to the less reliable in the lightest tone on the left and it matches with the corresponding bounds in figure 5.5. The horizontal black line lies at the conformal value $\xi = 1/6$. Figure included in [2].

In Fig. 5.4, we present the effect of the choice of $N_{\rm end}$, which we parameterise by the adiabaticity parameter $\dot{H}/H^2$, on the lower ξ-bounds for the central value $m_t = 172.76$ GeV. A more negative $\dot{H}/H^2$ corresponds to lower $N_{\rm end}$ and therefore leads to a significantly stronger bound on $\xi_{\rm EW}$, approaching the conformal value at $\dot{H}/H^2 = -2$. However, because they violate the validity condition (4.11), these bounds probably cannot be trusted. However, the darkest purple

area, which corresponds to $\dot{H}/H^2 > -1/4$, should be valid, and therefore we can conclude that vacuum stability requires $\xi_{\rm EW} \gtrsim 0.1$.

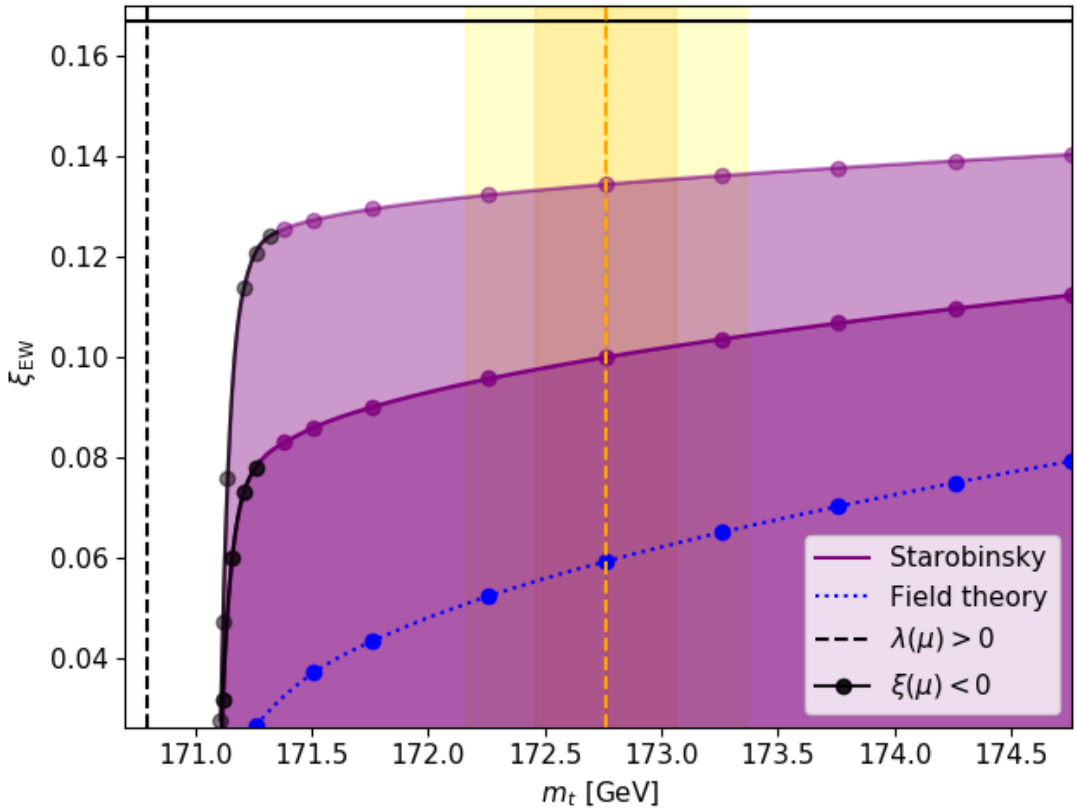

Figure 5.5: Lower bounds on the non-minimal Higgs curvature coupling $\xi_{\rm EW}$ as a function of the top quark mass m_t. The vertical dashed orange line with its accompanying shaded regions depict $m_t \pm \sigma\,, 2\sigma$ [8]. The darker and lighter shades of purple show the excluded areas for two different choices of $N_{\rm end}$, corresponding to $\dot{H}/H^2 = -1/4$ and $\dot{H}/H^2 = -1$, respectively. The leftmost black parts of the curves show the lowest $\xi_{\rm EW}$ values below which $\xi(\mu)$ turns negative during its running, and thus "pushes" the EW vacuum to higher field values. Previous constraints with a Starobinsky-like power-law model are shown in the dotted blue curve (see Section 4.2.1). The vertical dashed black line stands at the threshold value of m_t, below which the EW vacuum is stable. Finally, the horizontal, black line illustrates the conformal point $\xi = 1/6$. Figure included in [2].

In figure 5.5, we present the lower bounds with respect to the input value of the top quark mass. The shaded areas are excluded by vacuum instability. The darker and lighter shades of purple correspond to different choices of $N_{\rm end}$, $\dot{H}/H^2 = -1/4$ and $\dot{H}/H^2 = -1$, respectively. The blackened portions of the curves correspond to the area of parameter space where the non-minimal coupling turns negative as it runs, and thus forces the metastable vacuum to higher field values close to the potential barrier. These bounds are obtained in a slightly different manner, since the height of the potential barrier is measured from the top of the barrier to

the now dynamic local minimum of the potential. For comparison, we also show with the blue dotted curve the bounds for the field theory inflation model as shown in Section 4.2.1. They are evidently weaker, since now extra terms have been generated in the effective potential that have negative sign, and therefore destabilise the vacuum increasingly towards the end of inflation.

Chapter 6

Conclusion

6.1 Summary

In this thesis, we have investigated the cosmological implications of the electroweak vacuum instability to constrain fundamental physics and gain insights into the dynamics of the Higgs field in the early universe. More specifically, we utilised the metastability of the Higgs vacuum, which is a feature of the Standard Model according to our experimental measurements, during the inflationary era, to obtain lower bounds on the Higgs curvature coupling ξ. The importance of these results lies on the fact that ξ is the last unknown renormalizable parameter of the SM which cannot be probed experimentally with accelerator experiments, because spacetime is not significantly curved in the present day universe. Hence, such cosmological constraints are orders of magnitude stronger than other methods. Given also that we made use of the state-of-the-art effective Higgs potential approximated with three-loop renormalization group improvement and one-loop curvature corrections in a time-dependent background, the bounds presented here are arguably the most accurate to date.

6.2 Field theory inflation

In Section 4.2, we provided vacuum decay bounds on the Higgs curvature coupling in three inflationary models, quadratic, quartic, and Starobinsky-like power-law inflation. For the calculation of the tunnelling probability we made use of the Hawking-Moss bounce, with the renormalization group improved effective potential calculated on a curved background without the usual assumption of strict de Sitter space. In the effective potential for the SM Higgs, we included the leading time-dependent curvature corrections from all SM constituents by making use of the results of Ref. [6] and choosing the renormalization scale such that the loop correction strictly vanishes, as written in Eq. (2.29). This amounts to a consistent inclusion of quantum induced curvature corrections to 1-loop order, which in previous works has not been addressed beyond de Sitter space. This analysis indicated that the bound for the Higgs non-minimal coupling at the electroweak scale is

$$\xi_{\rm EW}^{\rm FT} \gtrsim 0.06\,, \tag{6.1}$$

for the central value of the top quark mass. This is numerically close to bounds obtained earlier in the de Sitter approximation [5, 6]. From the results in Eqs. (4.14)–(4.16), one can also see that the bound is largely unchanged when varying the top quark mass by 2σ or less. Since for the non-minimal coupling in the SM, $\xi = 0$ is not a fixed point of the RG evolution, a small yet non-zero value is perfectly natural from the model building point of view.

Our work also revealed non-trivial insights concerning when precisely, during inflation, the vacuum bubbles are formed. Consistently in all three models that we studied, the bulk of bubble nucleation occurs close to the end of inflation. This is shown explicitly in Fig. 4.3, where the maximum probability for nucleation is at the peaks localised less than ten e-folds before the end of inflation, while dropping rapidly for large N. In Section 4.2.3, the dependence of the average number of bubbles on the total length of inflation was studied analytically. It was shown that the results are largely insensitive to the entire duration of inflation, unless one considers an extremely long period of primordial inflation lasting more than $10^{50}\,e$-folds.

Although a very large number, this might be significant for cases admitting eternal inflation [55], which warrants further study.

It would be useful to clarify the range of validity of our approach, that utilises the Hawking-Moss solution during high-scale inflation. In general, during the expansion in the inflationary models we considered, because of the high scales of the Hubble rates, the Coleman-de Lucia process is always subdominant [5]. The stochastic formalism on the other hand is only required either at the very end of inflation, when deviating from dS, or at the earlier times, when the Hubble scales are higher than the barrier. Thus, in our case, where we look at the last e-foldings of inflation, the HM approach is the dominant one and because bubble production takes place before the last e-fold or so, it is still valid to use it in the dS approximation until then. Since the early time contribution is irrelevant, as we showed in Section 4.2.3, that means that we can use the HM instanton confidently and only consider the stochastic formalism if we want to look towards the very end of inflation. Numerically, we are within the HM regime [43],

$$H^2 < \left(V_{\rm H}(h_{\rm bar})\right)^{1/2} \,, \tag{6.2}$$

where the CdL bounce does not exist since $|V''_{\rm H}(h_{\rm bar})| < 4H^2$, even though $|V''_{\rm H}(h_{\rm bar})| \geq H^2$.

As mentioned in the introduction, the issue of vacuum stability during inflation was similarly studied on a time-dependent background in Ref. [54]. The main difference to our work was making use of the stochastic approach of Ref. [131], instead of the Hawking-Moss bounce, and including Planck-suppressed derivative operators in the action. Furthermore, Ref. [54] made use of the RG improved tree-level potential with the scale choice $\mu^2 = h^2 + 12H^2$, in contrast to this study, where we used the 1-loop result in Eq. (2.30) with the scale choice from Eq. (2.29). For the cases where the analyses overlap, there is good agreement between the results.

6.3 Starobinsky inflation

In Chapter 5, we studied the vacuum stability of the Higgs in the minimal Starobinsky inflation model, in which inflation is driven by an R^2 term. In the Einstein frame, this term gives rise to negative time-dependent contributions to the Higgs effective potential, whose effect is to destabilise the electroweak vacuum further. In parallel with our method in Chapter 4, we incorporated quantum effects in the Higgs effective potential by using the three-loop RGI effective potential, together with one-loop curvature corrections, computed in the de Sitter approximation with a constant inflaton field. We used this potential to compute the Hawking-Moss vacuum decay rate, and by demanding that no bubble nucleation events took place in the entirety of our past lightcone, we obtained a lower bound on the Higgs curvature coupling,

$$\xi_{\rm EW}^{R^2} \gtrsim 0.1\,. \tag{6.3}$$

This is significantly stronger than the corresponding bound (6.1), which was obtained for the Starobinsky-like field theory inflation model in Section 4.2.1.

These constraints exhibited similar mild dependence on the top quark mass as in Section 4.2.1, but were significantly more sensitive to the last moments of inflation, and therefore also to the precise choice of $N_{\rm end}$, the lower limit of the integral (4.4). Because vacuum bubble production is "pushed" towards the end of inflation, where our de Sitter approximations start to break down, we adopted a conservative choice for $N_{\rm end}$, corresponding to the condition $\dot{H}/H^2 = -1/4$. However, this suggests that the bounds may be improved significantly, by fully accounting for the transition from inflation to radiation dominated Hot Big Bang. Vacuum stability during reheating, in this same theory, was recently studied in Ref. [90], but further work is needed to bridge the gap between these two calculations.

On the other hand, when considering the shape of the effective potential at early times, we recover the results and the same cosmological implications from Section 4.2.3, where the bounds are not sensitive to the entire duration of inflation, unless it lasts for more than 10^{60} e-folds. Thus, eternal inflation appears to be inconsistent with vacuum metastability.

The result (6.3) is in agreement with a similar study [90], which considers the metastability of the Higgs potential in Starobinsky inflation, but focuses mainly on its dynamics during reheating. However, it is important to highlight the differences between the two approaches, especially in their overlap regarding inflation. Firstly, the conformal transformation in [90] is defined to include the ξ-term, and therefore there is no explicit non-minimal term ξRh^2 in the Higgs potential in the Einstein frame. This means that the additional terms that are generated in the effective Higgs potential are slightly different, since they originate from different field redefinitions that diagonalise the respective actions. Secondly, and more importantly, there is a discrepancy between the effective potentials used in these two studies, where it is just the quartic self-interaction term, without loop or curvature corrections, in [90]. In addition, the scale choice is limited to $\mu = h$, which misses the contribution from spacetime curvature R, that dominates during the inflationary epoch. Finally, an equally important difference lies in the manner in which vacuum decay is studied, where the instability is treated classically in [90] without considering any instanton solutions.

6.4 Future directions

It is evident from our analysis and results in Chapter 5, that it is essential to incorporate the period of reheating in vacuum decay calculations during Starobinsky inflation, because bubble production is predominantly taking place very close to the end of inflation. If we wish to provide stronger and more accurate constraints on ξ, and also follow the survival of the metastable vacuum after inflation, it is essential to extend our treatment to incorporate the oscillatory behaviour of the inflaton field during reheating. For this purpose, we would have to develop new techniques that would allow us to study closely the transition from inflation to reheating in a consistent manner, which is a particularly difficult and unexplored endeavour. The usual approach has been to investigate inflation and reheating separately, and introduce either an instantaneous transition or a gradual procedure in a phenomenological way. Furthermore, it is crucial for these studies to embed the SM consistently in the particular cosmological scenarios, since the loop and curvature corrections to the effective potential and its RG improvement

are not trivial on curved spacetime. Finally, since the usual de Sitter space approximation starts to break down in this regime, it would be necessary to adapt our numerical methods to accommodate these complications, so that we can probe the quantities of interest with increased confidence.

Another possibility relates to the possible effects on the effective potential from the inclusion of higher dimensional operators in the Lagrangian. This is motivated by [54], where it was suggested that such operators affect significantly the probability of vacuum decay. However, that study was performed in the stochastic rather than the Hawking-Moss regime. In this respect, we may also need to consider the case where the Coleman-de Lucia instanton dominates, as this can be relevant when including operators of higher dimensionality. A different option would be to consider thermal corrections to the effective Higgs potential, which become significant towards the end of inflation and the beginning of reheating. This could provide a route to constraining the reheating temperature and thus expanding our scope of constraining power. To that end, we may have to incorporate the stochastic dynamics of the Higgs field in the theory, as they would dominate the bounce solution when deviating increasingly from de Sitter.

In this work, we have not considered a direct coupling between the Higgs and the inflaton field. In the slow-roll limit, there are examples in which its effects are similar to those of the curvature coupling, and therefore one can translate the bounds on the curvature coupling to include the direct Higgs-inflaton coupling [65]. Unfortunately, this is not possible in general beyond slow roll, and therefore a new calculation is required to include the effects of a direct coupling. Lastly, within the proposed minimal framework of this thesis, there is the possibility to expand our approach and consider a family of plateau models, such as Higgs and mixed scalaron inflation as in [100], and different formalisms of gravity, such as Palatini [132, 133], teleparallel [134], affine [135, 136], and Einstein-Cartan [137] gravity. This would potentially allow us to confront our models with observations, constrain the number of viable inflationary models, and gain novel insights into theories beyond General Relativity, with respect to the desired features for their short scale signatures and the survival of the electroweak vacuum throughout our cosmological history.

Bibliography

[1] A. Mantziris, T. Markkanen and A. Rajantie, *Vacuum decay constraints on the Higgs curvature coupling from inflation*, *JCAP* **03** (2021) 077, [2011.03763].

[2] A. Mantziris, T. Markkanen and A. Rajantie, *The effective Higgs potential and vacuum decay in Starobinsky inflation*, 2207.00696.

[3] A. Mantziris, *Cosmological implications of EW vacuum instability: constraints on the Higgs-curvature coupling from inflation*, *PoS* **EPS-HEP2021** (2022) 127, [2111.02464].

[4] A. Mantziris, *On the cosmological implications of the electroweak vacuum instability: constraining the non-minimal coupling with inflation*, *J. Phys. Conf. Ser.* **2156** (2021) 012239, [2111.02497].

[5] T. Markkanen, A. Rajantie and S. Stopyra, *Cosmological Aspects of Higgs Vacuum Metastability*, *Front. Astron. Space Sci.* **5** (2018) 40, [1809.06923].

[6] T. Markkanen, S. Nurmi, A. Rajantie and S. Stopyra, *The 1-loop effective potential for the Standard Model in curved spacetime*, *JHEP* **06** (2018) 040, [1804.02020].

[7] C. W. Misner, K. S. Thorne and J. A. Wheeler, *Gravitation*. W. H. Freeman, San Francisco, 1973.

[8] Particle Data Group collaboration, P. Zyla et al., *Review of Particle Physics*, *PTEP* **2020** (2020) 083C01.

[9] CMS collaboration, S. Chatrchyan et al., *Observation of a New Boson at a Mass of 125 GeV with the CMS Experiment at the LHC*, *Phys. Lett. B* **716** (2012) 30–61, [1207.7235].

[10] ATLAS collaboration, G. Aad et al., *Observation of a new particle in the search for the Standard Model Higgs boson with the ATLAS detector at the LHC*, *Phys. Lett. B* **716** (2012) 1–29, [1207.7214].

[11] W. Cottingham and D. Greenwood, *An introduction to the standard model of particle physics*. Cambridge University Press, 4, 2007.

[12] A. Eichhorn, M. Fairbairn, T. Markkanen and A. Rajantie, eds., *Proceedings, Higgs cosmology: Newport Pagnell, Buckinghamshire, UK, March 27-28, 2017*, 2018.

[13] J. Espinosa, *Cosmological implications of Higgs near-criticality*, *Phil. Trans. Roy. Soc. Lond. A* **376** (2018) 20170118.

[14] H. Gies and R. Sondenheimer, *Renormalization Group Flow of the Higgs Potential*, *Phil. Trans. Roy. Soc. Lond. A* **376** (2018) 20170120, [1708.04305].

[15] E. A. R. Rojas, *The Higgs Boson at LHC and the Vacuum Stability of the Standard Model*. PhD thesis, Colombia, U. Natl., 2015. 1511.03651.

[16] G. Degrassi, S. Di Vita, J. Elias-Miro, J. R. Espinosa, G. F. Giudice, G. Isidori et al., *Higgs mass and vacuum stability in the Standard Model at NNLO*, *JHEP* **08** (2012) 098, [1205.6497].

[17] D. Buttazzo, G. Degrassi, P. P. Giardino, G. F. Giudice, F. Sala, A. Salvio et al., *Investigating the near-criticality of the Higgs boson*, *JHEP* **12** (2013) 089, [1307.3536].

[18] A. Bednyakov, B. Kniehl, A. Pikelner and O. Veretin, *Stability of the Electroweak Vacuum: Gauge Independence and Advanced Precision*, *Phys. Rev. Lett.* **115** (2015) 201802, [1507.08833].

[19] P. Q. Hung, *Vacuum Instability and New Constraints on Fermion Masses*, *Phys. Rev. Lett.* **42** (1979) 873.

[20] M. Sher, *Precise vacuum stability bound in the standard model*, *Phys. Lett. B* **317** (1993) 159–163, [hep-ph/9307342].

[21] J. Casas, J. Espinosa and M. Quiros, *Standard model stability bounds for new physics within LHC reach*, *Phys. Lett. B* **382** (1996) 374–382, [hep-ph/9603227].

[22] G. Isidori, G. Ridolfi and A. Strumia, *On the metastability of the standard model vacuum*, *Nucl. Phys. B* **609** (2001) 387–409, [hep-ph/0104016].

[23] J. Ellis, J. Espinosa, G. Giudice, A. Hoecker and A. Riotto, *The Probable Fate of the Standard Model*, *Phys. Lett. B* **679** (2009) 369–375, [0906.0954].

[24] J. Elias-Miro, J. R. Espinosa, G. F. Giudice, G. Isidori, A. Riotto and A. Strumia, *Higgs mass implications on the stability of the electroweak vacuum*, *Phys. Lett. B* **709** (2012) 222–228, [1112.3022].

[25] O. Lebedev, *On Stability of the Electroweak Vacuum and the Higgs Portal*, *Eur. Phys. J. C* **72** (2012) 2058, [1203.0156].

[26] V. Branchina and E. Messina, *Stability, Higgs Boson Mass and New Physics*, *Phys. Rev. Lett.* **111** (2013) 241801, [1307.5193].

[27] A. Salvio, A. Strumia, N. Tetradis and A. Urbano, *On gravitational and thermal corrections to vacuum decay*, *JHEP* **09** (2016) 054, [1608.02555].

[28] A. Rajantie and S. Stopyra, *Standard Model vacuum decay with gravity*, *Phys. Rev. D* **95** (2017) 025008, [1606.00849].

[29] S. Chigusa, T. Moroi and Y. Shoji, *State-of-the-Art Calculation of the Decay Rate of Electroweak Vacuum in the Standard Model*, *Phys. Rev. Lett.* **119** (2017) 211801, [1707.09301].

[30] S. Chigusa, T. Moroi and Y. Shoji, *Decay Rate of Electroweak Vacuum in the Standard Model and Beyond*, *Phys. Rev. D* **97** (2018) 116012, [1803.03902].

[31] S. Chigusa, T. Moroi and Y. Shoji, *Precise Calculation of the Decay Rate of False Vacuum with Multi-Field Bounce*, 2007.14124.

[32] J. Espinosa, *Vacuum Decay in the Standard Model: Analytical Results with Running and Gravity*, *JCAP* **06** (2020) 052, [2003.06219].

[33] S. Stopyra, *Standard Model Vacuum Decay with Gravity*. PhD thesis, Imperial Coll., London, 2018.

[34] J. Callan, Curtis G. and S. R. Coleman, *The Fate of the False Vacuum. 2. First Quantum Corrections*, *Phys. Rev. D* **16** (1977) 1762–1768.

[35] S. R. Coleman and F. De Luccia, *Gravitational Effects on and of Vacuum Decay*, *Phys. Rev. D* **21** (1980) 3305.

[36] J. R. Espinosa, G. F. Giudice, E. Morgante, A. Riotto, L. Senatore, A. Strumia et al., *The cosmological Higgstory of the vacuum instability*, *JHEP* **09** (2015) 174, [1505.04825].

[37] P. Burda, R. Gregory and I. Moss, *The fate of the Higgs vacuum*, *JHEP* **06** (2016) 025, [1601.02152].

[38] J. R. Espinosa, G. F. Giudice and A. Riotto, *Cosmological implications of the Higgs mass measurement*, *JCAP* **05** (2008) 002, [0710.2484].

[39] W. E. East, J. Kearney, B. Shakya, H. Yoo and K. M. Zurek, *Spacetime Dynamics of a Higgs Vacuum Instability During Inflation*, *Phys. Rev. D* **95** (2017) 023526, [1607.00381].

[40] O. Lebedev and A. Westphal, *Metastable Electroweak Vacuum: Implications for Inflation*, *Phys. Lett. B* **719** (2013) 415–418, [1210.6987].

[41] A. Kobakhidze and A. Spencer-Smith, *Electroweak Vacuum (In)Stability in an Inflationary Universe*, *Phys. Lett. B* **722** (2013) 130–134, [1301.2846].

[42] M. Fairbairn and R. Hogan, *Electroweak Vacuum Stability in light of BICEP2*, *Phys. Rev. Lett.* **112** (2014) 201801, [1403.6786].

[43] A. Hook, J. Kearney, B. Shakya and K. M. Zurek, *Probable or Improbable Universe? Correlating Electroweak Vacuum Instability with the Scale of Inflation*, *JHEP* **01** (2015) 061, [1404.5953].

[44] K. Kamada, *Inflationary cosmology and the standard model Higgs with a small Hubble induced mass*, *Phys. Lett. B* **742** (2015) 126–135, [1409.5078].

[45] J. Kearney, H. Yoo and K. M. Zurek, *Is a Higgs Vacuum Instability Fatal for High-Scale Inflation?*, *Phys. Rev. D* **91** (2015) 123537, [1503.05193].

[46] K. Enqvist, T. Meriniemi and S. Nurmi, *Higgs Dynamics during Inflation*, *JCAP* **07** (2014) 025, [1404.3699].

[47] K. Bhattacharya, J. Chakrabortty, S. Das and T. Mondal, *Higgs vacuum stability and inflationary dynamics after BICEP2 and PLANCK dust polarisation data*, *JCAP* **12** (2014) 001, [1408.3966].

[48] M. Herranen, T. Markkanen, S. Nurmi and A. Rajantie, *Spacetime curvature and the Higgs stability during inflation*, *Phys. Rev. Lett.* **113** (2014) 211102, [1407.3141].

[49] O. Czerwińska, Z. Lalak and L. u. Nakonieczny, *Stability of the effective potential of the gauge-less top-Higgs model in curved spacetime*, *JHEP* **11** (2015) 207, [1508.03297].

[50] O. Czerwińska, Z. Lalak, M. Lewicki and P. Olszewski, *The impact of non-minimally coupled gravity on vacuum stability*, *JHEP* **10** (2016) 004, [1606.07808].

[51] A. Rajantie and S. Stopyra, *Standard Model vacuum decay in a de Sitter Background*, *Phys. Rev. D* **97** (2018) 025012, [1707.09175].

[52] D. Rodriguez Roman and M. Fairbairn, *Gravitationally produced Top Quarks and the Stability of the Electroweak Vacuum During Inflation*, *Phys. Rev. D* **99** (2019) 036012, [1807.02450].

[53] S. Rusak, *Destabilization of the EW vacuum in non-minimally coupled inflation*, *JCAP* **05** (2020) 020, [1811.10569].

[54] J. Fumagalli, S. Renaux-Petel and J. W. Ronayne, *Higgs vacuum (in)stability during inflation: the dangerous relevance of de Sitter departure and Planck-suppressed operators*, *JHEP* **02** (2020) 142, [1910.13430].

[55] M. Jain and M. P. Hertzberg, *Eternal inflation and reheating in the presence of the standard model Higgs field*, *Phys. Rev. D* **101** (2020) 103506, [1910.04664].

[56] M. P. Hertzberg and M. Jain, *Explanation for why the Early Universe was Stable and Dominated by the Standard Model*, 1911.04648.

[57] Z. Lalak, A. Nakonieczna and L. u. Nakonieczny, *Two interacting scalars system in curved spacetime – vacuum stability from the curved spacetime Effective Field Theory (cEFT) perspective*, 2004.12327.

[58] P. Adshead, L. Pearce, J. Shelton and Z. J. Weiner, *Stochastic evolution of scalar fields with continuous symmetries during inflation*, *Phys. Rev. D* **102** (2020) 023526, [2002.07201].

[59] V. De Luca, A. Kehagias and A. Riotto, *On the Cosmological Stability of the Higgs Instability*, 2205.10240.

[60] M. Herranen, T. Markkanen, S. Nurmi and A. Rajantie, *Spacetime curvature and Higgs stability after inflation*, *Phys. Rev. Lett.* **115** (2015) 241301, [1506.04065].

[61] K. Kohri and H. Matsui, *Higgs vacuum metastability in primordial inflation, preheating, and reheating*, *Phys. Rev. D* **94** (2016) 103509, [1602.02100].

[62] C. Gross, O. Lebedev and M. Zatta, *Higgs–inflaton coupling from reheating and the metastable Universe*, *Phys. Lett. B* **753** (2016) 178–181, [1506.05106].

[63] Y. Ema, K. Mukaida and K. Nakayama, *Fate of Electroweak Vacuum during Preheating*, *JCAP* **10** (2016) 043, [1602.00483].

[64] K. Enqvist, M. Karciauskas, O. Lebedev, S. Rusak and M. Zatta, *Postinflationary vacuum instability and Higgs-inflaton couplings*, *JCAP* **11** (2016) 025, [1608.08848].

[65] Y. Ema, M. Karciauskas, O. Lebedev and M. Zatta, *Early Universe Higgs dynamics in the presence of the Higgs-inflaton and non-minimal Higgs-gravity couplings*, *JCAP* **06** (2017) 054, [1703.04681].

[66] M. Postma and J. van de Vis, *Electroweak stability and non-minimal coupling*, *JCAP* **05** (2017) 004, [1702.07636].

[67] D. G. Figueroa, A. Rajantie and F. Torrenti, *Higgs field-curvature coupling and postinflationary vacuum instability*, *Phys. Rev. D* **98** (2018) 023532, [1709.00398].

[68] D. Croon, N. Fernandez, D. McKeen and G. White, *Stability, reheating and leptogenesis*, *JHEP* **06** (2019) 098, [1903.08658].

[69] J. Kost, C. S. Shin and T. Terada, *Massless preheating and electroweak vacuum metastability*, *Phys. Rev. D* **105** (2022) 043508, [2105.06939].

[70] M. Kawasaki, K. Mukaida and T. T. Yanagida, *Simple cosmological solution to the Higgs field instability problem in chaotic inflation and the formation of primordial black holes*, *Phys. Rev. D* **94** (2016) 063509, [1605.04974].

[71] P. Burda, R. Gregory and I. Moss, *Gravity and the stability of the Higgs vacuum*, *Phys. Rev. Lett.* **115** (2015) 071303, [1501.04937].

[72] J. Espinosa, D. Racco and A. Riotto, *Cosmological Signature of the Standard Model Higgs Vacuum Instability: Primordial Black Holes as Dark Matter*, *Phys. Rev. Lett.* **120** (2018) 121301, [1710.11196].

[73] K. Kohri and H. Matsui, *Electroweak Vacuum Collapse induced by Vacuum Fluctuations of the Higgs Field around Evaporating Black Holes*, *Phys. Rev. D* **98** (2018) 123509, [1708.02138].

[74] J. R. Espinosa, D. Racco and A. Riotto, *Primordial Black Holes from Higgs Vacuum Instability: Avoiding Fine-tuning through an Ultraviolet Safe Mechanism*, *Eur. Phys. J. C* **78** (2018) 806, [1804.07731].

[75] G. Franciolini, G. Giudice, D. Racco and A. Riotto, *Implications of the detection of primordial gravitational waves for the Standard Model*, *JCAP* **05** (2019) 022, [1811.08118].

[76] J. M. Cline and J. R. Espinosa, *Axionic landscape for Higgs coupling near-criticality*, *Phys. Rev. D* **97** (2018) 035025, [1801.03926].

[77] J. R. Espinosa, D. Racco and A. Riotto, *A Cosmological Signature of the SM Higgs Instability: Gravitational Waves*, *JCAP* **09** (2018) 012, [1804.07732].

[78] A. Hook, J. Huang and D. Racco, *Searches for other vacua. Part II. A new Higgstory at the cosmological collider*, *JHEP* **01** (2020) 105, [1907.10624].

[79] T. Hayashi, K. Kamada, N. Oshita and J. Yokoyama, *On catalyzed vacuum decay around a radiating black hole and the crisis of the electroweak vacuum*, *JHEP* **08** (2020) 088, [2005.12808].

[80] A. Strumia and N. Tetradis, *Higgstory repeats itself*, 2207.00299.

[81] J. S. Cruz, S. Brandt and M. Urban, *Quantum and Gradient Corrections to False Vacuum Decay on a de Sitter Background*, 2205.10136.

[82] J. E. Camargo-Molina, M. C. González and A. Rajantie, *Phase Transitions in de Sitter: Quantum Corrections*, 2204.03480.

[83] J. E. Camargo-Molina and A. Rajantie, *Phase transitions in de Sitter: The stochastic formalism*, 2204.02875.

[84] S. Vicentini, *New bounds on vacuum decay in de Sitter space*, 2205.11036.

[85] D. N. Maeso, L. Marzola, M. Raidal, V. Vaskonen and H. Veermäe, *Primordial black holes from spectator field bubbles*, *JCAP* **02** (2022) 017, [2112.01505].

[86] N. Chernikov and E. Tagirov, *Quantum theory of scalar fields in de Sitter space-time*, *Ann. Inst. H. Poincare Phys. Theor. A* **9** (1968) 109.

[87] E. A. Tagirov, *Consequences of field quantization in de Sitter type cosmological models*, *Annals Phys.* **76** (1973) 561–579.

[88] J. Callan, Curtis G., S. R. Coleman and R. Jackiw, *A New improved energy - momentum tensor*, *Annals Phys.* **59** (1970) 42–73.

[89] M. Bounakis and I. G. Moss, *Gravitational corrections to Higgs potentials*, *JHEP* **04** (2018) 071, [1710.02987].

[90] Q. Li, T. Moroi, K. Nakayama and W. Yin, *Instability of the Electroweak Vacuum in Starobinsky Inflation*, 2206.05926.

[91] D. G. Figueroa, A. Florio, T. Opferkuch and B. A. Stefanek, *Dynamics of Non-minimally Coupled Scalar Fields in the Jordan Frame*, 2112.08388.

[92] S. Clery, Y. Mambrini, K. A. Olive, A. Shkerin and S. Verner, *Gravitational Portals with Non-Minimal Couplings*, 2203.02004.

[93] O. Lebedev and J.-H. Yoon, *On gravitational preheating*, 2203.15808.

[94] K. Chetyrkin and M. Zoller, *Three-loop β-functions for top-Yukawa and the Higgs self-interaction in the Standard Model*, *JHEP* **06** (2012) 033, [1205.2892].

[95] F. Bezrukov, M. Y. Kalmykov, B. A. Kniehl and M. Shaposhnikov, *Higgs Boson Mass and New Physics*, *JHEP* **10** (2012) 140, [1205.2893].

[96] F. Bezrukov and M. Shaposhnikov, *Standard Model Higgs boson mass from inflation: Two loop analysis*, *JHEP* **07** (2009) 089, [0904.1537].

[97] A. A. Starobinsky, *A New Type of Isotropic Cosmological Models Without Singularity*, *Adv. Ser. Astrophys. Cosmol.* **3** (1987) 130–133.

[98] A. Vilenkin, *Classical and Quantum Cosmology of the Starobinsky Inflationary Model*, *Phys. Rev. D* **32** (1985) 2511.

[99] Planck collaboration, Y. Akrami et al., *Planck 2018 results. X. Constraints on inflation*, *Astron. Astrophys.* **641** (2020) A10, [1807.06211].

[100] Y. Ema, *Higgs Scalaron Mixed Inflation*, *Phys. Lett. B* **770** (2017) 403–411, [1701.07665].

[101] M. He, A. A. Starobinsky and J. Yokoyama, *Inflation in the mixed Higgs-R^2 model*, *JCAP* **05** (2018) 064, [1804.00409].

[102] T. Lancaster and S. J. Blundell, *Quantum Field Theory for the Gifted Amateur*. Oxford University Press, 2014.

[103] Particle Data Group collaboration, M. Tanabashi et al., *Review of Particle Physics*, *Phys. Rev. D* **98** (2018) 030001.

[104] H. B. Nielsen, *PREdicted the Higgs Mass*, *Bled Workshops Phys.* **13** (2012) 94–126, [1212.5716].

[105] M. Holthausen, K. S. Lim and M. Lindner, *Planck scale Boundary Conditions and the Higgs Mass*, *JHEP* **02** (2012) 037, [1112.2415].

[106] T. Hambye and K. Riesselmann, *Matching conditions and Higgs mass upper bounds revisited*, *Phys. Rev. D* **55** (1997) 7255–7262, [hep-ph/9610272].

[107] P. B. Arnold and S. Vokos, *Instability of hot electroweak theory: bounds on m(H) and M(t)*, *Phys. Rev. D* **44** (1991) 3620–3627.

[108] S. Hawking and I. Moss, *Supercooled Phase Transitions in the Very Early Universe*, *Adv. Ser. Astrophys. Cosmol.* **3** (1987) 154–157.

[109] S. R. Coleman, *The Fate of the False Vacuum. 1. Semiclassical Theory*, *Phys. Rev. D* **15** (1977) 2929–2936.

[110] A. D. Linde, *Quantum creation of an open inflationary universe*, *Phys. Rev. D* **58** (1998) 083514, [gr-qc/9802038].

[111] T. Markkanen, S. Nurmi and A. Rajantie, *Do metric fluctuations affect the Higgs dynamics during inflation?*, *JCAP* **12** (2017) 026, [1707.00866].

[112] J. C. Collins, *Renormalization: An Introduction to Renormalization, The Renormalization Group, and the Operator Product Expansion*, vol. 26 of *Cambridge Monographs on Mathematical Physics*. Cambridge University Press, Cambridge, 1986, 10.1017/CBO9780511622656.

[113] R. J. Hardwick, T. Markkanen and S. Nurmi, *Renormalisation group improvement in the stochastic formalism*, *JCAP* **09** (2019) 023, [1904.11373].

[114] D. Y. Cheong, S. M. Lee and S. C. Park, *Primordial Black Holes in Higgs-R^2 Inflation as a whole dark matter*, 1912.12032.

[115] C. Ford, D. Jones, P. Stephenson and M. Einhorn, *The Effective potential and the renormalization group*, *Nucl. Phys. B* **395** (1993) 17–34, [hep-lat/9210033].

[116] A. H. Guth, *The Inflationary Universe: A Possible Solution to the Horizon and Flatness Problems*, *Phys. Rev. D* **23** (1981) 347–356.

[117] A. R. Liddle and D. Lyth, *Cosmological inflation and large scale structure*. Cambridge University Press, 9, 2000.

[118] N. Turok, *A critical review of inflation*, *Class. Quant. Grav.* **19** (2002) 3449–3467.

[119] J. A. Vázquez, L. E. Padilla and T. Matos, *Inflationary Cosmology: From Theory to Observations*, 1810.09934.

[120] G. Lazarides, *Introduction to inflationary cosmology*, in *Corfu Summer Institute on Elementary Particle Physics (Corfu 2001)*, 2001. hep-ph/0204294.

[121] A. R. Liddle, *An introduction to modern cosmology*. Wiley, 1998.

[122] A. G. Riess et al., *A 2.4% Determination of the Local Value of the Hubble Constant*, *Astrophys. J.* **826** (2016) 56, [1604.01424].

[123] Planck collaboration, N. Aghanim et al., *Planck intermediate results. XLVI. Reduction of large-scale systematic effects in HFI polarization maps and estimation of the reionization optical depth*, *Astron. Astrophys.* **596** (2016) A107, [1605.02985].

[124] A. A. Starobinsky, *Spectrum of relict gravitational radiation and the early state of the universe*, *JETP Lett.* **30** (1979) 682–685.

[125] A. Kehagias, A. Moradinezhad Dizgah and A. Riotto, *Remarks on the Starobinsky model of inflation and its descendants*, *Phys. Rev. D* **89** (2014) 043527, [1312.1155].

[126] T. Markkanen and A. Tranberg, *A Simple Method for One-Loop Renormalization in Curved Space-Time*, *JCAP* **08** (2013) 045, [1303.0180].

[127] A. De Felice and S. Tsujikawa, *f(R) theories*, *Living Rev. Rel.* **13** (2010) 3, [1002.4928].

[128] J. Martin, C. Ringeval and V. Vennin, *Encyclopædia Inflationaris*, *Phys. Dark Univ.* **5-6** (2014) 75–235, [1303.3787].

[129] D. S. Gorbunov and A. G. Panin, *Scalaron the mighty: producing dark matter and baryon asymmetry at reheating*, *Phys. Lett. B* **700** (2011) 157–162, [1009.2448].

[130] Y. Ema, K. Mukaida and J. van de Vis, *Renormalization group equations of Higgs-R^2 inflation*, *JHEP* **02** (2021) 109, [2008.01096].

[131] A. A. Starobinsky and J. Yokoyama, *Equilibrium state of a selfinteracting scalar field in the De Sitter background*, *Phys. Rev. D* **50** (1994) 6357–6368, [astro-ph/9407016].

[132] F. Bauer and D. A. Demir, *Inflation with Non-Minimal Coupling: Metric versus Palatini Formulations*, *Phys. Lett. B* **665** (2008) 222–226, [0803.2664].

[133] K. Dimopoulos, A. Karam, S. S. López and E. Tomberg, *Palatini R^2 Quintessential Inflation*, 2206.14117.

[134] S. Raatikainen and S. Rasanen, *Higgs inflation and teleparallel gravity*, *JCAP* **12** (2019) 021, [1910.03488].

[135] H. Azri and D. Demir, *Affine Inflation*, *Phys. Rev. D* **95** (2017) 124007, [1705.05822].

[136] C. Rigouzzo and S. Zell, *Coupling Metric-Affine Gravity to a Higgs-Like Scalar Field*, 2204.03003.

[137] M. Shaposhnikov, A. Shkerin, I. Timiryasov and S. Zell, *Higgs inflation in Einstein-Cartan gravity*, *JCAP* **02** (2021) 008, [2007.14978].

Appendix A

Explicit calculations in quadratic inflation

A.1 Analysis in terms of physical time

This illustrative calculation is performed in the slow-roll regime for the quadratic inflationary model (3.41). We define that inflation ends at $t_{\rm inf} = 0$, and consider the time interval from the start to the end of inflation, $t_{\rm start} < t < 0$, during which the inflaton field is positive. We can obtain the time dependence of the inflaton field ϕ and the Hubble rate H, by inserting the potential (3.41) into (3.13) and (3.14):

$$\left\{ \begin{array}{l} H^2 = \frac{V(\phi)}{3M_P^2} \\ 3H\dot{\phi} = -V'(\phi) \end{array} \right. \Rightarrow \left\{ \begin{array}{l} H^2 = \frac{m^2\phi^2}{6M_P^2} \\ 3H\dot{\phi} = -m^2\phi \end{array} \right. \Rightarrow \left\{ \begin{array}{l} \frac{m^2\phi^2}{6M_P^2} = H^2 = \frac{m^4\phi^2}{9\dot{\phi}^2} \\ H = -\frac{m^2\phi}{3\dot{\phi}} \end{array} \right. \Rightarrow \left\{ \begin{array}{l} \dot{\phi}^2 = \frac{2m^2M_P^2}{3} \\ H = -\frac{m^2\phi}{3\dot{\phi}} \end{array} \right. \Rightarrow$$

$$\left\{ \begin{array}{l} \dot{\phi} = \pm\sqrt{\frac{2}{3}}mM_P \\ H = \mp\frac{m^2\phi}{3\sqrt{\frac{2}{3}}mM_P} \end{array} \right. \Rightarrow \left\{ \begin{array}{l} \phi(t) = \pm\sqrt{\frac{2}{3}}mM_Pt + c_1 \\ H = \mp\frac{m}{M_P\sqrt{6}}\left(\pm\sqrt{\frac{2}{3}}mM_Pt + c_1\right) \end{array} \right. \Rightarrow$$

$$\phi(t) = -\sqrt{\frac{2}{3}} m M_P t + c_1 \tag{A.1}$$

$$H = -\left(\frac{m^2}{3}\right) t + c_2 \tag{A.2}$$

where c_1 and $c_2 = \frac{m}{M_P\sqrt{6}} c_1$ are integration constants, and the signs of $\phi, \dot{\phi}$ and H have been fixed according to the conventions mentioned above. At the end of inflation, we have $c_1 = M_P\sqrt{2}$ and thus $c_2 = H_{\rm inf} = \frac{m}{\sqrt{3}}$. Hence,

$$\phi(t) = -\left(\sqrt{\frac{2}{3}} m M_P\right) t + M_P\sqrt{2}\,, \tag{A.3}$$

$$H(t) = -\left(\frac{m^2}{3}\right) t + \frac{m}{\sqrt{3}}\,. \tag{A.4}$$

We can also obtain $a = a(t)$ using the Friedmann equation (3.8),

$$\frac{\dot{a}}{a} = H(t) \;\Rightarrow\; \frac{{\rm d}a}{a} = \left[-\left(\frac{m^2}{3}\right) t + \frac{m}{\sqrt{3}}\right] {\rm d}t \;\Rightarrow\; \int^a \frac{{\rm d}a'}{a'} = \int^t \left[-\left(\frac{m^2}{3}\right) t' + \frac{m}{\sqrt{3}}\right] {\rm d}t' \;\Rightarrow$$

$$\ln a(t) = -\left(\frac{m^2}{6}\right) t^2 + \frac{m}{\sqrt{3}} t + c_3\,, \tag{A.5}$$

$$a(t) = a_{\rm inf} \exp\left[-\left(\frac{m^2}{6}\right) t^2 + \frac{m}{\sqrt{3}} t\right]\,, \tag{A.6}$$

where c_3 is the integration constant, and $a_{\rm inf} = a(t_{\rm inf} = 0) = e^{c_3}$. This constant can be found by inserting the potential (3.41) at $t_{\rm inf}$ in (3.18), and via (3.19) we can also obtain the value of the scale factor at the start of inflation for the minimum value of e-foldings $N_{\rm start}$,

$$V_{\rm inf} = (mM_P)^2 \;\Rightarrow\; a_{\rm inf} = \frac{a_0 H_0 e^{60}}{10^{16}} \frac{\sqrt{mM_P}}{m/\sqrt{3}} \;\Rightarrow$$

$$a_{\rm inf} = \frac{a_0 H_0 e^{60}}{10^{16}} \sqrt{\frac{3M_P}{m}}\,, \tag{A.7}$$

$$a_{\rm start} = \frac{a_0 H_0 e^{60-N_{\rm start}}}{10^{16}} \sqrt{\frac{3M_P}{m}}\,. \tag{A.8}$$

Using (A.6) and (A.8), provides $t_{\rm start}$ as a function of $N_{\rm start}$:

$$a(t_{\rm start}) = a_{\rm inf}\exp\left[-\left(\frac{m^2}{6}\right)t_{\rm start}^2 + \frac{m}{\sqrt{3}}t_{\rm start}\right] = a_{\rm inf}\,e^{-N_{\rm start}} \;\Rightarrow\; t_{\rm start}^2 - \frac{2\sqrt{3}}{m}t_{\rm start} - \frac{6N_{\rm start}}{m^2} = 0,$$

$$\Delta = \frac{4\times 3}{m^2} + \frac{4\times 6N_{\rm start}}{m^2} = \frac{4\times 3(1+2N_{\rm start})}{m^2} \;\Rightarrow$$

$$t(N_{\rm start}) = \frac{\frac{2\sqrt{3}}{m} \pm \frac{2}{m}\sqrt{3(1+2N_{\rm start})}}{2} = \frac{\sqrt{3}}{m}\left(1 \pm \sqrt{1+2N_{\rm start}}\right) \xRightarrow{t_{\rm start}<0}$$

$$t(N_{\rm start}) = \frac{\sqrt{3}}{m}\left(1 - \sqrt{1+2N_{\rm start}}\right), \tag{A.9}$$

where for the minimum value of $N_{\rm start} = 60$, we get $t_{\rm start} = -10\sqrt{3}/m$. The factor $\eta_0 - \eta(t) = (\eta_0 - \eta_{\rm inf}) + (\eta_{\rm inf} - \eta(t))$, present in the number of bubbles integral (4.4), can be calculated from (3.3), (3.21) and (A.6):

$$\begin{aligned}
\eta_{\rm inf} - \eta(t) &= \int_t^0 \frac{dt'}{a(t')} = \frac{1}{a_{\rm inf}}\int_t^0 \exp\left[\frac{m^2}{6}t'^2 - \frac{m}{\sqrt{3}}t'\right]dt' \\
&= \frac{1}{a_{\rm inf}}\int_t^0 \exp\left[\frac{m^2}{6}t'^2 - \frac{m}{\sqrt{3}}t' + \frac{1}{2} - \frac{1}{2}\right]dt' = \frac{e^{-1/2}}{a_{\rm inf}}\int_t^0 \exp\left(\frac{m}{\sqrt{6}}t' - \frac{1}{\sqrt{2}}\right)^2 dt' \\
&= \frac{1}{a_{\rm inf}\sqrt{e}}\int_t^0 \exp\left[\frac{1}{2}\left(\frac{m}{\sqrt{3}}t' - 1\right)^2\right]dt' \xRightarrow[dt'=\frac{\sqrt{3}}{m}dx]{x=\frac{m}{\sqrt{3}}t'-1} \frac{\sqrt{3}}{a_{\rm inf}m\sqrt{e}}\int_{\frac{m}{\sqrt{3}}t-1}^{-1} e^{\frac{x^2}{2}}dx \\
&= \frac{\sqrt{3}}{a_{\rm inf}m\sqrt{e}}\sqrt{\frac{\pi}{2}}\left[\mathrm{erfi}\left(\frac{-1}{\sqrt{2}}\right) - \mathrm{erfi}\left(\frac{\frac{m}{\sqrt{3}}t-1}{\sqrt{2}}\right)\right] \Rightarrow
\end{aligned}$$

$$\eta_0 - \eta(t) = \frac{3.21}{a_0 H_0} + \frac{1}{a_{\rm inf}m}\sqrt{\frac{3\pi}{2e}}\left[\mathrm{erfi}\left(\frac{-1}{\sqrt{2}}\right) - \mathrm{erfi}\left(\frac{\frac{m}{\sqrt{3}}t-1}{\sqrt{2}}\right)\right], \tag{A.10}$$

where $\mathrm{erfi}(x)$ is the imaginary error function.

A.2 Analysis in terms of the scale factor

We repeat the previous analysis in terms of the scale factor a, which is a more suitable variable than time t for inflationary cosmology. With a simple change of variables, we can write $\dot{\phi} = \frac{d\phi}{dt} = \frac{d\phi}{da}\frac{da}{dt} = aH(a)\frac{d\phi}{da}$, and thus perform the same calculation more efficiently:

$$\left\{ \begin{array}{l} H^2 = \frac{V(\phi)}{3M_P^2} \\ 3H\dot{\phi} = -V'(\phi) \end{array} \right. \Rightarrow \left\{ \begin{array}{l} H^2 = \frac{V(\phi)}{3M_P^2} \\ 3aH^2\frac{d\phi}{da} = -V'(\phi) \end{array} \right. \Rightarrow \left\{ \begin{array}{l} 3H^2 = \frac{m^2\phi^2}{2M_P^2} \\ 3aH^2\frac{d\phi}{da} = -m^2\phi \end{array} \right. \Rightarrow a\frac{d\phi}{da} = \frac{-2M_P^2}{\phi} \Rightarrow$$

$$\phi\, d\phi = -2M_P^2\frac{da}{a} \;\Rightarrow\; \frac{\phi^2(a)}{2} = -2M_P^2\ln(a) + c_4 \;\Rightarrow\; \phi(a) = \pm\sqrt{2c_4 - 4M_P^2\ln(a)} \;\Rightarrow$$

$$\phi(a) = \sqrt{2c_4 - 4M_P^2\ln(a)}\,, \tag{A.11}$$

where c_4 is an integration constant, and we have used the convention $\phi > 0$ during inflation. We can express c_4 in terms of $a_{\rm inf}$ via

$$\phi_{\rm inf}^2 = 2M_P^2 = 2c_4 - 4M_P^2\ln(a_{\rm inf}) \;\Rightarrow\; c_4 = M_P^2\left(1 + 2\ln(a_{\rm inf})\right)\,, \tag{A.12}$$

and thus rewrite (A.11) as

$$\phi(a) = M_P\sqrt{2 + 4\ln(a_{\rm inf}) - 4\ln(a)} = \left(M_P\sqrt{2}\right)\sqrt{1 + 2\left(\ln(a_{\rm inf}) - \ln(a)\right)} \;\Rightarrow$$

$$\phi(a) = \left(M_P\sqrt{2}\right)\sqrt{1 + 2\ln\left(a_{\rm inf}/a\right)}\,. \tag{A.13}$$

Now that we have $\phi(a)$, we can get $H(a)$ via (3.13),

$$H^2(a) = \left(\frac{m^2}{6M_P^2}\right)2M_P^2\left[1 + 2\ln\left(\frac{a_{\rm inf}}{a}\right)\right] = \frac{m^2}{3}\left[1 + 2\ln\left(\frac{a_{\rm inf}}{a}\right)\right] \;\Rightarrow$$

$$H(a) = (m/\sqrt{3})\sqrt{1 + 2\ln\left(a_{\rm inf}/a\right)}\,. \tag{A.14}$$

Similarly as before, the factor $\eta_0 - \eta(a)$, present in the number of bubbles integral (4.4), can be calculated from (3.3), (3.21) and (A.14)

$$\begin{aligned}\eta_{\rm inf} - \eta(a) &= \int_a^{a_{\rm inf}} \frac{da'}{a'^2 H(a')} = \frac{\sqrt{3}}{m}\int_a^{a_{\rm inf}} \frac{da'}{a'^2\sqrt{1 + 2\ln\left(a_{\rm inf}/a'\right)}} \\ &= \frac{\sqrt{3}}{a_{\rm inf} m}\sqrt{\frac{\pi}{2e}}\left[\mathrm{erfi}\left(\sqrt{\ln\left(\frac{a_{\rm inf}}{a}\right) + \frac{1}{2}}\right) - \mathrm{erfi}\left(\frac{1}{\sqrt{2}}\right)\right]\,,\end{aligned} \tag{A.15}$$

resulting ultimately into

$$\eta_0 - \eta(a) = \frac{3.21}{a_0 H_0} + \frac{1}{a_{\rm inf} m}\sqrt{\frac{3\pi}{2e}}\left[\mathrm{erfi}\left(\sqrt{\ln\left(\frac{a_{\rm inf}}{a}\right) + \frac{1}{2}}\right) - \mathrm{erfi}\left(\frac{1}{\sqrt{2}}\right)\right]\,. \tag{A.16}$$

A.3 Analysis in terms of the number of e-foldings

Using (4.10), we can obtain the expression for ϕ in terms of N, and subsequently find $H(N)$ through (3.13), as

$$\phi(N) = \left(M_P\sqrt{2}\right)\sqrt{1 + 2N}\,, \tag{A.17}$$

$$H(N) = (m_\phi/\sqrt{3})\sqrt{1 + 2N}\,, \tag{A.18}$$

The conformal time term present in (4.4) can be derived via (3.22), where we calculate it in the interval from N e-foldings to the end of inflation $N = 0$, as

$$\eta_{\rm inf} - \eta(N) = \frac{\sqrt{3}}{a_{\rm inf} m_\phi}\int_0^N \frac{e^{N'} dN'}{\sqrt{1 + 2N'}} = \frac{1}{a_{\rm inf} m_\phi}\sqrt{\frac{3\pi}{2e}}\left[\mathrm{erfi}\left(\sqrt{N + \frac{1}{2}}\right) - \mathrm{erfi}\left(\sqrt{\frac{1}{2}}\right)\right]\,, \tag{A.19}$$

where erfi is the imaginary error function. Combining (A.19) with (3.21), gives the total conformal time of our lightcone, from the present day to N e-foldings before the end of inflation,

$$\eta_0 - \eta(N) = \frac{3.21}{a_0 H_0} + \frac{1}{a_{\rm inf} m_\phi}\sqrt{\frac{3\pi}{2e}}\left[\text{erfi}\left(\sqrt{N+\frac{1}{2}}\right) - \text{erfi}\left(\sqrt{\frac{1}{2}}\right)\right]. \tag{A.20}$$

Thus, we can calculate the number of bubbles of true vacuum $\langle\mathcal{N}\rangle$ in terms of e-folds via (4.4). This number is sensitive to the value of the integral's upper limit, which is not fixed but only bounded, $60 \leq N_{\rm start} \leq N_{\rm max}\left(\rho = M_p^4\right)$, as explained in Section 3.3.1.

In order to simplify calculations, and especially the numerical computation in slow-roll, we can use the asymptotic expansion of the imaginary error function $\text{erfi}\left(\sqrt{N+1/2}\right)$ for large N,

$$\text{erfi}(x) = \frac{e^{x^2}}{\sqrt{\pi}x}\left(\sum_{k=0}^{\infty}\frac{(2k-1)!!}{(2x^2)^k}\right), \tag{A.21}$$

where $-1!! = 0!! = 1$ and

$$n!! = \begin{cases} n(n-2)(n-4)...(4)(2)\,, \text{ even } n. \\ n(n-2)(n-4)...(3)(1)\,, \text{ odd } n. \end{cases}$$

Therefore, we can expand the erfi term in (A.20) accordingly as

$$\text{erfi}\left(\sqrt{N+\frac{1}{2}}\right) = \sqrt{\frac{2e}{\pi}}\frac{e^N}{\sqrt{2N+1}}\left(1 + \frac{1}{(2N+1)} + \frac{3}{(2N+1)^2} + ...\right). \tag{A.22}$$

As we see in (4.4), we can combine the $(\eta_0 - \eta\,(N))^3$ factor with the e^{-3N} factor to simplify the form of the integrand, as

$$\begin{aligned}\frac{\eta_0 - \eta\,(N)}{e^N} &= \frac{3.21e^{-N}}{a_0 H_0} + \frac{e^{-N}}{a_{\rm inf} m_\phi}\sqrt{\frac{3\pi}{2e}}\left[\text{erfi}\left(\sqrt{N+\frac{1}{2}}\right) - \text{erfi}\left(\sqrt{\frac{1}{2}}\right)\right] \\ &= \frac{\left(\frac{3.21}{a_0 H_0} - \frac{\text{erfi}\left(\sqrt{\frac{1}{2}}\right)}{a_{\rm inf} m_\phi}\sqrt{\frac{3\pi}{2e}}\right)}{e^N} + \frac{\sqrt{3}(2N+1)^{-1/2}}{a_{\rm inf} m_\phi}\left(1 + \frac{1}{(2N+1)} + \frac{3}{(2N+1)^2} + ...\right).\end{aligned} \tag{A.23}$$

We can also see that from the other terms in (4.4), $\Gamma(N)/H(N) = H^3(N)e^{-B_{HM}(N)}$, there is a factor of H^3 that can be also combined with the previous expression and simplify it further

$$\frac{\eta_0 - \eta\,(N)}{e^N} H(N) = \left(\frac{3.21}{a_0 H_0} - \frac{\text{erfi}\left(\sqrt{\frac{1}{2}}\right)}{a_{\text{inf}} m_\phi} \sqrt{\frac{3\pi}{2e}} \right) \left(\frac{m_\phi}{\sqrt{3}} \right) \frac{\sqrt{2N+1}}{e^N} + \frac{1}{a_{\text{inf}}} \left(1 + \frac{1}{(2N+1)} + ... \right). \tag{A.24}$$

Finally, inserting also the a_{inf}^3 term in the above expression and rewriting $m_\phi/\sqrt{3} = H_{\text{inf}}$, leads to

$$\begin{aligned} \frac{\eta_0 - \eta\,(N)}{e^N} H(N) a_{\text{inf}} &= \left[3.21 \left(\frac{a_{\text{inf}} H_{\text{inf}}}{a_0 H_0} \right) - \text{erfi}\left(\sqrt{\frac{1}{2}} \right) \sqrt{\frac{\pi}{2e}} \right] \frac{\sqrt{2N+1}}{e^N} + 1 + ... \\ &= Q \left(\frac{\sqrt{2N+1}}{e^N} \right) + 1 + ..., \end{aligned} \tag{A.25}$$

where we have calculated the numerical factor $Q = 3.21 \left(\frac{a_{\text{inf}} H_{\text{inf}}}{a_0 H_0} \right) - \text{erfi}\left(\sqrt{\frac{1}{2}} \right) \sqrt{\frac{\pi}{2e}} = 2.4269 \times 10^{26}$. Hence, we can express (4.4) as

$$\langle \mathcal{N} \rangle = \langle \mathcal{N} \rangle |_0^{N_{\text{large}}} + \frac{4\pi}{3} \int_{N_{\text{large}}}^{N_{\text{start}}} dN \left[Q \left(\frac{\sqrt{2N+1}}{e^N} \right) + (1 + ...) \right]^3 e^{-B_{HM}(N)}, \tag{A.26}$$

where $\langle \mathcal{N} \rangle |_0^{N_{\text{large}}}$ corresponds to the number of bubbles formed between the end of inflation $N_{\text{inf}} = 0$ and a sufficiently large number of e-folds N_{large} ($N_{\text{inf}} \ll N_{\text{large}} < N_{\text{start}}$), where the asymptotic expansion is not valid, and it is given by

$$\langle \mathcal{N} \rangle |_0^{N_{\text{large}}} = (4\pi/3) \int_0^{N_{\text{large}}} dN \left[(\eta_0 - \eta\,(N))\, a_{\text{inf}} H(N) e^{-N} \right]^3 e^{-B_{HM}(N)}. \tag{A.27}$$

For large values of N_{large} and N_{start}, the terms in the integrand of (A.26) vanish, as $e^{-N}\sqrt{2N+1}$ and $(2N+1)^{-1,-3,\cdots}$ both tend to zero, so we can rewrite it in a very simplified form as

$$\langle \mathcal{N} \rangle = \langle \mathcal{N} \rangle |_0^{N_{\text{large}}} + \frac{4\pi}{3} \int_{N_{\text{large}}}^{N_{\text{start}}} e^{-B_{HM}(N)} dN. \tag{A.28}$$

A.4 Toy model vacuum decay in slow-roll

With the assumptions of slow-roll inflation and approximately constant bounce action $B_{\rm HM}$, we can obtain explicit lower bounds on the non-minimal coupling ξ, in an almost completely analytical manner. Following the formalism of Section 4.1 and inserting (2.23) in (A.26) results into

$$\begin{aligned}\langle\mathcal{N}\rangle &= \frac{4\pi}{3}e^{-\frac{96\pi^2\xi^2}{|\lambda|}}\left(\int_0^{N_{\rm large}} dN\left[\left(\eta_0-\eta\left(N\right)\right)a_{\rm inf}H(N)e^{-N}\right]^3\right.\\ &+ \left.\int_{N_{\rm large}}^{N_{\rm start}} dN\left[Q\left(\frac{\sqrt{2N+1}}{e^N}\right)+\left(1+\frac{1}{(2N+1)}+...\right)\right]^3\right). \qquad \text{(A.29)}\end{aligned}$$

We can rewrite this expression in a more compact way as

$$\langle\mathcal{N}\rangle = e^{-\frac{96\pi^2\xi^2}{|\lambda|}}\left[\Delta A(0,N_{\rm large})+\Delta B(N_{\rm large},N_{\rm start})\right], \qquad \text{(A.30)}$$

$$\Delta A(0,N_{\rm large}) = \frac{4\pi}{3}\int_0^{N_{\rm large}} dN\left[\left(\eta_0-\eta\left(N\right)\right)a_{\rm inf}H(N)e^{-N}\right]^3, \qquad \text{(A.31)}$$

$$\Delta B(N_{\rm large},N_{\rm start}) = \frac{4\pi}{3}\int_{N_{\rm large}}^{N_{\rm start}} dN\left[Q\left(\frac{\sqrt{2N+1}}{e^N}\right)+\left(1+\frac{1}{(2N+1)}+...\right)\right]^3. \qquad \text{(A.32)}$$

Unfortunately, there is no analytical expression for the ΔA term, but we can calculate its value at a valid $N_{\rm large}$ that is numerically attainable. We choose $N_{\rm large}=600$, which results in $\Delta A(0,600)=\frac{4\pi}{3}\left(1.0817\times10^{79}\right)$. However, note that we would get the same answer for ΔA at a value as low as $N=11$ e-folds. On the other hand, we can perform the integral in ΔB analytically

$$\begin{aligned}B(N) &= \left[\frac{1}{3}e^{\frac{3}{2}}Q^3\left(\sqrt{\frac{\pi}{6}}\right)\mathrm{erf}(\sqrt{\frac{3}{2}(1+2N)})+\frac{3}{2}\ln(1+2N)-3Q\sqrt{2e\pi}-\frac{1}{3}e^{\frac{3}{2}}Q^3\sqrt{\frac{\pi}{6}}\right.\\ &- \frac{2Q^3e^{-3N}}{3\sqrt{1+2N}}(2N^2+3N+1)+3Q\left(\sqrt{2e\pi}\right)\mathrm{erf}(\sqrt{\frac{1}{2}(1+2N)})\\ &+ \left.N-\frac{3}{2(1+2N)}-\frac{6Qe^{-N}}{\sqrt{1+2N}}(N+1)-3Q^2e^{-2N}\left(N+\frac{3}{2}\right)\right]\frac{4\pi}{3}, \qquad \text{(A.33)}\end{aligned}$$

where erf is the error function. For large values of N, Eq. (A.33) can be written in a much more simple form, since most of its terms get suppressed and $\mathrm{erf}(x\to\infty)\approx1$, as

$$B(N) \approx \frac{4\pi}{3}\left(N + \frac{3}{2}\ln(1+2N)\right) \approx \frac{4\pi}{3}N\,. \tag{A.34}$$

The value of the ΔA term is very large, of order 10^{79}, and thus dominates the contribution to the number of bubbles of true vacuum in (A.30). In order for the the early universe contribution $\Delta B(N_{\rm large}, N_{\rm start}) \approx \frac{4\pi}{3}(N_{\rm start} - N_{\rm large}) \approx \frac{4\pi}{3}N_{\rm start}$ to be comparable and eventually dominate, we need to go beyond $N = 10^{78}$ e-folds, which is inconsistent with the maximum duration of quadratic inflation (3.45).

Imposing the condition $\langle\mathcal{N}\rangle \leq 1$ to (A.30), we can obtain an analytic relationship between ξ and $N_{\rm start}$, as

$$|\xi| \geq \frac{\sqrt{|\lambda|}}{4\pi\sqrt{6}}\sqrt{\ln\left[\Delta A(0, N_{\rm large}) + \Delta B(N_{\rm large}, N_{\rm start})\right]}\,, \tag{A.35}$$

where the equality holds at the boundary $\langle\mathcal{N}\rangle = 1$, and for $N_{\rm large} = 600$ reduces to

$$|\xi| \geq \frac{\sqrt{|\lambda|}}{4\pi\sqrt{6}}\sqrt{\ln(4\pi/3) + \ln\left(1.0817\times 10^{79} + N_{\rm start}\right)}\,. \tag{A.36}$$

Thus, for quadratic inflation in slow-roll, we obtain the lower bound on the Higgs curvature coupling at high curvature scales $\xi(\mu \approx 10^{15}\,{\rm GeV}) \geq 0.044$, for $60 \leq N_{\rm start} \leq N_{\rm max} \approx 10^{10}$.

The expected number of bubbles $\langle\mathcal{N}\rangle$ scales with the number of e-folds and follows (A.30). For $\xi \approx 0.044$, we can approximate (A.30) in the very early universe as

$$\langle\mathcal{N}\rangle \approx 9.2451\times 10^{-80}\left[1.0817\times 10^{79} + N_{\rm start}\right]. \tag{A.37}$$

It is evident that we have approximately one bubble forming, even if inflation does not begin much earlier than $N_{\rm large}$. However, this is a consequence of the condition that we set in order to find the bound on ξ. Nevertheless, we see that when $N_{\rm start}$ becomes comparable with 10^{79}, the number of bubbles becomes proportional to the number of e-foldings, with enhanced bubble production in the very early universe, as illustrated in Section 4.2.3.